

Lattice Physics Calculations for
Alternative Fuels for the Canadian
SCWR

LATTICE PHYSICS CALCULATIONS FOR ALTERNATIVE FUELS FOR THE CANADIAN
SCWR

By EDWARD MATTHEW GLANFIELD, B.Sc.

A Thesis Submitted to the School of Graduate Studies in Partial Fulfilment of the
Requirements for the Degree Master of Applied Science

McMaster University © Copyright by E.M. Glanfield, July 2017

Master of Applied Science, 2017

Department of Engineering Physics

McMaster University

Hamilton, Ontario, Canada

TITLE: Comparison of Fuel Types for the Pressure-Tube Super-Critical Water Cooled Reactor

AUTHOR: Edward Matthew Glanfield, B.Sc.

SUPERVISOR: Dr. David Novog

NUMBER OF PAGES: ix, 122

Abstract

The Canadian-designed Super-Critical Water-cooled Reactor (SCWR) has been in development since the early 2000s and has undergone many design changes since its initial conception. Initially the reactor was designed to use a fuel bundle modeled after the Canada Deuterium Uranium (CANDU) pressurized heavy water reactor bundles. Over time, this fuel bundle evolved into its current design of a re-entrant coolant channel with two fuel rings in the outer portion of the channel. Throughout the development of this design, the fuel composition has remained relatively constant, with only minor changes to enrichment.

The initial SCWR design was intended to utilize a fuel mix of reactor grade plutonium and thorium. The thorium filler is an easily attainable material, being about three times more common than uranium. More importantly, the majority of thorium is made of ^{232}Th , which breeds more fissile material than ^{238}U in the SCWR reactor. This leads to production of ^{233}U that can significantly extend the lifetime of fuel in the reactor, compared to fuels with either ^{238}U or no fertile source.

Even though the plutonium-thorium fuel cycle seems generally advantageous compared to traditional uranium fuels, or even other fuel types, it may not ultimately be preferable to other fuels in a specific reactor design such as the SCWR. The geometry, operation conditions, and cycle length can all have a large influence on the performance of a specific fuel in a reactor. Therefore it is important to compare the performance of different fuels when utilized in the reactor of interest.

The SCALE suite of programs is used in this work to evaluate the performance of plutonium-thorium (PuTh), mixed oxide (MOX), and enriched uranium (UO_2) fuels in the SCWR reactor. TRITON was used to deplete the fuel and obtain nuclide concentrations in 100 day intervals over the lifetime of the fuel. NEWT was used to perform lattice calculations for the determination of reactivity coefficients. In both cases, the ENDF/B-VII nuclear data library was used.

In order to achieve similar burnups for all three fuel types, the enrichment of the UO_2 and MOX fuels was adjusted. The standard PuTh fuel mix used in this work has an average enrichment of 10% plutonium, of which around 50% is ^{239}Pu . An

average enrichment of 7.6% ^{235}U was used for the uranium fuel, while the MOX fuel retained the same enrichment as the PuTh. All three fuel types share the same ratio of enrichment between the inner and outer fuel rings.

Besides adjusting the composition of the fuel, all other reactor parameters were kept identical. Varying the fuel type could change the operating temperatures and other thermalhydraulic properties of the reactor, but this was not considered for ease of computation as well as allowing for more direct comparison of the neutronic differences between fuels. As an alternative, the feedback coefficients for each fuel type were also investigated.

The reactivity changes with burnup of both the PuTh and MOX fuels are extremely similar. The UO_2 fuel, in contrast, decreases in reactivity at a faster rate. This results in the uranium fuel requiring a higher k-eff at zero burn-up to maintain the same cycle length. This also indicates that the PuTh and MOX fuels are being used more efficiently in the reactor. Additionally, a reactor with a more stable reactivity over time is generally easier to refuel.

In general, the UO_2 fuel has feedback coefficients of reactivity closer to zero than either the PuTh or MOX fuels. This is most pronounced in the Coolant Void Reactivity coefficients (CVR), where the uranium fuel has a significantly smaller coefficient than the others. The most notable exception to this is the Coolant Temperature Coefficient of reactivity (CTC), where the uranium fuel has a higher reactivity coefficient at large burnups. It is important to note that in nearly all cases the sign of the reactivity coefficients does not change with fuel selection, meaning that reactor behaviour could be expected to be quite similar between the three fuels.

The originally proposed PuTh fuel seems adequate for use in the SCWR compared to the two alternative fuels. It shows no significant advantages or disadvantages in regards to the reactivity coefficients analyzed in this work. The MOX fuel performs very similarly to the PuTh option, with many reactivity coefficients being nearly the same. Its main benefit would be the availability of existing operational experience in comparison to PuTh fuels. An enriched uranium fuel benefits the most from historic operational experience, and in general has the most optimal reactivity coefficients. However, it burns less efficiently, requiring the fuel to be enriched to around 8.5%, well above the level currently used in power reactors.

From this work there does not seem to be a single, best fuel choice. The multitude of factors considered are a small portion of those that influence the choice of fuel in an operating reactor. Furthermore, some studies have demonstrated the need for advanced fuel materials that would lower the centreline melting temperature and hence some form of nitride or accident tolerant fuel may be needed in the future. Additionally, the fuel that stands out based on a single criterion does not necessarily perform well in other criteria, and further analysis would be beneficial.

Acknowledgements

Without the guidance of David Novog, this thesis would not have been possible. He is responsible for giving me the opportunity to pursue a Master's degree, providing assistance and patience throughout the process, and ensuring that I have completed it successfully. His experience and counsel were invaluable.

Although their knowledge and advice was frequently questionable, I have to thank the familiar faces that I would see each week at WEB. They welcomed and introduced me to Canada, and provided a variety of wonderful extracurricular distractions during my time at McMaster. I also thank the people I met through PNB, Makeshift, and FIRST Canada for their friendship and support.

I would also like to thank Haley Kragness for bringing me to Canada, providing advice and support whenever needed, and for being there from the beginning to the end. And most of all, I appreciate the constant support of my family over the two decades of my education.

Table of Contents

Abstract.....	ii
Acknowledgements.....	v
Table of Contents.....	vi
List of Figures	viii
List of Tables	ix
Chapter 1: Introduction	1
1.1 Development of Canadian Nuclear Industry.....	1
1.2 Development of the SCWR	2
1.3 Current Design	7
1.4 SCWR Fuel	12
Chapter 2: Theory	14
2.1 Nuclides of Interest.....	14
2.2 Fuels	15
2.3 Multiplication Factor.....	16
2.4 Coefficients of Reactivity	17
2.5 Path of a Neutron.....	20
2.6 Dancoff Factors	21
Chapter 3: Literature Review	22
3.1 Work on Early Designs	22
3.2 Work on the 64-Element Design.....	23
3.3 Variations on the 64-Element Design	24
3.4 Analysis of fuels in non-Canadian SCWRs	25
Chapter 4: Methodology.....	27
4.1 Code	27
4.2 Meshing.....	28
4.3 Depletion Time Steps.....	31
4.4 Dancoff Factors	32
4.5 Enrichment.....	33

4.6	Simulations.....	33
Chapter 5: Data & Analysis		35
5.1	Multiplication Factor.....	35
5.2	Coefficient of Void Reactivity.....	38
5.3	Coolant Temperature Coefficient of Reactivity	45
5.4	Moderator Temperature Coefficient of Reactivity	51
5.5	Fuel Temperature Coefficient of Reactivity	54
5.6	Validity	58
Chapter 6: Conclusions		63
Chapter 7: Future Work.....		65
References		66
Appendix A: Raw Data		62
A.1	PuTh.....	62
A.1.1	125mm	62
A.1.2	2375mm	68
A.1.3	4875mm	72
A.2	MOX.....	77
A.1.4	125mm	77
A.1.5	2375mm	81
A.1.6	4875mm	86
A.3	UO ₂	91
A.1.7	125mm	91
A.1.8	2375mm	95
A.1.9	4875mm	100
Appendix B: Additional Plots		105
B.1	PuTh.....	105
B.2	MOX.....	111
B.3	UO ₂	117

List of Figures

Figure 1: CANFLEX-style 43-element fuel bundle adapted for use in SCWR (2).....	3
Figure 2: 54-element fuel bundle design for the SCWR (2)	4
Figure 3: 78-element fuel bundle design for the SCWR (2)	5
Figure 4: 64-element fuel bundle design for the SCWR (2)	7
Figure 5: Current pressure tube and fuel bundle design for the SCWR (2)	8
Figure 6: Simplified diagram of SCWR reactor vessel and internals (10).....	11
Figure 7: IAEA ENDF (n,f) cross section data for the Pu239 nuclide, showing the 0.3eV peak.....	19
Figure 8: Final meshing scheme for SCWR geometry, as displayed by NEWT's graphical output	30
Figure 9: Multiplication factor over burn-up for all three types of fuel at 2375mm.....	35
Figure 10: Number densities of various nuclides of interest over burn-up for the three fuel types.....	36
Figure 11: Four factors for the three fuel types over burn-up	37
Figure 12: Inner Coefficient of Void Reactivity for the three fuel types at 2375mm	39
Figure 13: Change in four factors for ICVR in PuTh fuel at 2375mm	40
Figure 14: ICVRs for PuTh fuel at three reactor heights	41
Figure 15: Outer Coefficient of Void Reactivity for the three fuel types at 2375mm	42
Figure 16: Change in four factors for OCVR in UO ₂ fuel at 2375mm	43
Figure 17: Total Coefficient of Void Reactivity for the three fuel types at 2375mm.....	44
Figure 18: ICTC for the three fuel types at 2375mm	45
Figure 19: Change in four factors for ICTC in PuTh fuel at 2375mm	46
Figure 20: OCTC for the three fuel types at 2375mm.....	47
Figure 21: Change in four factors for OCTC in PuTh fuel at 2375mm.....	48
Figure 22: TCTC for the three fuel types at 2375mm	49
Figure 23: Change in four factors for TCTC in PuTh fuel at 2375mm	50
Figure 24: TCTC for the PuTh fuel at various heights.....	51
Figure 25: MTC for the three fuel types at 2375mm	52
Figure 26: Change in four factors for PuTh fuel at 2375mm	53
Figure 27: MTC at various heights for PuTh fuel.....	54
Figure 28: FTC for three fuel types at 2375mm	55
Figure 29: Change in four factors for PuTh fuel at 2375mm	55
Figure 30: Change in four factors for UO ₂ fuel at 2375mm	56
Figure 31: IAEA ENDF (n,f) cross section data for Th232 and U238 nuclides	57
Figure 32: Comparison of Multiplication Factors to Sharpe et al. Benchmark.....	58
Figure 33: Comparison of CVRs to Sharpe et al. Benchmark.....	60

List of Tables

Table 1: Specifications for the 64-Element Fuel Assembly and Channel (8)	9
Table 2: Results of meshing optimization search. Case 0 has an overly fine mesh to establish a reference case, with the later meshes being increasingly coarser while attempting to retain accuracy.	29
Table 3: Comparison of four factors and multiplication factor to Moghrabi paper	61

Chapter 1: Introduction

1.1 Development of Canadian Nuclear Industry

The first Canadian nuclear reactors had a unique set of criteria constrained by the country's post-war manufacturing abilities. As part of the US Manhattan Project, heavy water was being produced in Trail, British Columbia, but there were no domestic uranium enrichment facilities. Canada also lacked the capability to manufacture a large pressure vessel. When designing the first Canadian reactors, these restrictions led to the criteria that a Canadian reactor must contain heavy water to allow for use of natural uranium and that the design would not require a large pressure vessel.

These criteria led Canada through the Generation I prototypes of the ZEEP, NRX, and NRU reactors and the unique Generation II CANDU reactor. The CANDU reactor has experienced a successful lifetime, due to its advantages of online refuelling, utilization of natural uranium, and use of multiple pressure tubes rather than a single pressure vessel. These benefits were largely continued and improved upon in Canada's Generation III and III+ designs, such as the EC6 and ACR-1000 (1).

Looking forward to Generation IV designs, Canada became a founding member of the Generation IV International Forum (GIF). The GIF developed a number of goals that Generation IV reactors should meet such as sustainability, safety and reliability, economics, proliferation resistance, and physical protection. From these goals, six "classes" of reactors were chosen. The reactor designs pursued by various countries were the Very High Temperature Reactor, Sodium-cooled Fast Reactor, Supercritical Water Reactor, Gas Fast Reactor, Lead-cooled Fast Reactor, and Molten Salt Reactor (2). Of these six, Canada chose to focus on the SCWR.

There are a few SCWR designs currently under development by various countries, each of which is fairly distinct in comparison to the others. A major difference in the Canadian SCWR design is the use of pressure tubes rather than

a pressure vessel. This design calls upon the use of circular fuel bundles and a bulk moderator separated from the coolant, analogous to the Generation II and III CANDU designs, but cannot use natural uranium due to reduced lattice pitch compared to other designs, the use of stainless steel structural material, and the use of supercritical light water coolant rather than the heavy water coolant used in CANDU reactors. The temperatures and pressures of the supercritical water prevent online refuelling, as the requirements for a refuelling machine that could withstand the conditions would be prohibitive.

The SCWR is still identifiable as a Canadian reactor design, even without the use of natural uranium or online refuelling, but its departures from the well-known CANDU design present a unique opportunity for the Canadian nuclear industry. Given that the SCWR will require batch refuelling and utilize supercritical light water, the fuel must be enriched well above natural uranium levels. Other countries, such as the United States or France, would likely turn to traditional uranium dioxide (UO_2) or mixed-oxide ($\text{PuO}_2\text{-UO}_2$) fuels due to their experience with those fuels and existing manufacturing capabilities. However, Canada does not have sufficient uranium enrichment facilities to easily utilize enriched UO_2 fuel, and could just as easily build reprocessing facilities to remove plutonium from spent fuel. Therefore, PuTh becomes a more attractive option for the Canadian industry than UO_2 fuels.

1.2 Development of the SCWR

The development of the SCWR core hinged on four major criteria that were chosen to best allow a reactor to meet the safety and economic standards of a Generation IV reactor (2). The criteria are:

1. High burnup (~ 40 MWd/kgHE) (3)
2. Low-negative Coolant Void Reactivity (CVR)
3. Maximum Linear Element Rate (LER) of 40kW/m (4)
4. Maximum Fuel Cladding Temperature of 850° C (5)

One of the earliest concepts for the SCWR was similar to existing CANDU designs. It used a 43-element bundle that was similar to CANFLEX designs (6), and placed these in horizontal fuel channels with the goal of being able to make use of online refuelling. A diagram of this bundle design is shown in Figure 1. With an

average enrichment of 5% of heavy elements across the bundle, it was calculated that a burn-up of 40 MWd/kgHE would be achievable. Given the difficulties that were anticipated with fuelling machines interfacing with 25MPa coolant in the fuel channels, online fuelling was rejected as an option at an early stage of SCWR development. Once online refuelling was abandoned, burn-up of only 30 MWd/kgHE would be achievable, and only with significant grading of the fuel enrichment between the inner and outer rings. This made the ability of the original design to satisfy Coolant Void Reactivity (CVR) and Linear Element Rate (LER) doubtful (2).

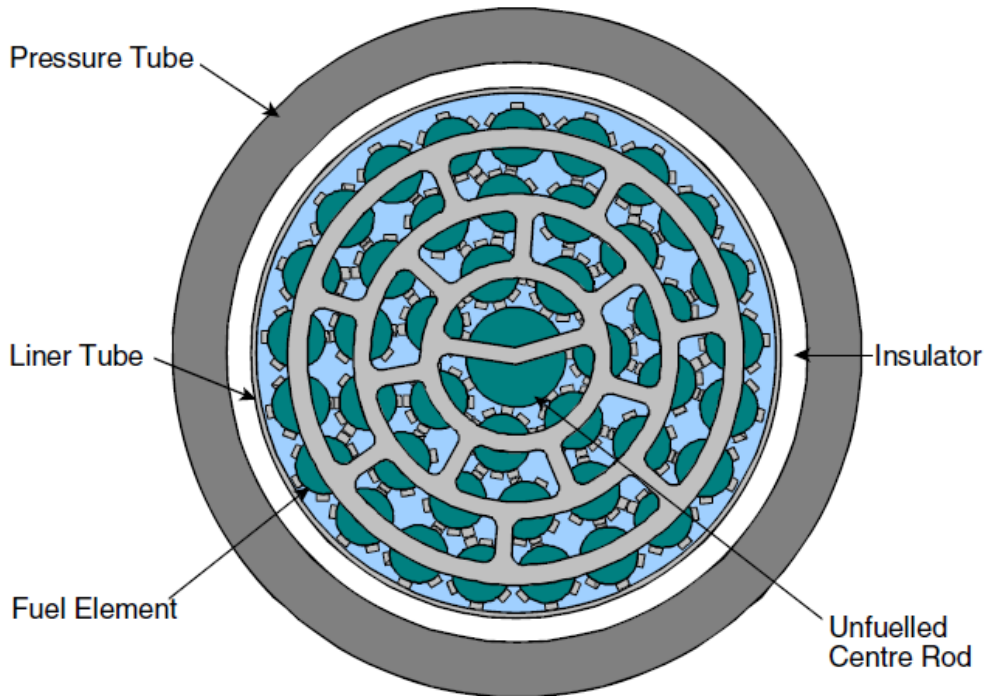


Figure 1: CANFLEX-style 43-element fuel bundle adapted for use in SCWR (2)

A new 54-element, 3-ringed assembly, as shown in Figure 2, was designed to improve upon the initial design. This concept used a vertical pressure tube and no longer allowed for online refuelling. This design did not rely upon graded enrichment, which was expected to lower manufacturing costs and simplify analysis and did not rely on a poison pin in the centre of the fuel. Instead, it used a non-fueled centre tube to ensure that the CVR would remain negative. Although the 54-element design met the burnup requirements, the LER was too high and it had unsatisfactory fuel utilization. Further analysis of the design

revealed that the outer elements had an LER of around 76.8 kW/m, almost double the criterion. It was suspected that due to the non-uniformity of gaps between the fuel, the design would also create an unbalanced flow distribution. This could further exacerbate the significant power differential between the outer and inner fuel pins (2).

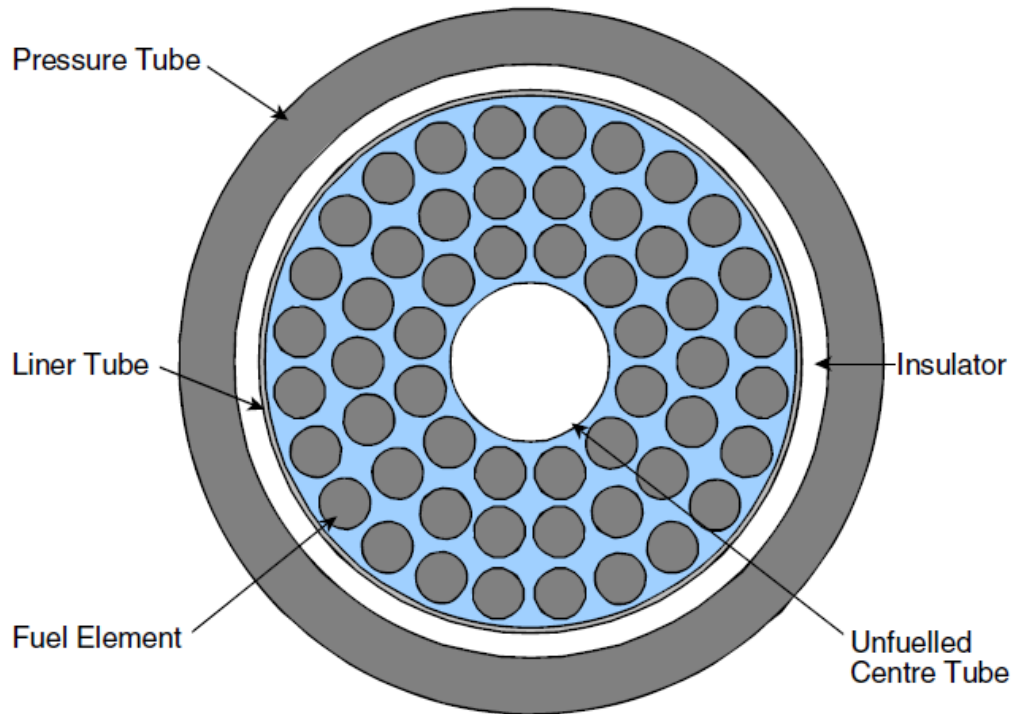


Figure 2: 54-element fuel bundle design for the SCWR (2)

In order to significantly reduce the LER of the outer pins, they were subdivided from 27 to 42 pins, each with a smaller diameter. This 78-element design, shown in Figure 3, met the burnup and LER criteria, but worsened both the CVR and fuel utilization. Subsequent analyses revealed that the clad temperature of the outer ring would greatly exceed the criterion of 850° C. By varying the enrichment of fuel pins in the bundle, both the LER and clad temperature could be reduced at the cost of burnup and fuel utilization (2).

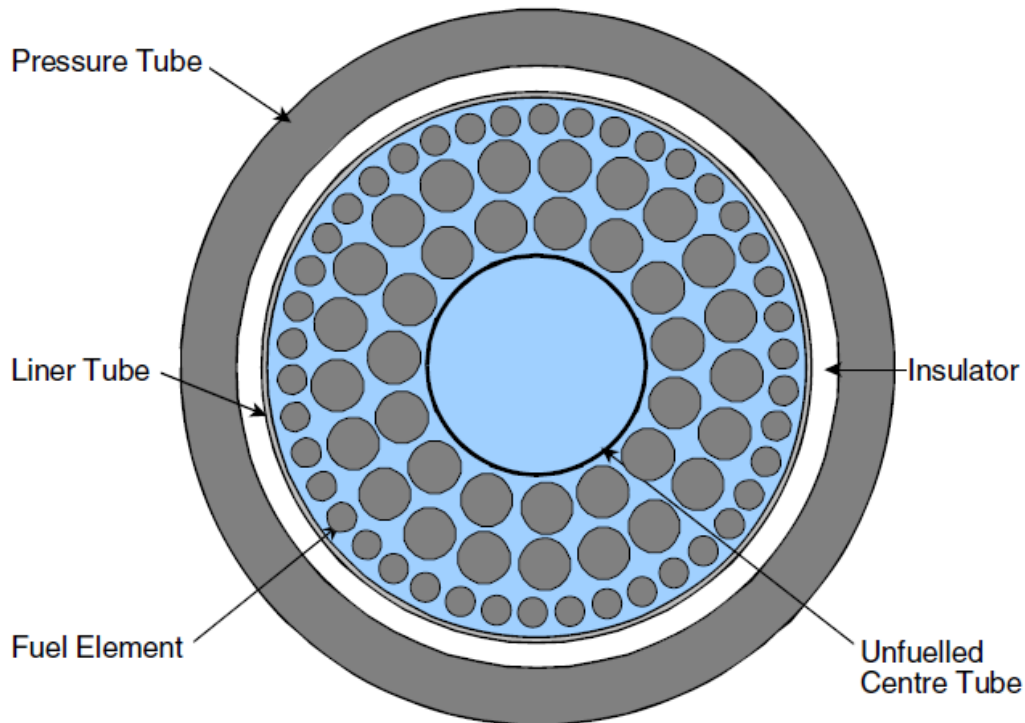


Figure 3: 78-element fuel bundle design for the SCWR (2)

From the three-ringed fuel designs, a number of lessons were learned. The chief lesson was that the designs created a significant disparity between the inner and outer fuel pins in regard to power production, LER, and clad temperatures. Second, due to the difficulty in meeting the four major criteria through design (primarily the high temperatures needed to achieve high cycle thermal efficiencies), fine-tuning of thermalhydraulic properties would be very restricted. The third, and possibly most important lesson, was that the non-fuelled centre tube offered significant neutronic benefit. Not only does having a large volume of coolant in the centre of the bundle help to ensure a negative CVR, it also increases moderation in the inner fuel elements. This contributes to higher power generation in the centre of the bundle that flattens the power, LER, and clad temperature across the bundle (2). An additional constraint was then identified – that a large number of feeders was undesirable at the bottom of the core – since any rupture of a feeder under the core would impede core refill in the event of an accident. Therefore, future work focused on re-entrant fuel designs in which lower feeder pipes are eliminated.

To emphasize the effect of the inner coolant channel and decrease the differences between the inner and outer rings, the design was changed to two concentric rings, with fewer fuel pins of smaller diameter than the other designs. This helps both rings of fuel to have similar parameters as well as meet power, LER, and clad temperature criteria. Another significant difference of the two-ring design is the division between the centre coolant area and the fuelled area. In previous designs, the inner and outer coolant flowed in the same direction. However, in the re-entrant design, the flow is bidirectional, with the inner coolant travelling downward through the centre tube then upward through the fuel (2). With an integral double-pass design, lower temperature central coolant enters the central region of the bundle at the location where the outer coolant has the lowest density. This lends significant moderation to the area of fuel that, in most other reactor designs, has the least moderation.

The two-ring design represented a significant improvement on previous proposals. The thermal hydraulic optimization was much more feasible, allowing variation in the gap size, pellet diameter, and other geometry specifications of the fuel pins. With a two-ring design, experimenting with these parameters does not necessarily violate LER, CVR, or maximum cladding temperature considerations and makes fine tuning of parameters much easier (2).

Although several two-ring designs were considered, the 64-element design is the current lead-concept for the SCWR concept. Each ring is made of 32 fuel pins, with the inner ring fuel elements being a slightly smaller diameter than the outer as can be seen in Figure 4. In addition to the thermalhydraulic and neutronic benefits discussed, the 64-element design has the benefit of eighth symmetry on the lattice level. While not necessarily an economic benefit, it makes computation of reactor properties much simpler.

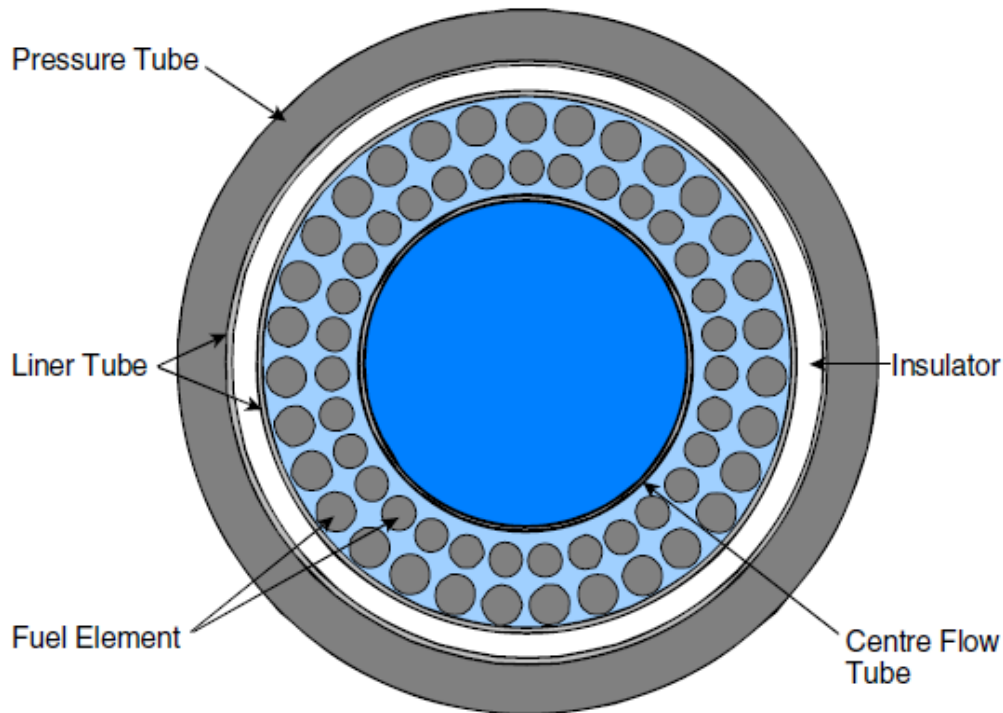


Figure 4: 64-element fuel bundle design for the SCWR (2)

1.3 Current Design

The current SCWR design utilizes a thermodynamically efficient, supercritical-water coolant, a separate, low-pressure, heavy-water moderator (with pressure tubes as boundaries), and a multi-pass core. Although the lattice level fuel bundle design has undergone much iteration, a single design has been widely adopted in the past few years, the 64-element bundle. However, very recent analyses suggest that fuel centre-line temperatures for this design exceed acceptable limits (7). Thus, the reactor geometry will likely need improvements in the future.

The centre of the fuel channel is made up of a central coolant tube. This tube allows cold coolant to flow from the top of the reactor to the bottom where it is redirected upward through the fuel region of the tube. This forms an outer, upward-flowing coolant ring that is concentric with the inner, downward-flowing coolant. The two coolant regions are separated by a thin cylinder of stainless steel. The outward coolant flows past two concentric rings, each comprised of 32

fuel pins. This design avoids the need for complex inlet and outlet headers and feeder pipe networks like those required by the pressure tubes in a CANDU reactor (8). An illustration of this is presented in Figure 5.

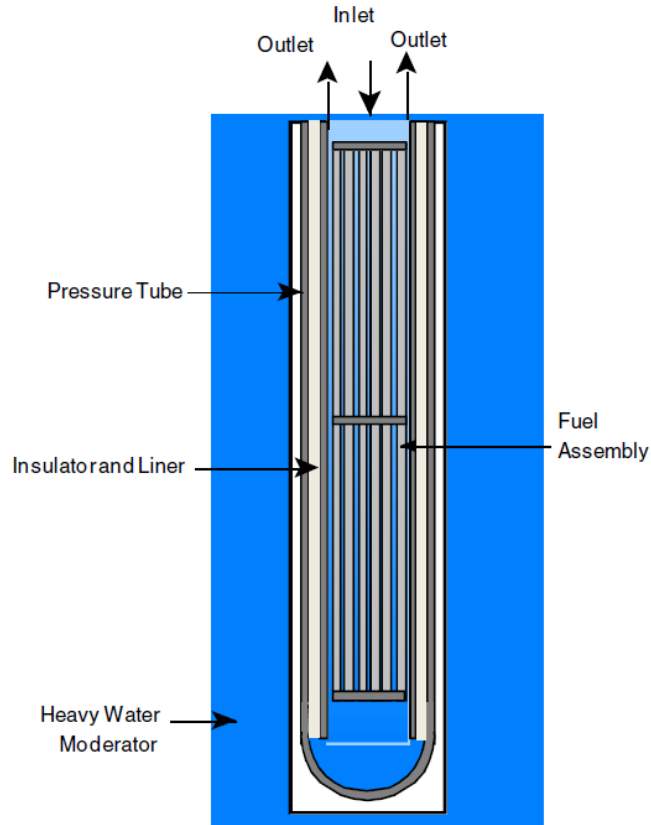


Figure 5: Current pressure tube and fuel bundle design for the SCWR (2)

The outer coolant channel is bound by an inner liner of stainless steel, a zirconia insulator, and an outer liner made of a zirconium alloy. Although the exact materials for the SCWR have not been finalized, the materials listed here are a reasonable approximation for this stage of the design. Unlike Generation II and III reactors, the temperatures and pressures associated with an SCWR design do not allow traditional zircalloy materials to be used. Instead, for areas that may be contacted by supercritical water, a zirconium modified stainless steel is used. This has the advantage of being more robust in the SCWR environment at the cost of reducing the neutron economy. Therefore, for areas that do not contact supercritical water, such as the outer liner and the pressure tube, zirconium alloys are used.

As shown in Figure 6, the outside of the pressure tube is surrounded by a heavy water moderator that has the added benefit of acting as a significant heat sink in the event of an accident, similar to CANDU reactors. The heavy water adds significant moderation to the cell, allowing the overall enrichment of the fuel to be much lower than it would otherwise need to be. The bulk of the volume of the reactor is moderator, with the pitch being close to twice the diameter of the pressure tubes.

The fuel is made of two concentric rings of 32 fuel elements, for a total of 64 elements. The inner ring of fuel has a smaller diameter than the outer ring, although the gap and cladding width are the same. The current fuel design is a Plutonium-Oxide and Thorium-Oxide mixture (PuTh), with the inner ring enriched to approximately 12 wt% PuO₂, and the outer ring enriched to approximately 15 wt% ThO₂. The remainder of the fuel pellet is filled with natural ThO₂ (8). The remainder of the compositions of materials used in the SCWR core can be found in Table 1.

Table 1: Specifications for the 64-Element Fuel Assembly and Channel (8)

Component	Dimension	Material	Composition (wt%)	Density (g/cm ³)
Central Coolant (inside flow tube)	3.60 cm radius	Light Water	100% H ₂ O	Variable
Flow Tube Inner Cladding	3.60 cm radius (IR), 0.05 cm thick	Zr-modified 310 Stainless Steel (Zr-mod SS)	C:0.034; Si:0.51; Mn:0.74; P:0.016; S:0.0020; Ni:20.82; Cr:25.04; e:51.738; Mo:0.51; Zr:0.59	7.90
Flow Tube	3.65 cm IR, 1.00 cm thick	Zirconium Hydride	Zr:98.26; H:1.74	5.64

Flow Tube Outer Cladding	4.65 cm IR, 0.05 cm thick	Zr-mod SS	As above	7.90
Inner Pins (32)	0.415 cm radius 5.4 cm pitch no displacement angle	15 wt% PuO ₂ /ThO ₂	Pu:13.23; Th:74.70; O:12.07	9.91
Outer Pins (32)	0.440 cm radius 6.575 cm pitch no displacement angle	12 wt% PuO ₂ /ThO ₂	Pu:10.59; Th:77.34; O:12.08	9.87
Cladding	0.06 cm thick	Zr-mod SS	As above	7.90
Coolant	n/a	Light Water	100% H ₂ O	variable
Liner Tube	7.20 cm IR 0.05 cm thick	Zr-mod SS	As above	7.90
Insulator	7.25 cm IR 0.55 cm thick	Zirconia (ZrO ₂)	Zr:66.63; Y:7.87; O:25.5	5.83
Outer Liner	7.80 cm IR 0.05 cm thick	Excel (Zirconium Alloy)	Sn:3.5; Mo:0.8; Nb:0.8; Zr:94.9	6.52
Pressure Tube	7.85 cm IR 1.2 cm thick	Excel (Zirconium Alloy)	As above	6.52
Moderator	25 cm square lattice pitch	D ₂ O	99.833 D ₂ O; 0.167 H ₂ O	Variable (1.0851 nominal)
Plutonium Enrichment	N/A	Pu	Pu-238:2.75; Pu-239:51.96; Pu-240:22.96; Pu-241:15.23; Pu-242:7.10	N/A

The control system design for the SCWR has not been finalized. The use of control blades – similar to a boiling water reactor (BWR) – that travels through the moderator, outside of the pressure tube is one option under consideration. The use of burnable poison in the fuel bundle such as gadolinium, used in a number of other reactor designs, is also under consideration (3) (7) (9).

The SCWR is not at the stage of design for active shutdown systems, although it is likely it would have features similar to Generation III+ and other Generation IV reactors, such as fast-acting control rods and a boron injection system. Because it is a design goal of Generation IV reactors to be inherently safe, many passive safety considerations were established early in the design of the reactor.

The first major passive safety consideration is the reactor vessel having no penetrations below the top of the fuel. This is possible due to the double-pass pressure tube allowing for both inlet and outlet piping being located at the top of the vessel. Because of this, there is a high probability that any primary loop coolant lost during an accident will end up in the reactor vessel.

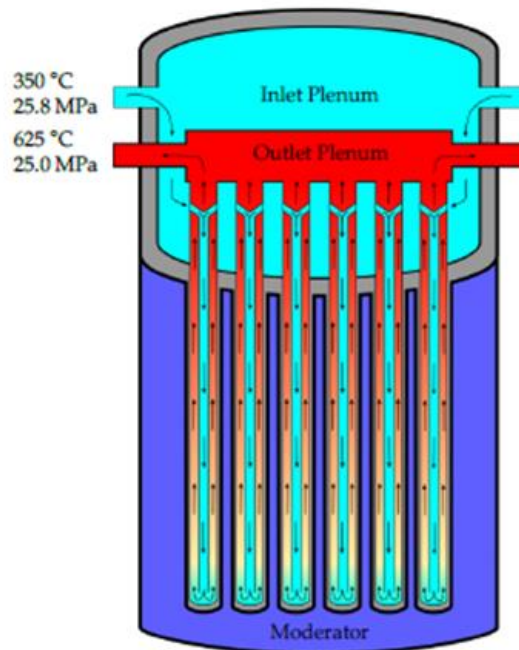


Figure 6: Simplified diagram of SCWR reactor vessel and internals (10)

Additionally, the large mass of moderator acts as an excellent emergency heat sink. If the fuel were to become uncovered, heat would radiate to the pressure tube and be removed through the moderator. The moderator is then able to naturally circulate through an isolation condenser and be removed to the environment.

These passive safety features are intended to meet the “no core melt” design objective of Generation IV reactors. It is hoped that they will prevent situations that lead to core damage, such as the Three Mile Island and Fukushima accidents (10).

1.4 SCWR Fuel

While the design of the fuel geometry has changed greatly since the first proposal, the fuel composition has not undergone as much iteration. Initially, it was intended that the reactor could use natural uranium like the Generation II CANDU reactors, but this quickly became impossible. With the elimination of natural uranium from consideration, many other fuel options were examined (11). The current forerunner is a mix of Plutonium Oxide and Thorium Oxide that was first proposed alongside the first fuel bundle, the CANFLEX analogue (2). Although this fuel choice may have been re-evaluated along the way, no formal, published documentation was found. Therefore, it is valuable to re-evaluate the choice of PuTh fuels and their performance in the SCWR.

The main advantage of Plutonium-Thorium fuels is the use of thorium. Thorium is about three times more abundant than uranium, making it a more sustainable choice. Thorium 232 also breeds more fissile material in the SCWR than Uranium 238, resulting in higher reactivity at high burnups. Reactor grade plutonium is also an attractive driver fuel source as it can be sourced from spent light water reactor (LWR) fuel.

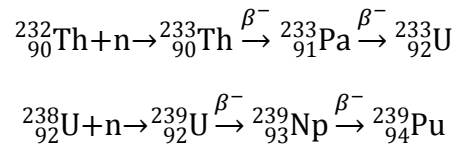
Although the general advantages of Plutonium-Thorium fuels seem to make it an attractive option for the SCWR, it is also important to consider its neutronic behaviour. Comparisons dealing with utilization in other reactors (including CANDU, LWR, and other SCWR designs) may not be adequate for the SCWR design (12) (13) (14). The SCWR has some significant neutronic differences from other reactor designs, mainly the centre coolant channel that acts as a second

moderator. This makes the moderation for the SCWR a mix of heavy water and light water. Along with the materials, temperature, pressures, and geometry of the SCWR, the neutronic behaviour of the reactor is distinct and warrants individual analysis before a consensus can be reached.

Chapter 2: Theory

2.1 Nuclides of Interest

In reactor physics, nuclides of interest are split into three categories: fissionable, fissile, and fertile. Nearly all nuclides useful for nuclear reactions that can be found in nuclear fuel fall into one of these categories. The first, fissionable, refers to nuclides that have the ability to fission when they absorb a neutron. The second category is fissile nuclides. These are a subset of the fissionable nuclides with the distinction that, when fissioned, produce enough neutrons of appropriate energy to sustain a nuclear chain reaction. In general, actinide nuclides with an odd number of neutrons are fissile. The most common fissile nuclides used in nuclear reactors are ^{233}U , ^{235}U , ^{239}Pu , and ^{241}Pu . The final category of distinction for nuclear physics is fertile nuclides. These are nuclides that, when a neutron is absorbed, are either directly fissionable or eventually decay into fissionable nuclides. Some important fertile nuclides are ^{232}Th , which produces ^{233}U , ^{238}U , which produces ^{239}Pu , and the plutonium nuclides with even neutron numbers (non-fissile), which generally produce plutonium nuclides with odd neutron numbers (fissile). The transmutation chains of ^{232}Th and ^{238}U are below:



Nuclear Power reactors require a fissile fuel to sustain nuclear chain reactions. In the majority of existing reactors, this fissile nuclide is uranium-235. ^{235}U makes up 0.7% of natural uranium, with almost all of the remainder being ^{238}U . ^{235}U is much more readily fissionable than ^{238}U . Therefore, the majority of power reactors use uranium fuel that has been enriched to contain 3-5% ^{235}U . A notable exception to this is the CANDU, which utilizes natural uranium, with the trade-off being the requirement of using heavy water as a moderator.

2.2 Fuels

In nearly all current uranium-driven reactors, ^{235}U is responsible for the majority of energy production. However, the large amount of fertile ^{238}U leads to significant production of Plutonium-239. ^{239}Pu is fissile and contributes greatly to end-of-life power generation in a uranium-fuelled reactor. The combination of ^{235}U and ^{238}U meshes well, creating a sufficiently fissile fuel at the beginning of the reactor cycle that replenishes some of its reactivity due to the conversion of some ^{238}U to ^{239}Pu , prolonging the time that the reactor can produce power. This relationship is not limited to uranium fuels; it can also be achieved by mixing other fissile and fertile nuclides. A common alternative is mixing plutonium oxide fuel with natural uranium oxide, known as mixed oxide fuel (MOX). This fuel primarily uses ^{239}Pu to initiate the fission reaction, and relies on fertile ^{238}U producing additional ^{239}Pu to elongate the lifetime of the fuel.

Although both of these fuels convert ^{238}U to ^{239}Pu , other fertile nuclides can be used. An interesting option is ^{232}Th , which produces ^{233}U . Thorium fuel's increasing popularity comes primarily from its higher abundance, more manageable waste, and relative ease of reprocessing (15). Thorium is not fissile, so it is commonly mixed with uranium or plutonium fuels to initiate the production of fissile isotopes. However, depending on the isotope with which the thorium is mixed, some of these benefits may be lost.

Existing operators of power reactors do not often have the opportunity to radically change the fuel that they use. Often, the effort required to evaluate the safety and performance of a new fuel composition outweighs potential benefits of utilizing that fuel. Some options currently being explored in the Canadian nuclear industry include the use of NEU, RU, and low-CVR fuels for CANDU reactors (1). These seek to gain performance increases by changing the initial enrichment of fuel, recycling used fuel, or improving the safety margins by adding various nuclides. However, when designing an entirely new reactor, other fuel types may be considered. This allowed the groups responsible for designing the SCWR to choose a PuTh fuel, rather than the more traditional UO₂ or MOX fuel.

A PuTh fuel type was chosen due its general benefits over traditional uranium fuels. Plutonium can be sourced from reprocessed fuel or nuclear weapons,

making it economical and contributing to non-proliferation of nuclear weapons. Thorium is also much more abundant than uranium, which could potentially make it cheaper and an option that will be available for centuries longer.

These advantages are shared for all thermal reactors that would choose a PuTh fuel cycle, but specifics of a reactor type have not been considered. A reactor's fuel composition has a great influence on the reactor's performance and behaviour when exposed to transients. It is important to not only consider the general advantages, but also the performance of a fuel in an operating reactor. Because a SCWR reactor has never been constructed and there is little operating experience with PuTh fuels in power reactors, this fuel type is less well-understood than a traditional uranium fuel.

In this work, the proposed PuTh fuel will be compared to a traditional, enriched uranium fuel, as well as a MOX fuel. Similar to the PuTh fuel, the fission reaction in the MOX fuel is primarily driven by Plutonium nuclides. However, the production of new fuel is primarily from ^{238}U , similar to an enriched uranium fuel. These three fuel types give us a good breadth of data to consider their behaviour.

2.3 Multiplication Factor

One of the most fundamental units for comparison of nuclear systems is the multiplication factor (k). This unit is the average number of neutrons from a fission reaction that cause an additional fission.

There are three main realms of criticality in which all nuclear reactions occur. The first is subcriticality, in which $k < 1$. In a system that is subcritical, the nuclear chain reaction cannot be sustained and will eventually die out. For each fission in this system, an average total of $1/(1-k)$ fissions occur.

The second realm is criticality; $k = 1$ and thus each fission causes, on average, one fission. This is a stable state and therefore the realm in which reactors operate.

The final area is supercriticality, in which $k > 1$. This is where each fission causes, on average, k more fissions, leading to exponential growth in the number of fission reactions. This region is subdivided into prompt and delayed

supercriticality. Prompt supercriticality ($k > 1/(1 - \beta)$) is the region in which the nuclear chain reaction is sustained entirely by neutrons created directly from fissions.

Power reactors are generally within the critical range, but occasionally stray a small amount into subcriticality or supercriticality to change power levels. The multiplication factor is conceptually simple, but can actually be quite difficult to calculate as neutrons cannot easily be individually counted, and the path a neutron takes from fission to fission is not consistent or easily traceable. One of the most common ways to examine the multiplication factor of a reactor is through the Four Factor Formula:

$$k = \eta f p \epsilon$$

The first factor is the reproduction factor (η) that is equivalent to the ratio of neutrons produced from fission to neutrons absorbed in the fuel. The thermal utilization factor (f) is the ratio of neutrons that are absorbed in the fuel to neutrons that are absorbed in any material. The resonance escape probability (p) is the fraction of fission neutrons that are able to slow to thermal energies without being absorbed in resonances. The final factor is the fast fission factor (ϵ). This is the ratio of the number of fission neutrons of all energies to the number of fission neutrons from only thermal fissions. Additional terms can also be included that account for leakage in the fast and thermal portions of the neutron spectra.

2.4 Coefficients of Reactivity

The most fundamental criteria for evaluating performance of a specific fuel in a reactor are the fuel's coefficients of reactivity. These coefficients are usually presented as the Fuel, Coolant, and Moderator Temperature Coefficients (FTC, CTC, and MTC respectively) and the Coolant Void Reactivity Coefficient (CVR). The Power Coefficient of Reactivity (PCR) is also very commonly studied, and in many cases can be more useful than the other coefficients of reactivity. However, determining the PCR requires coupling of thermalhydraulic and neutronic codes; a task that is beyond the scope of this work.

The temperature coefficient is the change in neutron multiplication that occurs due to temperature changes and is determined by perturbing the temperature of

a reactor material (fuel coolant or moderator) and calculating the change in reactivity per change in temperature. For example, the fuel temperature would be raised by 100 K, and the resulting change in reactivity would be observed. For the temperature coefficients, the result is expressed as the percent error between the two reactivities in the units of mk/K, according to the following formula:

$$\frac{(k_{\text{original}} - k_{\text{new}})}{k_{\text{original}}} \times \frac{1000}{\Delta T}$$

The coolant density reactivity, or alternatively coolant void reactivity (CVR), corresponds to the change in neutron multiplication caused by density changes in the coolant. CVR is numerically determined by perturbing the coolant void to a near zero value (0.01 g/cm³) and calculating the change in reactivity. Because the initial value of the density is different for various heights in the SCWR core, as well as for the inner and outer coolants, it is difficult to determine a reactivity change per degree of void that would be comparable across all situations. Therefore, a simple change in reactivity is used.

These reactivity coefficients are often used for traditional pressure water reactors (PWR) or BWR reactors, in which the coolant and moderator are the same material. However, in the CANDU and Canadian SCWR, the issue becomes more complex. First, the moderator and coolant of the SCWR are separated and hence separate reactivity coefficients are needed. In the SCWR, the coolant is divided into two regions – an inner region with no fuel and an outer region with fuel – that may have very different properties, especially at the top of the core, where the temperature and density differences are the largest. This requires having three different CTCs and CVRs: one for the inner coolant, one for the outer coolant, and one for both coolants. As we will see, these three coefficients will have different behaviours, and are not strictly additive.

Understanding the reactivity coefficients of a certain fuel in the SCWR can lead to reliable inferences about its behaviour. It would be ideal to couple neutronic and thermal-hydraulic codes in order to simulate transients and also to determine the power coefficient of reactivity. However, this requires considerable effort and was deemed outside the scope of this work. Even so, by knowing the relative strengths of the reactivity coefficients, coupled with a basic

understanding of thermal-hydraulics, we can speculate on the responses of a reactor system to transients.

The cause of variation in a coefficient of reactivity, whether as a function of burnup, fuel type, or location in the bundle, can often be better understood by examining the impact on each of the components of the four-factor formula. For example, an increase in coolant temperature in fuels containing plutonium most affects the thermal utilization factor that relies on two fundamental parameters, the macroscopic cross-section of absorption in the fuel and the macroscopic cross-section of absorption everywhere in the lattice cell. Because the increase in coolant temperature causes a corresponding increase in this factor, we can assume that there is either an increase in the macroscopic cross-section of absorption in the fuel, or a decrease elsewhere.

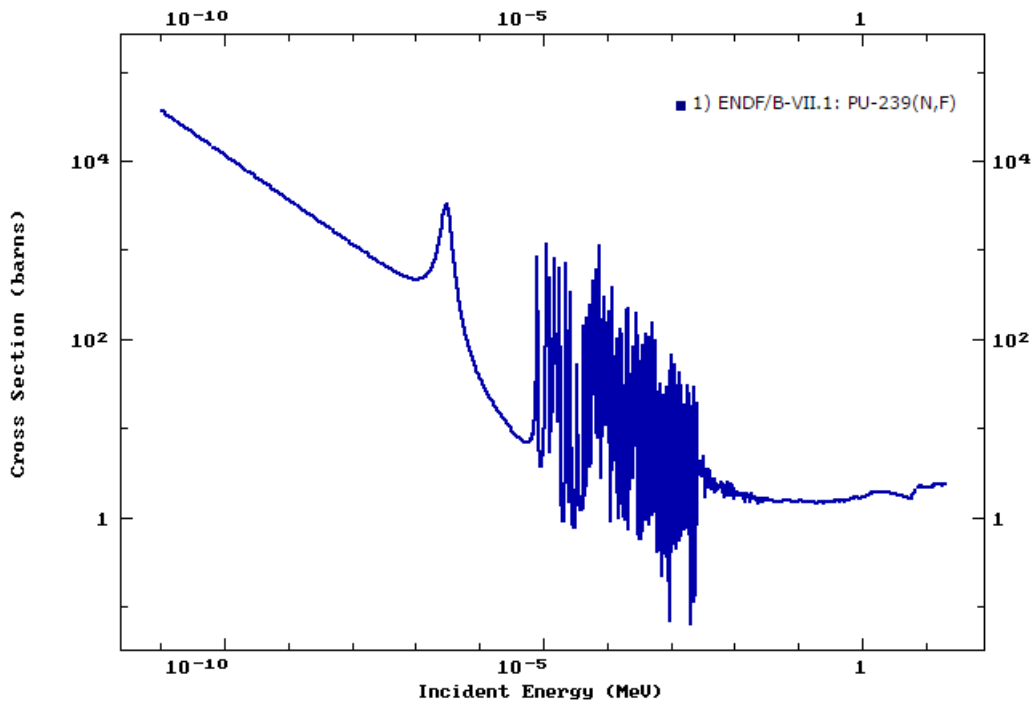


Figure 7: IAEA ENDF (n,f) cross section data for the Pu239 nuclide, showing the 0.3eV peak

By investigating the cross sections of materials in the lattice cell, we can theorize that the increase in the thermal utilization factor, and therefore the multiplication factor, is caused by a 0.3eV absorption peak in Plutonium that can be seen in Figure 7. Due to the higher temperature of the coolant, upscattering,

as well as decreased moderation, would cause more absorption in this peak, resulting in a higher ratio of absorption in the fuel. Since SCALE considers all energies below 0.625eV to be thermal, this would result in an increase in the thermal utilization factor.

2.5 Path of a Neutron

To understand the effects of changing the temperature or density of a material, it can be helpful to review the path a neutron takes from emission to absorption in the reactor. For the SCWR, this lifecycle usually involves the fuel, inner and outer coolants, and moderator. Everything else in the reactor can generally be treated as transparent, or at the very least, considered as a collective loss term.

A significant majority of neutrons are born as a result of fissions, though a small percentage – the delayed neutron fraction (β) – are created from the beta decays of fission products. These neutrons then travel out of the fuel, into the inner coolant, outer coolant, or moderator, where they see their first interactions. The majority of the interactions that occur during a neutron's lifetime will be in these coolant or moderator regions, where they are slowed from their fission energies (>0.5 MeV) to near thermal energies (<0.625 eV).

Thermal neutrons correspond to temperatures of about 290 K. Such a low temperature is only achievable through scattering reactions in the moderator. The coolant temperature is about 300 K hotter at its lowest, so neutrons moderated by the coolant would have significantly higher energies. Neutrons that are able to achieve energies corresponding to the moderator temperature frequently up-scatter to higher energies in the outer coolant before being absorbed in the fuel. Hence there is continuous up-scatter in energy caused by the coolant temperature being greater than the moderator temperature.

Once a neutron returns to the fuel, it will be absorbed in a fissile or fertile nuclide, or within a poison. This is determined by the macroscopic cross sections of each nuclide. A thermal neutron is much more likely to cause fission in a fissile nuclide than is a fast neutron. Similarly, fast neutrons are likely to be absorbed by all nuclides, but because the majority of the nuclides are non-fissile materials (^{232}Th , ^{238}U , etc.), most of the absorptions occur in these nuclides.

2.6 Dancoff Factors

An assumption that is regularly made when solving the transport equation is that neutrons that leave fuel do not have their first subsequent interaction in fuel. This is clearly not the case when fuel pins are separated only by a small portion of coolant. To correct for this, rod shadowing effects are considered to develop a modified collision probability for many lattice-level neutron codes. This is heavily dependent on the Dancoff factor that is determined by fuel geometry and cross sections. The modified collision probability is also highly correlated with the coolant density. If the coolant is less dense, there is an increased probability that the next interaction will not be in the coolant. The SCWR reactor, particularly in the upper portions of the channel, has extremely low coolant densities at normal operating conditions. These densities have a huge influence on the Dancoff factor and its implementation, and must be treated very cautiously. The treatment in this thesis is outlined in the Methodology: Dancoff Factors Section.

Chapter 3: Literature Review

3.1 Work on Early Designs

Much of the early work on the SCWR focused on its feasibility. Typically, a fuel bundle or channel design is proposed and subsequently evaluated to determine if it meets the four major requirements of a Generation IV reactor. Among these, the burn-up, CVR, and linear element rating appear to have received the most attention from researchers. For instance, an early paper by Boczar et al. discusses the relationship between burn-up and CVR (16).

In this work, the bundle being considered was the 54-element bundle, with a significantly large zirconium centre pin. Boczar et al. found that while the CVR could be improved, it came at the cost of decreased burn-up. That paper also assumed that continuous refueling similar to that of a CANDU reactor was feasible, resulting in burn-ups of the order of 40 MWd/kgHE. Subsequent studies found that for a similar bundle in batch fuelled reactor, a burn-up of only 30 MWd/kgHE would be feasible (17).

Although the Boczar et al. considered the PuTh fuel type, their contemporaries explored other fuel variations. Magill and colleagues, inspired by the use of the thorium fuel cycle in CANDU reactors, considered various thorium based fuels, including the PuTh fuel type (18). That study evaluated the performance of the fuels primarily on initial enrichments, ^{233}U recycling, and exit burn-up. A similar work from McDonald explored the performance of a more traditional UO_2 fuel (19), rather than the PuTh cycle, which was recently adopted at the time.

Subsequent studies refined the calculation of neutronic properties for the SCWR, but retained the use of the non-re-entrant fuel bundle. Harrisson and Marleau initially posited that, due to the large changes in temperature and density along the height of the SCWR, a calculation intensive 3D model may be required. However, they later demonstrated that a series of isolated 2D calculations followed by a 1D simulation could adequately replace a 3D model (20). This significantly reduced the effort required to evaluate the SCWR in subsequent works.

3.2 Work on the 64-Element Design

Following the initial SCWR designs, a paper by Pencer et al. introduced the re-entrant fuel bundle by replacing the centre zirconium pin with coolant (21). This improved the reactor performance on multiple criteria, primarily CVR and burnup. The 64-element re-entrant bundle outlined by Pencer et al. became the standard for the SCWR and is used in the majority of subsequent works. The burnup was improved by around 40%, and a negative CVR was achieved for the lifetime of the fuel. In a subsequent work discussing the progression of the SCWR design, Pencer stated that during some transients, the coolant density could increase, hinting at some of the difficulties with the SCWR design (17).

Works using the 64-element design were able to further refine the evaluation of the SCWR. A benchmark performed by Sharpe et al. compares a number of neutronic properties of the SCWR as calculated by DRAGON, TRITON, MCNP6, KENO V.a, and KENO-VI. (22). That benchmark showed that there is agreement for multiplication factors, CVRs, FTC, and power ratios, for both cold and hot zero powers over burnup between the evaluated codes. It also cautions that appropriate meshings, burn-up steps, and other parameters must be used to obtain an accurate evaluation, regardless of choice of code. The recommendations of the authors of the Sharpe et al. benchmark were followed during the creation of this work.

Concurrent with the present work, works by Moghrabi and Novog explore the variation of the reactivity coefficients in PuTh fuel for fresh and burnt fuel, with particular emphasis placed on the sensitivities of particular cross sections of nuclides (23) (24). In their 2016 paper, Moghrabi and Novog found that the relatively small lattice pitch of the SCWR leads to a hardened neutron spectrum, resulting in heightened sensitivity of the resonance escape probability and fast fission factor. This is also the source of an increased importance in up-scattering, due to the 0.3eV absorption cross section peaks found in plutonium isotopes. An additional finding was that, in the specific condition where the outer coolant of the SCWR is voided, the reactivity increases. This is usually counteracted by the overwhelmingly negative void reactivity of the central coolant channel, but is a potential source of positive feedback.

In Moghrabi and Novog's 2017 work, similar evaluations were performed with burnt fuel and the findings were largely similar. New findings included the importance of xenon, ^{233}U , and plutonium cross sections at high burnups, the reproduction rate being the primary influence of changes in reactivity over burn-up and reactivity coefficients over burn-up.

Works by Hummel and Novog discussed a full-core couple model, with fuel bundles at different stages of burnup (25) (10). In those works, Hummel and Novog found that the CVR is generally negative, but in specific scenarios can be made positive resulting in possible power excursions. Even with a positive power excursion, all transients evaluated were self-terminating. It is likely that these excursions could be controlled by a fast-acting shutdown system similar to CANDU designs.

3.3 Variations on the 64-Element Design

A paper by Colton and Pencer described a method to improve CVR control, and thus improve transient response, via the insertion of a solid moderator in the inner coolant channel (26). This would allow finer control of the CVR based on the displacement of the coolant in the central flow tube by a zirconium hydride rod. Although this would improve the CVR of the SCWR, it comes with some drawbacks: the exit burnup would be reduced by the implementation of a solid moderator, there is a potential for hydrogen embrittlement of the solid moderator, and there is the potential for additional hydrogen gas release as a result of increased coolant temperature.

The issue of reactivity control systems was addressed in a paper by Salaun and Novog (7). By combining fuel-integrated burnable absorbers and control blades, improvements on maximum sheath surface temperature (MSST), coolant exit temperatures, and graded enrichments were shown to be possible. However, it was found that some criteria, primarily the MSST, were unable to be held at acceptable levels over the length of the fuelling cycle. Some adjustments were suggested to improve the performance, such as graded burnable poisons and partial length control rods, but it remains difficult to keep the MSST within acceptable levels.

Some of the issues with the SCWR design can be addressed by adding features, such as reactivity control or solid moderators, but it may also be beneficial to reconsider choices made before the adoption of the 64-element re-entrant bundle design. One such choice is the use of PuTh fuel rather than other fuel types, as the fuel has a large influence on the reactor's response to transients, in particular the magnitude of the CVR and its role during transients.

3.4 Analysis of fuels in non-Canadian SCWRs

There are very few studies examining non-PuTh fuels in the 64-element Canadian SCWR design. Therefore, relevant literature comes primarily from evaluations of previous Canadian SCWR designs such as the aforementioned McDonald (19) and Magill (18), or from evaluations of fuels in other reactor designs.

For instance, a comparison was done for the U.S.-SCWR design between PuTh, UO₂, ²³³UTh, and ²³⁵UTh fuels (13). That study found that the rate of reactivity loss for the plutonium fuel was more gradual than that of the uranium fuels. This indicates that for the same initial reactivity, a plutonium-driven fuel would have a longer cycle length than a uranium-driven fuel. However, this study only evaluated fuels with thorium as the breeder. A possible alternative to breeding ²³³U via ²³²Th would be to use ²³⁸U to breed ²³⁹Pu. This is the process that occurs in current Generation II and III reactors. A fuel with ²³⁸U would have a different reactivity profile than the thorium breeder fuels, and possibly a different profile than in non-SCWR reactors due to the differing neutron spectrum.

The moderator temperature coefficient for each fuel varied by less than 0.0015 mk/K from each other over the range of burnup. Only the UO₂ fuel has a noticeable difference in shape, but still remains within the range of the other fuels. For all four fuels, the coolant temperature coefficient has a larger magnitude than the moderator temperature coefficient, as well as having a greater variation along burnup. This seems to indicate that a temperature change in the coolant is more influential than a temperature change in the moderator for this reactor type.

The fuel temperature coefficient as a function of burnup is less influential for all fuels than that of the moderator or coolant. Additionally, the profile of each fuel's temperature coefficient varies wildly over burnup, with no fuel having a

consistently higher magnitude than the other. Though the shape of each fuel is different, the variation between fuel types remains within 0.000005 mk/K for the majority of the fuel's life. This indicates that the difference between one fuel type and the other is most likely negligible with regard to the fuel temperature's effect on reactivity.

The study did not investigate the coolant density coefficient of reactivity directly, but did tangentially through an analysis of the Moderator-to-Fuel Ratio (MFR). The MFR was varied by changing the fuel density rather than by changing the moderator density. Although some information regarding the reactor's behaviour in voided conditions could be inferred through this data, it would likely be inaccurate due to a multitude of factors including the study involving a different geometry, MFR variation due to fuel pellet radius and moderator density not being directly comparable. However, the coolant density coefficient is possibly the most important of the reactivity coefficients for the SCWR design, and must be investigated.

It is also important to note that this study showed positive reactivity coefficients after burnups of approximately 30GWd/t for all three temperature coefficients. For the SCWR, it is an important design goal that all coefficients remain negative throughout the reactor's cycle, so these fuel designs would most likely not be preferred for the future of the SCWR. However, this work did present similar results for the PuTh fuel types to the results of Sharpe et al. (22) and Moghrabi and Novog (23), indicating that its results for the other fuel types may be a good initial reference for the SCWR.

As there is not sufficient literature evaluating the performance of UO₂ or MOX fuel types in the 64-element Canadian SCWR, this thesis seeks to provide a foundation for future work to evaluate fuel types other than PuTh. Regardless of whether there is an immediately obvious benefit to using UO₂ or MOX fuels in the current Canadian SCWR design, it may still be valuable to reconsider a specification that may be limiting the performance of the reactor design, and provide a starting point for future analyses to consider these options more fully.

Chapter 4: Methodology

4.1 Code

To evaluate the lattice cell neutronic behaviour and determine each of the four factors, a neutronic code must be used. This code must be capable of properly evaluating the SCWR geometry, providing cross sections for each material used, and performing calculations for the conditions of the SCWR channel. Although there are many codes that meet these criteria, the SCALE suite was selected, in particular NEWT (New ESC-based Weighting Transport code) (27) and TRITON (28).

NEWT is a transport code that solves complex geometric models and is capable of outputting eigenvalues, critical-buckling corrections, source calculations, and can prepare collapsed weighted cross sections in AMPX format. It can also be combined with TRITON to perform 2D depletion calculations. NEWT and TRITON were developed at Oak Ridge National Laboratory as part of the SCALE suite (29). This makes NEWT well-suited to the topics of this thesis, as it allows for a multitude of cases with varying materials and burn-ups to be evaluated.

NEWT was used to evaluate a 2D lattice “slice” of the SCWR channel. In total, 3 slices were used to allow for vertical variations in temperatures and densities throughout the channel. These slices were located 125mm, 2375mm, and 4875mm from the bottom of the channel. The individual parameters for each slice are outlined in Table 1 (8). Cross sections used in the calculations were obtained from the 238-group ENDF/B-VII library.

TRITON was used to model the initial lattice cell and simulate the compositional changes in the fuel throughout its lifetime. The anticipated cycle length of the SCWR is 470 days with three-batch refueling, so the fuel was burnt for 1415 days. Because the bundles are expected to operate at 47.28 MW/ kg, this corresponds to approximately 67 GWD/MTIHM (Mega-Ton Initial Heavy Metal). Compositional snapshots were taken every day for the first ten days, then every ten days until the 1415th day.

4.2 Meshing

In order to solve the neutron transport equation, NEWT subdivides the geometry into sections. This is done primarily through the interfaces between materials (with each material being a separate area), but homogenous regions can further be subdivided. This subdivision is referred to as the meshing of the cell.

Even with identical geometries, variations in meshing can cause differences in k_{inf} on the order of tens of milli- k . While an extremely fine mesh may be more accurate than a coarse mesh, coarser meshing is often used as a compromise to reduce computation time.

To ensure that the meshing does not introduce bias, a meshing scheme can be used that has a similar k_{eff} to an accurate reference case. For this work, the reference case was a NEWT model of the same geometry with the finest subdivisions reasonably possible. This very fine meshing was used as an accurate reference case that was compared with coarse meshing schemes. By varying the meshing options on the cell, the mesh features that are most critical to accuracy and computation time can be determined. Using the accurate reference case, individual meshing options were varied to find the individual influence of each variable. For instance, the concentric subdivisions in the inner-coolant channel were varied from a maximum of 44 rings, to a minimum of 0 rings, with the final meshing using 22 rings.

In total, close to 7 meshing options were varied to determine each part's influence on the time and accuracy of the solution. Then, by combining elements of individual variations that showed promise of retaining accuracy while significantly decreasing time, several major meshing options were tested. To ensure that the accuracy of a meshing scheme wasn't a result of a few large errors with cancelling magnitudes, the schemes were run for conditions found elsewhere in the core. The method with the best accuracy/time trade-off over all core conditions was selected.

Table 2: Results of meshing optimization search. Case 0 has an overly fine mesh to establish a reference case, with the later meshes being increasingly coarser while attempting to retain accuracy.

Case Number	Symmetry	Rect. Lattice Grid divisions	Rect. Fuel Pin Grid divisions	Number of Sides in Circular Elements	Number of Rings in Fuel Pin	Number of Rings in Inner Coolant	Number of Rings in Outer Coolant	Reactivity change (mk)	Multiplication Factor (k_{inf})	Number of Iterations	Runtime
0	1/1	25x25	10x10	120	1	0	0	0.000	1.2908	435	14990
1	1/8	25x25	10x10	120	1	0	0	0.690	1.2920	48	487
2	1/1	4x4	10x10	120	1	0	0	0.936	1.2924	308	9868
3	1/1	25x25	2x2	120	1	0	0	0.181	1.2911	284	9896
4	1/1	25x25	10x10	12	1	0	0	0.236	1.2912	321	10623
5	1/1	25x25	10x10	120	0	0	0	9.716	1.3072	386	12765
6	1/1	25x25	10x10	120	1	22	0	0.295	1.2903	501	16547
7	1/1	25x25	10x10	120	1	0	25	0.000	1.2908	454	14990
8	1/8	25x25	2x2	120	1	22	25	0.507	1.2900	58	526
9	1/8	10x10	2x2	120	1	22	25	0.917	1.2893	35	554
10	1/8	25x25	2x2	12	1	22	25	0.250	1.2904	25	223
11	1/8	25x25	2x2	12	1	11	13	0.180	1.2911	18	178
12	1/8	25x25	2x2	12	1	6	7	0.594	1.2918	15	149
13	1/8	25x25	2x2	12	1	6	13	0.493	1.2917	18	180
14	1/8	25x25	2x2	12	1	11	7	0.280	1.2913	14	143
15	1/8	25x25	2x2	12	1	22	7	0.058	1.2907	16	142
16	1/8	25x25	2x2	12	1	44	7	0.227	1.2905	19	168
17	1/8	25x25	2x2	12	1	22	0	0.121	1.2910	11	102
18	1/8	25x25	2x2	12	1	22	6*	0.005	1.2908	16	140
19	1/8	25x25	2x2	36	1	22	6*	0.244	1.2904	20	183
20	1/8	25x25	1x1	12	1	22	6*	0.041	1.2908	14	126
21	1/8	25x25	2x2	12	1	22	6*	0.152	1.2906	16	147
22	1/8	25x25	1x1	12	1	22	4**	0.079	1.2910	12	109

(*) – Four of the six outer coolant rings are tangential to fuel pins, with the other two rings bisecting the fuel pins

(**) – Four rings in the outer coolant, each tangential to the fuel pins

Although the numbers that were settled upon for this meshing may not be the most optimal, exploring every variation would take hundreds of thousands of hours of computation time, so a simplified approach such as this is appropriate. The original reference case took a total of 14990 seconds to run. The final meshing scheme took only 140 seconds, and had less than a thousandth of a percent error in the multiplication factor over various core conditions. The results of this search can be seen in Table 2 and the chosen meshing scheme, case 18, can be seen in Figure 8.

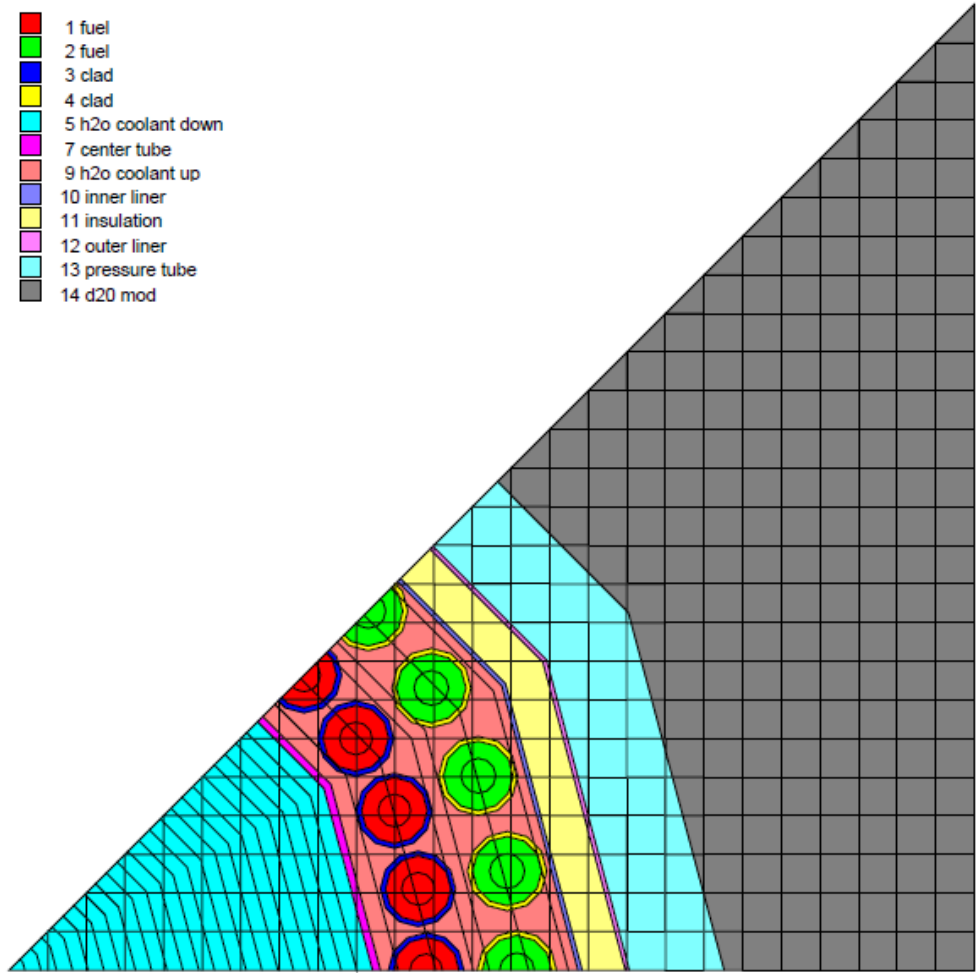


Figure 8: Final meshing scheme for SCWR geometry, as displayed by NEWT’s graphical output

4.3 Depletion Time Steps

The time between subsequent burnup steps in TRITON can have a large effect on the resultant outputs given that each future instance of time depends on the isotopic makeup of the fuel at each previous time step. In TRITON, fuel depletion is performed over a discrete time interval assuming that the flux spectrum and fuel composition is invariant over this small discrete time step. Strictly speaking, this is only true for very small time steps. Thus, taking a large numeric time step during intervals in which there are high isotopic changes is incorrect, since numeric errors related to large time steps are magnified at future time steps. This is particularly important in the first few days of burnup, as errors there can compound significantly. In this project, single-day time steps were used for the first ten days and the remainder was burnt using ten-day time steps.

This approach was chosen arbitrarily and not due to an optimization approach similar to that of the meshing. The time steps were picked at small enough increments that there should be no significant error. This was at the expense of runtime. However, since there were only nine cases that required burnup, this was decided to be an acceptable trade off. The time spent fine-tuning the time-steps would not have been well-invested, as TRITON was run hundreds of times less frequently than NEWT. When compared to the multiplication factor given in a benchmark by Sharpe et al. (22), both result in extremely similar values even though the benchmark used much smaller time steps. This indicates that time steps of this scale are adequate.

TRITON reports fuel composition at the mid-point of a time step rather than the start or end. For example, during the time step from 10-20 days, the fuel composition was reported at 15 days. Therefore, determination of reactivity coefficients was performed at 15 days. Fuel composition changes drastically in the first ten days of burning because the fuel is transitioning from pure, fresh fuel to fuel that contains fission products, and in particular, poisons. Therefore, the reactivity coefficients were determined at both 0 and 15 days, as well as every 100 days thereafter until the 1415th day, for a total of 16 points of interest.

4.4 Dancoff Factors

Dancoff factors can have a large influence on the overall k -eff of a lattice cell. Variations in core conditions (such as temperature and density of materials) necessitate that Dancoff factors be recalculated for each change in conditions. The calculation of Dancoff factors in NEWT is handled by MCDancoff (Monte Carlo Dancoff) (30). However, NEWT's interpretation of the Dancoff factor, analyzed using dan2pitch, has some errors. These errors are most noticeable when coolant densities drop below 0.3g/cm^3 (31). Therefore, it is important to analyze the conversion of Dancoff factors into effective pitches outside of the dan2pitch module, particularly to avoid using dan2pitch when coolant densities drop below the 0.3 threshold.

This is especially true for the SCWR, since a significant portion of coolant is below 0.3g/cm^3 , even in normal operating conditions. The method used to convert Dancoff factors to equivalent pitches was the iterative solving of a single fuel pin's equivalent pitch given a specific Dancoff factor. This method is described more fully in the 2016 work by Glanfield and Novog (31).

The method can be summarized as follows. First, the Dancoff factor is determined for a fuel pin, using the standard method of MCDancoff. The usual next step would be to feed the outputted Dancoff factor into the dan2pitch module of NEWT. Then, if an input of single pin with a pitch equal to the Dancoff equivalent pitch given by dan2pitch were evaluated, the expected result would be that the Dancoff factor given by MCDancoff would be the same as in the original full lattice. This is not often the case, and more frequently a different Dancoff factor is given for the original lattice and the single-pin approximation.

Therefore, this work recursively changes the pitch of a single pin cell until the Dancoff factor matches that of the original lattice. The pitch of the single pin when the Dancoff is identical is taken as the Dancoff equivalent pitch, and is used in the NEWT calculation, effectively bypassing the dan2pitch calculations. This method has been found to much more closely approximate KENO-CE models that do not rely on Dancoff Factor evaluations.

Dancoff factors do not change with variations in fuel composition, so they do not need to be recalculated for different fuels or different fuel burnups. However,

when evaluating coefficients of reactivity, changing material temperatures and densities can have a large effect on the Dancoff factor. For each case, the Dancoff factor must be recalculated and an appropriate equivalent pitch determined.

4.5 Enrichment

The current SCWR preferred cycle length is around 470 days (7), equivalent to a burnup of 22.3 Mega-Watt days per Mega-Ton Initial Heavy Metal (MWd/MTIHM). After burning the PuTh fuel at the prescribed enrichment (8), the k -eff at the centre of the channel at 470 days is 1.1597. Assuming, at the time of refuelling, that a third of the core is 470 day old fuel, a third is 940 day old fuel, and the remainder is 1410 day old fuel, the core-wide average k -eff would be 1.0609.

For the UO_2 and PuU MOX fuels, an assumption was made of the initial average enrichment that preserved the enrichment ratio of the two rings in the PuTh fuel. The enrichment was then adjusted until the average core reactivity for all three cases was very similar, so that the expected cycle length of each fuel would be similar. For UO_2 that enrichment was 7.65%, and for MOX that enrichment was 10% Pu, enriched to 51.9% ^{239}Pu .

The fuel enrichment in this work is not varied along the length of the bundle, nor is a whole-core analysis performed. The comparison of fuel types is not likely to be significantly affected by these variables, and considering them greatly increases the complexity. However, for any given fuel, such an analysis would need to be performed before a complete picture of the behaviour of the fuel could be obtained.

4.6 Simulations

After determining the appropriate meshing and enrichments of the fuel, each fuel type can be burned for the length of three cycles, approximately 67 GW/MTIHM or 1415 days. This gives a reference k -eff value for each burn-up of interest, and the fuel composition at that point can be used to evaluate coefficients of reactivity.

For each of the five important burn-ups, a case is run for the FTC, MTC, CTC, and CVC. Because the coolant flows through two distinct regions, the CTC and CVC are split into three parts. These are the inner, outer, and total coefficients.

Each temperature coefficient is determined by increasing the temperature by 100K and each void coefficient is determined by reducing the void to 0.01 g/cm^3 . The temperature coefficients are reported in units of mk/K , while the void coefficients are reported simply in mk . While it is common for void coefficients to be reported in mk/g/cm^3 , this approach is not well-suited to the SCWR. The operating density of the coolant varies by around 80% from the bottom to the top of the core, so the rate of change in the void coefficient cannot be expected to be constant over this range. Therefore the void coefficients were reported in terms of their reactivity change when fully voided from nominal conditions.

The reference case and eight coefficient cases, each evaluated at three heights in the fuel bundle, over 16 burnups for each of three fuel types, result in 1296 runs per fuel type. These burnups and locations were chosen to obtain a good neutronic understanding of each of these fuels' performance over a range of reactor conditions.

In order to ensure valid comparisons between fuel types and core locations, the input files for the calculation of each coefficient were kept the same with the exception of the fuel composition. Although an extremely detailed analysis would have different material temperatures and densities specific to the power shape of the fuel types and fuel burnups, such analyses would require thermalhydraulic–neutronic coupling. The coupling would greatly increase the complexity of the computation. The trade-off between increased accuracy and increased time is not likely to be beneficial until a more detailed analysis is required for the continuation of the reactor design.

Chapter 5: Data & Analysis

5.1 Multiplication Factor

The multiplication factor follows similar trends for all three fuel types. As can be seen in Figure 9, the multiplication factor is linear for most of the fuel's lifetime, with two exceptions. The first is the large drop in reactivity in the first 1.0 MWd/kgIHM. This is due to the build-up of fission products that are not present in fresh fuel. Many of these fission products are poisons that significantly reduce the reactivity of the lattice cell. The second non-linear feature of the multiplication factors is the decline in the last 10-20 MWd/kgIHM. As the quantity of fissile nuclides becomes sufficiently low, the reactivity drops sharply. This is noticeable for the UO_2 fuel, but barely perceptible for the MOX fuel in comparison to the PuTh fuel.

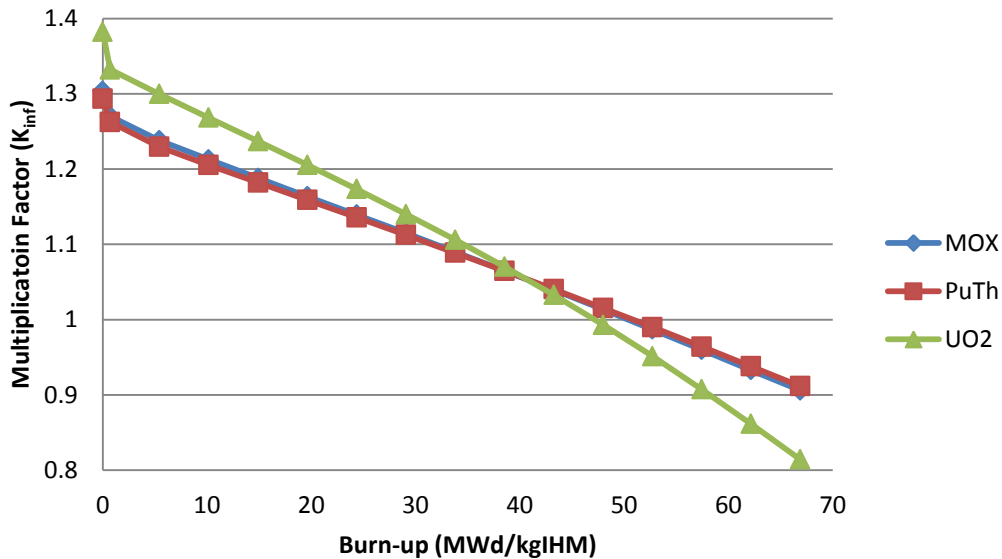


Figure 9: Multiplication factor over burn-up for all three types of fuel at 2375mm

The UO_2 fuel's k_{inf} decreases at a faster rate than either the MOX or PuTh due to the rate of the conversion of ^{238}U to ^{239}Pu . All three fuel types contain a fertile nuclide that breeds a fissile isotope to lend additional reactivity over burn-up. However, this conversion is less efficient in UO_2 than the equivalents in PuTh or MOX, leading to less breeding of new fuel inventory and the corresponding

greater rate of decrease in k_{inf} . Even though the MOX fuel also converts ^{238}U to ^{239}Pu , its reactivity does not drop as quickly as the UO_2 fuel. Therefore the effect cannot solely be due to the choice of fertile material.

Figure 10 shows the different concentrations of nuclide groups for the three fuel types. The PuTh and UO_2 fuels’ initial fissile nuclides decrease at a similar rate, even though they have different initial values. The MOX fuel has a distinct slope due to the ^{239}Pu that is bred being undistinguishable from the initial ^{239}Pu . When comparing the amount of bred nuclide in PuTh or UO_2 , it becomes clear that the PuTh fuel produces more ^{233}U than the UO_2 produces Pu. It is also clear that the decrease of the initial concentration of the fertile nuclide in the UO_2 fuel, which should be correlated with the production of fissile isotopes, is larger than the corresponding decrease in either the MOX or PuTh fuels. This suggests that even though more fertile material is burnt in the UO_2 fuel, it is less efficient at producing usable fissile nuclides. Therefore, at higher burnups, the UO_2 fuel would have a lower fissile content due to less efficient breeding, and a lower multiplication factor.

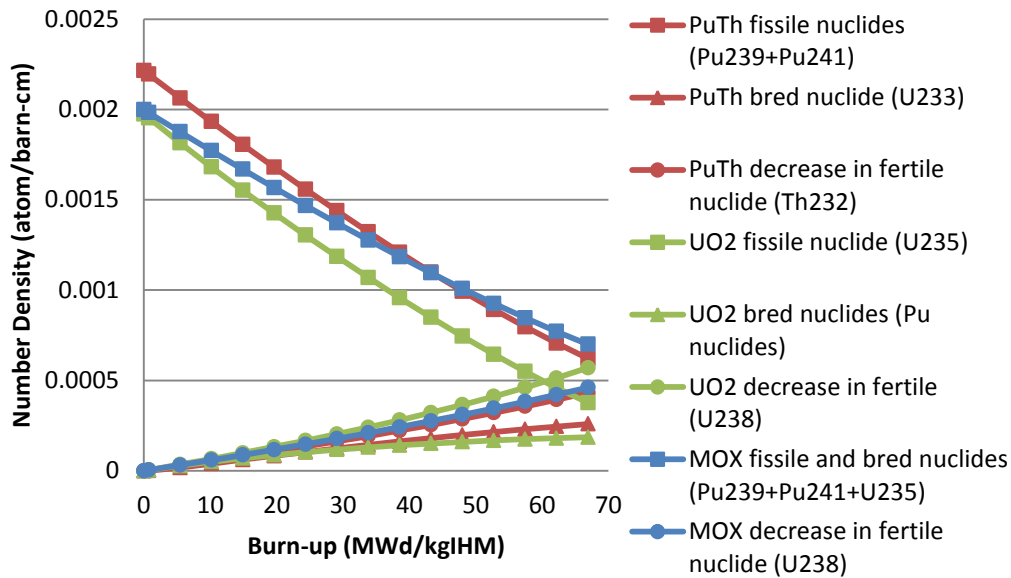


Figure 10: Number densities of various nuclides of interest over burn-up for the three fuel types

One source of this difference is likely to be the large absorption peaks in the plutonium isotopes, 0.3 eV in ^{239}Pu and ^{241}Pu and 1 eV in plutonium ^{240}Pu and

^{242}Pu . The ^{235}U in the UO_2 does not have any similar peaks, and therefore is not as well-suited to the harder neutron spectrum in the SCWR reactor. This can be seen in the higher fast fission factors of the PuTh and MOX fuels and in the higher resonance escape probability of the UO_2 fuel, as shown in Figure 11. Additionally, the thermal utilization factor is lower in the UO_2 fuel, indicating that fewer thermalized neutrons are absorbed in the fuel. Another difference between the fuels is that plutonium fissions release more energy than uranium fissions. This could result in plutonium-based fuels requiring a smaller number of fissions for the same power output as a uranium fuel. This would tend to burn the fuel more slowly, giving the multiplication factor a flatter slope.

However, in order to entirely determine the cause of the differences in multiplication factor, more research would need to be done. Since it is clear that an effect caused by the combination of the fissile and fertile material is responsible for the unique trend, a potential avenue of research would be manipulating cross sections or removing nuclides one at a time. These approaches have a good potential for identifying the root cause of the differences in multiplication factor, but are also fairly time intensive.

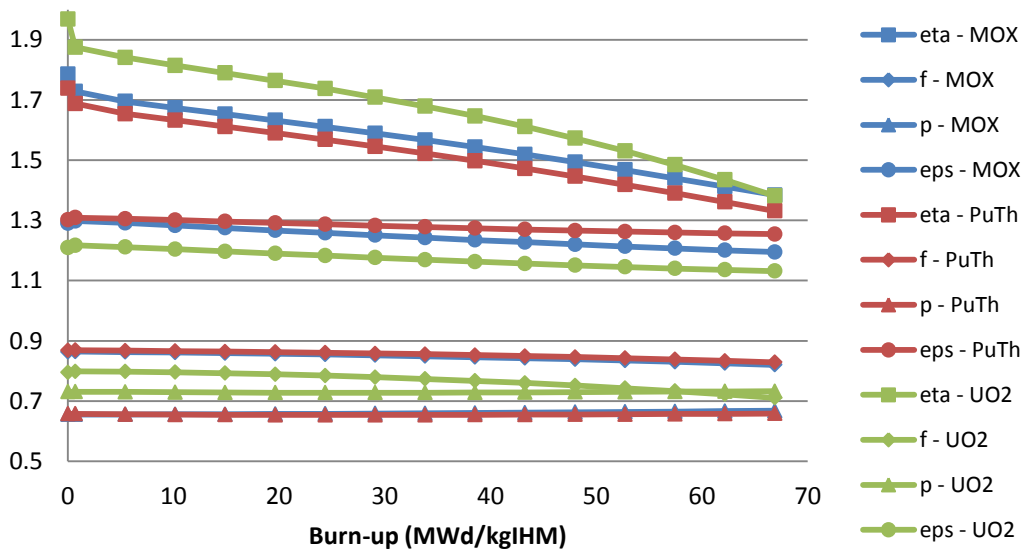


Figure 11: Four factors for the three fuel types over burn-up

The reproduction factor becomes especially important in the discussion of the coefficients of reactivity. In particular, in the final 30 MWd/kgIHM of burn-up, there is a significant change in the slope of the reproduction factor for the UO_2 fuel. This causes numerous non-linearities in the reactivity coefficients of the UO_2 fuel that are not present in the MOX or PuTh fuels. The reproduction factor is determined solely by the properties of the fuel isotopes, so all reproduction factor changes are the result of differences in the fuel composition. Both the MOX and PuTh fuel types have a majority of plutonium isotopes, while the UO_2 fuel has a majority of uranium, at least until very high burn-ups. This shift of almost entirely ^{235}U to nearly half ^{239}Pu , coupled with the much more significant drop in fissile inventory, is the cause of a large portion of the unique trend in the reproduction factor.

For all three fuel types, the multiplication factor remains extremely similar for all heights of the reactor. This implies that the neutron spectrum does not change significantly over the height of the reactor, even though the outer coolant density changes dramatically. As will be shown by the CVR and CTC results, the outer coolant is responsible for a miniscule amount of moderation that further supports this conclusion. Although plots of the multiplication factor over height for the three fuels are not included in the body of this text for brevity, they are shown in Additional Plots.

5.2 Coefficient of Void Reactivity

Much like other reactor designs, the SCWR has a negative total CVR. However, due to the unique geometry of the reactor, a discussion of CVR is not as straightforward as it is with other reactor types. Changes in coolant density in the separate coolant regions affect the reactivity of the lattice differently. The effect of varying the density in the inner coolant and the effect of varying the density in the outer coolant added together are not equivalent to the effect of varying the density of both coolants. Therefore, it is important to consider the effects of changing coolant density separately for the inner, outer, and total coolant regions.

For all three fuel types, the inner CVR is negative and becomes more negative as the fuel depletes, as shown in Figure 12. This is due to the large portion of moderation that the inner coolant provides. The removal of such a large source

of moderation causes a significant decrease in reactivity. The reason for this can be determined by looking at the changes in the four factors that are plotted for the PuTh fuel type at 2375mm in Figure 13 (MOX and UO₂ plots are similar and can be found in the appendix).

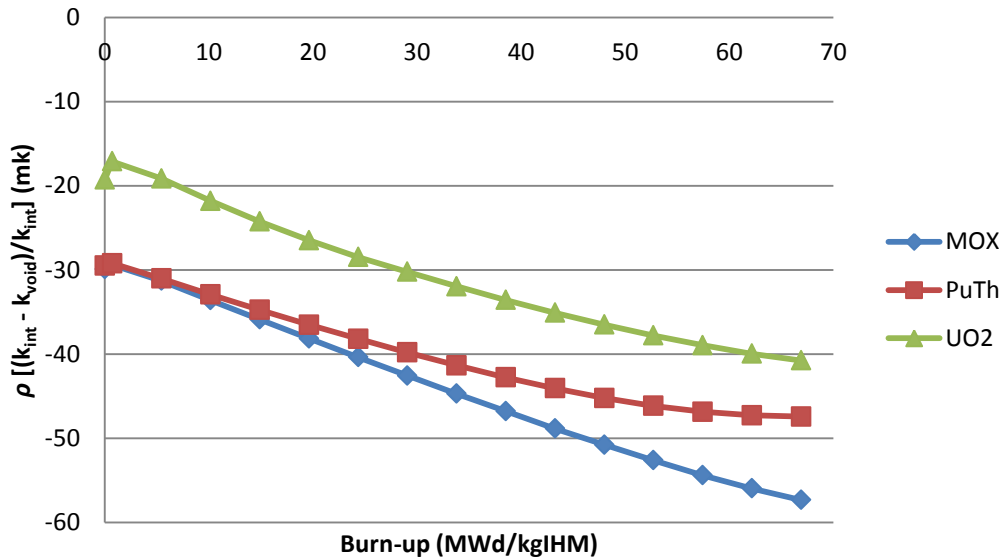


Figure 12: Inner Coefficient of Void Reactivity for the three fuel types at 2375mm

The two factors that change most significantly are the resonance escape probability and the fast fission factor. Even with the small positive contribution of the thermal utilization factor, the net effect on the multiplication factor as a result of the inner coolant voiding is negative due to the dominating decrease in the resonance escape probability. The large increase in the fast fission factor coupled with the large decrease in the resonance escape probability implies that fewer neutrons are being slowed below epithermal energies. Therefore, more neutrons are being absorbed at higher energies, and a higher proportion of fissions are occurring at higher energies. This is a logical conclusion of the complete voiding of a major source of moderation.

As seen in Figure 12, The ICVR becomes more negative over burn-up. This is due to the change in reproduction factor as the fuels ages. Looking at the four factors in Figure 13, the k_{inf} largely follows the trend of the reproduction factor, with the changes in the other three factors effectively cancelling each other out. The

reproduction factor is changing due to the coolant voiding leading to less moderation and a hardening of the neutron spectrum. This changes the fission-to-absorption ratio in the fuel, leading to the trend observed in the reproduction factor. In general, this is common to all of the reactivity coefficients, and will become clearer as more cases are discussed.

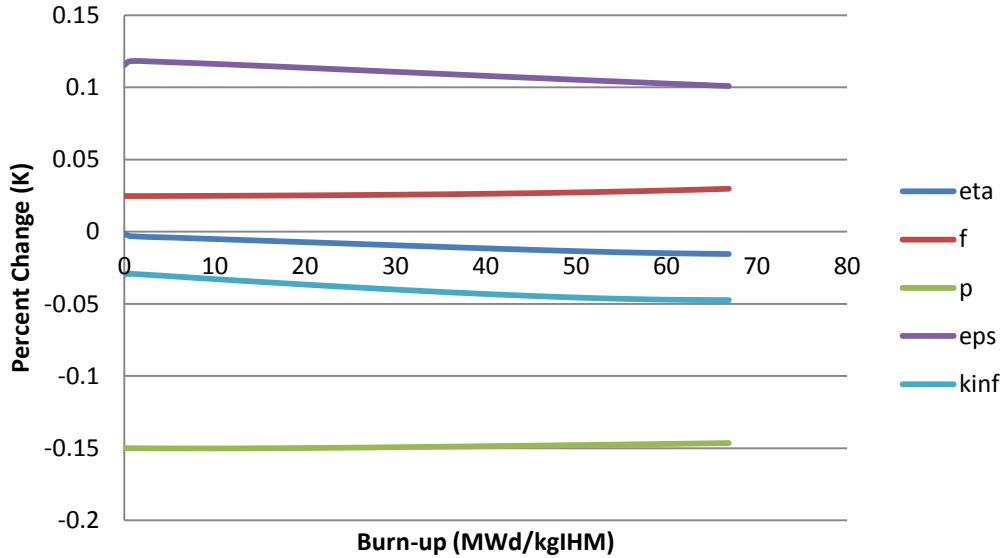


Figure 13: Change in four factors for ICVR in PuTh fuel at 2375mm

The ICVR is the smallest at 125mm, and roughly the same for the 2375 and 4875mm heights, as shown in Figure 14. This is due to the outer coolant being at its most dense at 0.54g/cm^3 , and contributing a larger share of moderation than anywhere else in the core. Therefore, voiding the inner coolant has less of an effect at this height in the core. Both the 2375 and 4875mm densities are extremely low, at 0.15 and 0.07g/cm^3 respectively. This makes the values for the ICVR very similar at these heights.

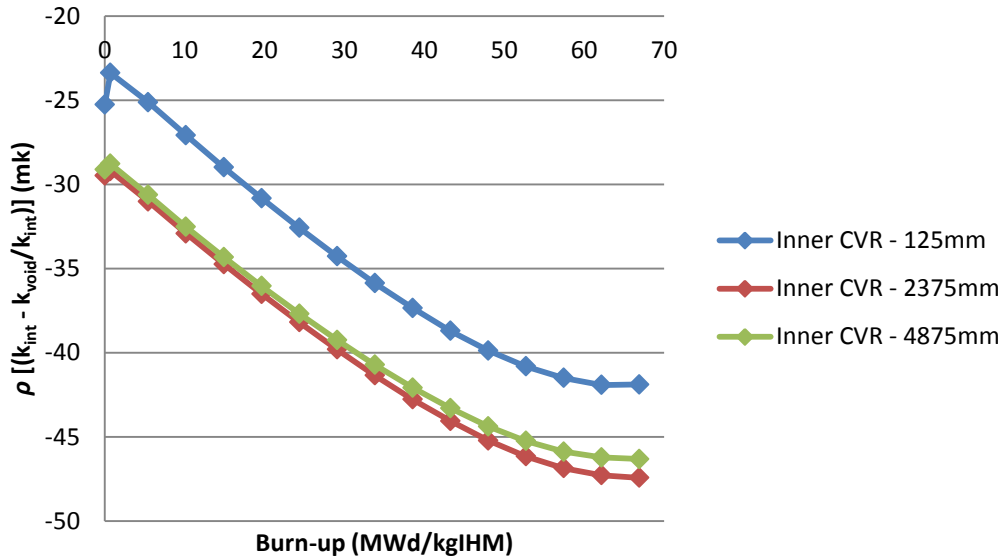


Figure 14: ICVRs for PuTh fuel at three reactor heights

As seen in Figure 12, the UO₂ fuel has a less negative ICVR than the MOX or PuTh fuel. This is due to the absorption peaks in the plutonium nuclides at energy levels relevant to coolant up scatter. These peaks cause the plutonium fuel to have a larger reaction to the loss of moderation that directly reduces the amount of neutrons available in the 0.3eV energy region. As the UO₂ fuel has very little plutonium, especially at low burn-ups, it is not as significantly affected by the reduced population of 0.3eV neutrons and therefore it is more sensitive at higher burn-ups. In contrast, the PuTh fuel replaces some of its original fissile plutonium with uranium, making it less sensitive at higher burn-ups. This causes its ICVR to shift towards the UO₂ fuel values (primarily uranium) and away from the MOX values (primarily plutonium) due to the lack of the 0.3eV absorption peak in uranium nuclides.

The OCVR, shown in Figure 15, is quite different from the ICVR, as it is responsible for a very small amount of moderation. In fact, the presence of the outer coolant decreases the likelihood of a fast fission as well as increases the likelihood of absorptions in materials other than the fuel. By voiding the outer coolant, the reactivity is increased due to an increase in fast fissions and a lower proportion of absorptions in the outer coolant. This effect is not as strong as the ICVR: it is about 1/3 of the magnitude.

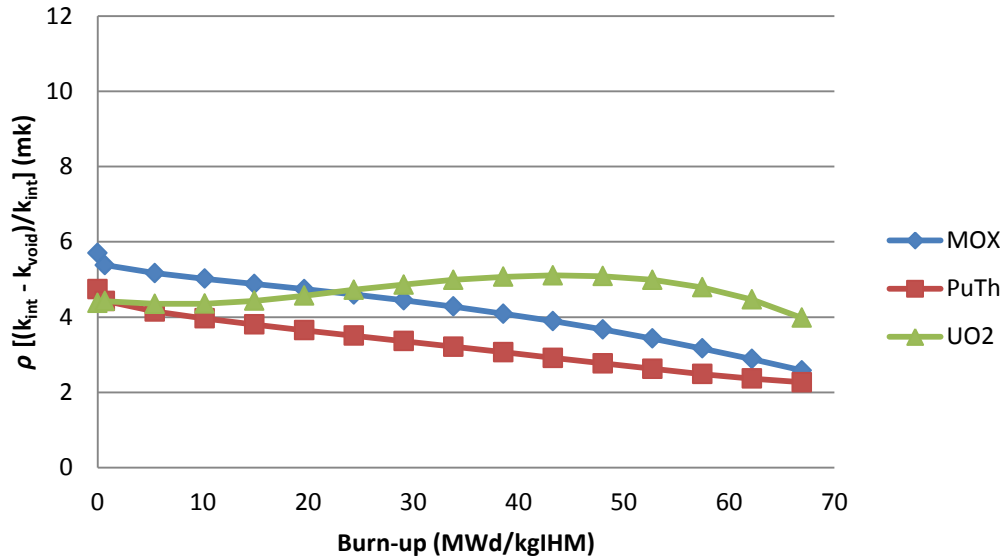


Figure 15: Outer Coefficient of Void Reactivity for the three fuel types at 2375mm

For both the MOX and PuTh fuel types, the OCVR decreases with increasing burn-up. This trend mirrors the decrease in the reproduction factor. When the outer coolant is voided, the ratio of the fission-to-absorption cross sections in the fuel changes, with an increasing likelihood of absorptions. This could be due to the spectrum hardening from a lack of moderation pushing a significant amount of neutrons above the 0.3eV peaks in plutonium, due to a lack of up-scattering leaving neutrons below the 0.3eV peaks, or a combination of the two effects.

The UO₂ is unique in that the change in reproduction factor is not solely responsible for the trend in the OCVR. For this fuel, the change in resonance escape probability has a more significant influence than in the Pu-based fuels. Because the primary fissile nuclide in UO₂ is ²³⁵U, rather than a plutonium nuclide as in PuTh or MOX fuels, there is not a significant absorption peak in the epithermal region until late in the fuel's life, when a moderate amount of plutonium has been bred. This gives the change in the resonance escape probability a sharp initial increase, followed by a levelling trend, as seen in Figure 16. The resonance escape probability is not solely responsible for the changes in the multiplication factor; the reproduction factor is still quite dominant. The

downward curve of the reproduction factor at high burnups is responsible for the sinusoidal shape of the OCVR.

The reproduction factor is also unique in the UO₂ case for the OCVR compared to the other fuel types, since it is positive. This is because the fuel primarily consists of uranium isotopes that lack the low-lying absorption peaks found in plutonium. As the fuel ages, the composition changes and the reproduction factor begins to mirror that of the PuTh and MOX fuels. The reproduction factor does not have a significant effect on the OCVR in the early-life of the fuel because the absence of up-scattering does not affect the UO₂ fuel as severely, due to the lack of the absorption peaks.

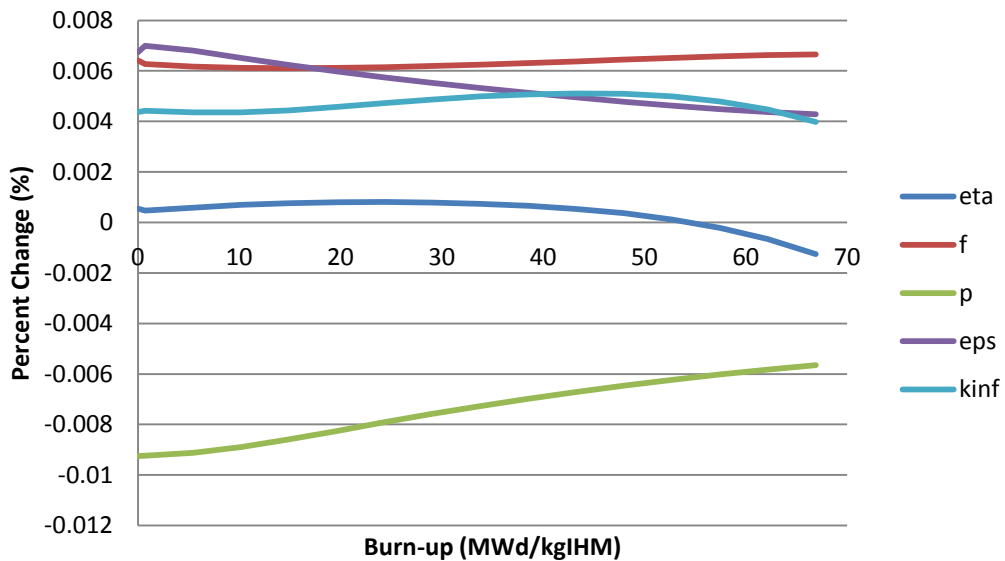


Figure 16: Change in four factors for OCVR in UO₂ fuel at 2375mm

Although it may be tempting to add the ICVR to the OCVR to determine the TCVR, the effect of removing all the coolant is not so simple. Neither coolant is truly independent; the removal of one changes the role of the other. For example, although at the beginning of cycle the OCVR is generally around +5mk and the ICVR is around -25mk, the TCVR is around -15mk, not -20mk. This reflects the non-additive behaviour of the reactivity phenomena in the lattice.

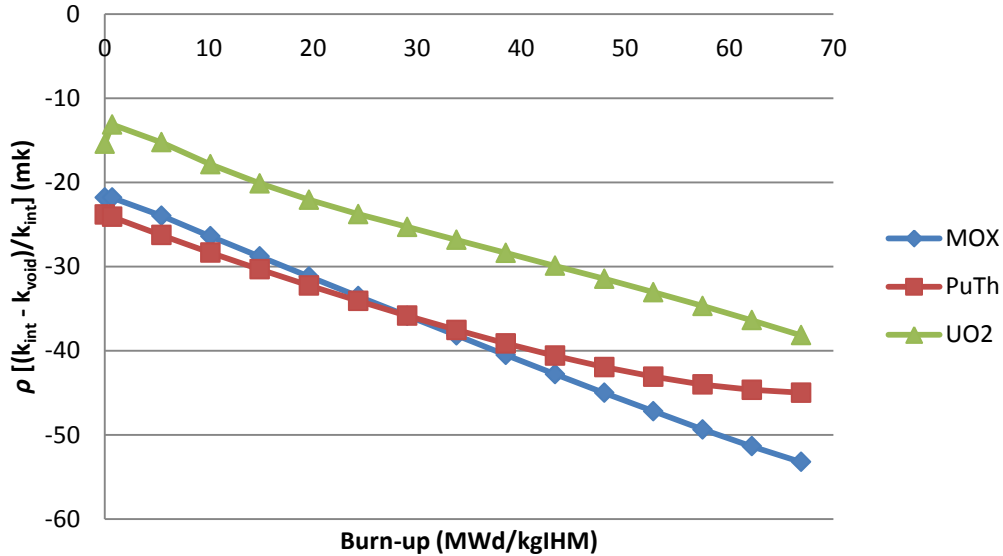


Figure 17: Total Coefficient of Void Reactivity for the three fuel types at 2375mm

That being said, since voiding the inner coolant has a much stronger effect than voiding the outer coolant, and the inner coolant is responsible for a significant portion of moderation in the SCWR core, the TCVR generally follows the same trends as the ICVR, as seen in Figure 17.

Like its ICVR, the UO₂ fuel's TCVR has a smaller magnitude due to the absorption peaks in the plutonium nuclides found in the PuTh and MOX fuels but not in the UO₂ fuel. As burn-up increases, the shifting of the fissile content from entirely ²³⁵U to a content with a significant portion of plutonium nuclides tends to shift the values close to those of the MOX fuel. This effect is not readily apparent because, like the effect demonstrated in the ICVR, it is overshadowed by the significantly decreased reactivity, as well as the effects of removing the outer coolant.

The MOX fuel, once again, is almost entirely linear, owing to its more consistent fissile composition. The PuTh fuel follows this trend until a significant portion of ²³³U is built up, when it starts to drift closer to the UO₂ curve.

5.3 Coolant Temperature Coefficient of Reactivity

The CTCs exhibit a similar response to the CVRs. There are distinct effects of increasing the temperature for the inner, outer, and both coolant regions, and these effects are fairly similar across fuel types. For all three fuels, the CTCs are generally positive, with the TCTC being the largest and the OCTC being the smallest. The CTCs for all three fuel types and locations in the core increase with burn-up.

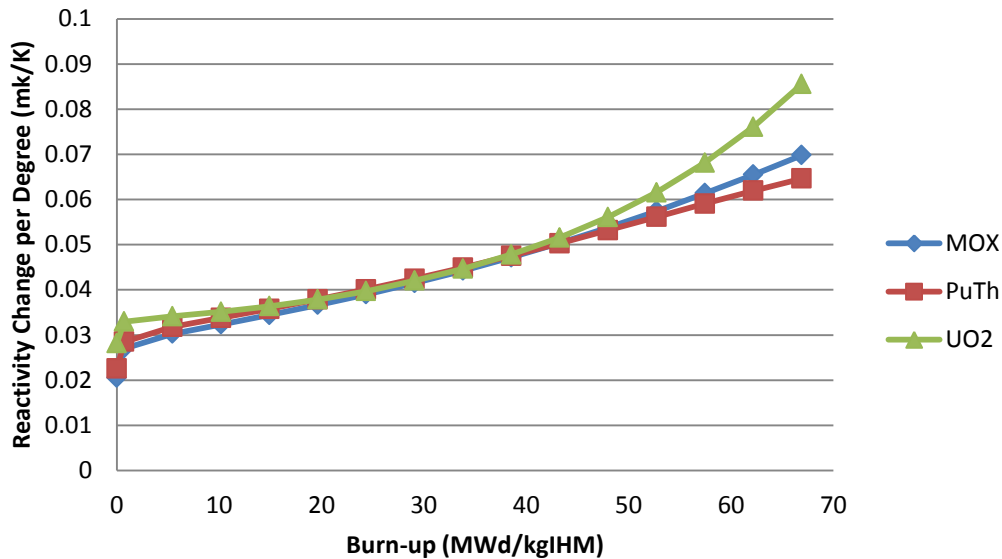


Figure 18: ICTC for the three fuel types at 2375mm

Starting with the ICTC, as shown in Figure 18, it is clear that all three fuel types have very similar values over much of their burn-up. Increasing the inner coolant's temperature by 1K increases the reactivity by 0.03 to about 0.07mk, depending on burn-up. The magnitude of the ICTC is largely due to the thermal utilization factor, as the other three factors do not change significantly at the beginning of the cycle for fresh fuel. As a result of increasing the temperature of the inner coolant, the neutron spectrum becomes hardened, both due to increased up-scattering in the inner coolant and a reduction in the capacity for moderation. As a result, there is a decrease in the amount of absorptions in the coolant in proportion to the amount of absorptions in the fuel. A higher energy neutron would have a decreased probability of absorption in ^1H in the coolant

and an equal (or possibly higher) chance of absorption in the 0.3eV plutonium peaks or resonance regions of uranium or plutonium nuclides.

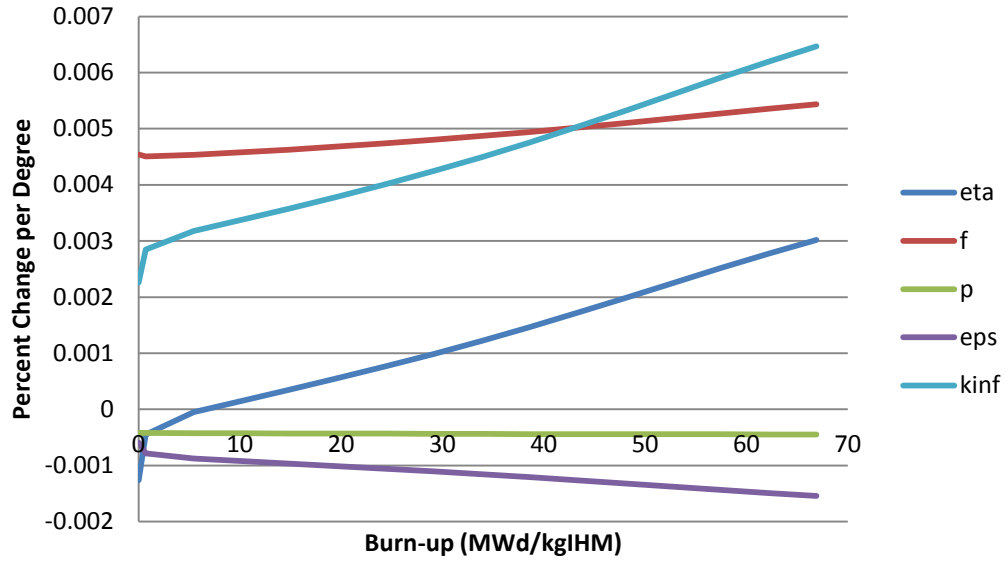


Figure 19: Change in four factors for ICTC in PuTh fuel at 2375mm

As can be seen in the plot of the change in the four factors for the PuTh in Figure 19, the main factor that influences the trend in the ICTC is the reproduction factor. Much like the CVR cases, the change in the reproduction factor is a result of a hardening of the neutron spectrum. As the coolant temperature increases, the neutron spectrum is hardened both through up-scattering and lack of moderation. This leads to an increase in fissions in the plutonium absorption peaks and uranium and plutonium resonances, and changes the fission to absorption ratio in the fuel.

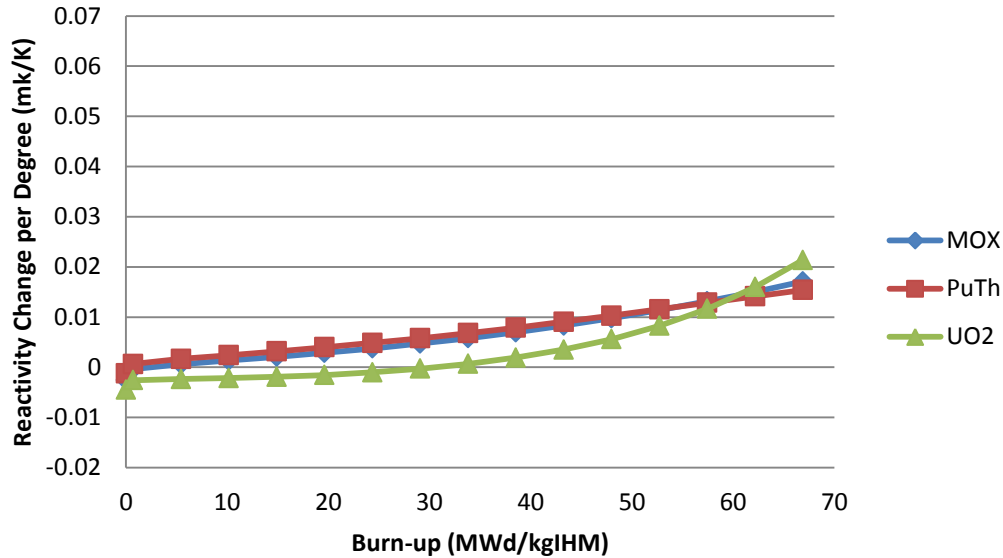


Figure 20: OCTC for the three fuel types at 2375mm

The OCTC is quite similar to the ICTC, the largest difference being that it is much smaller in magnitude, as shown in Figure 20. This is expected, as the outer coolant is less dense and has a generally smaller area to provide moderation. Since fewer interactions occur in the outer coolant, the effect of raising its temperature is not as large.

The four factors, shown in Figure 21, are also quite similar to the ICTC case; the thermal utilization factor, reproduction factor, and multiplication factor are all positive, and the resonance escape probability and fast fission factor are negative. As with the ICTC, the initial determinant of the magnitude of the effect is the thermal utilization factor, once again due to a lack of absorption in ^1H and an increase in fission in the fuel due to an increase up-scattering and decrease in moderation. However, because the outer coolant is a much lower density and covers a smaller area than the inner coolant, the magnitude of this effect, and the change in the other three factors, is much smaller than in the ICTC.

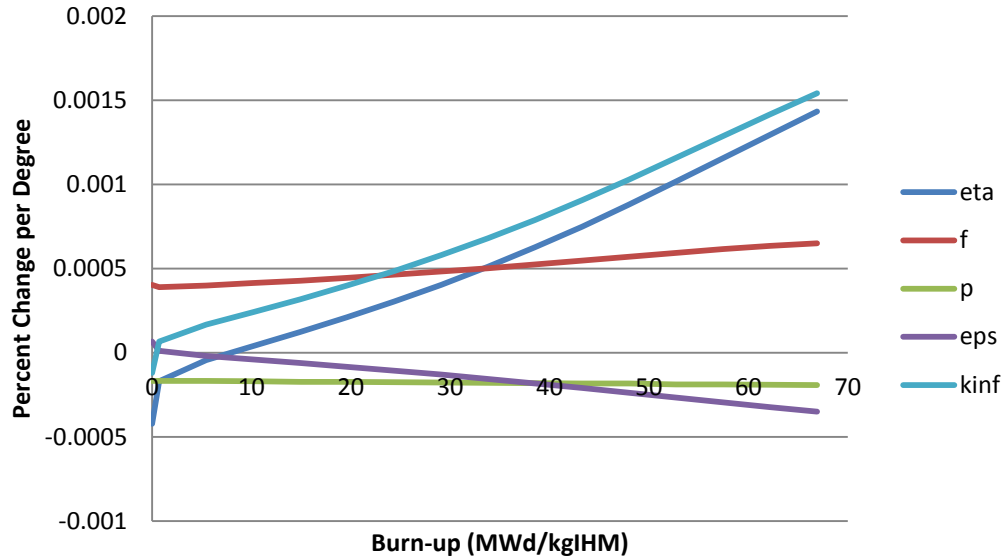


Figure 21: Change in four factors for OCTC in PuTh fuel at 2375mm

Once again, the trend in the OCTC is determined by the reproduction factor that is very clearly dominant in this case. Similarly, an increase in up-scattering and decrease in moderation due to the temperature increase results in an increase in the fission-to-absorption ratio in the fuel, due to the 0.3eV peaks in plutonium and resonances in uranium and plutonium isotopes.

The one notable, negative portion of the CTCs is the OCTC for the UO_2 fuel, particularly in the lower portions of the core. The outer coolant causes an increase in up-scattering when the temperature is raised. For the plutonium based fuels, this tends to increase the reactivity due to their strong 0.3 eV fission peaks. The uranium fuel has no such peak, so the reactivity tends to decrease as a result of up-scattering. As the UO_2 fuel burns out its uranium content and breeds plutonium, this effect is reversed and the reactivity starts to increase at later burn-ups. The opposite effect can be seen for the PuTh fuel as it breeds uranium. Although it is never negative, it does decrease noticeably compared to the MOX fuel. This effect is strongest near the top of the core where the coolant is nearly voided and the up-scattering effect is non-consequential. Conversely, the effect is stronger near the bottom of the core. The negative portion can be seen for the UO_2 fuel at the 2375mm height in Figure 23, and the rest of the OCTCs can be observed in Additional Plots.

Much like the CVRs for the three fuel types, the inner coolant is responsible for a larger amount of moderation than the outer coolant and therefore the ICTC is larger than the OCTC. Unlike the OCVR that has the opposite sign as the ICVR and TCVR, the OCTC has the same sign as the ICTC and TCTC. Also similar to the CVR, the TCTC is not strictly a result of adding the ICTC and OCTC. The increase in temperature of the two regions is not entirely independent, so the TCTC cannot be reliably predicted based on the ICTC and OCTC.

However, the TCTC does share a number of similarities with the ICTC and OCTC. The plot seen in Figure 22 is quite similar to the other coolant temperature coefficients in that it is positive, increases with a mostly linear trend, and is fairly similar for all three fuel types. The UO₂ fuel has a non-linear shape, similar to its shape in the ICTC and OCTC cases, caused by non-linearities in the reproduction factor. As discussed previously, this is the result of the changing fuel composition and, in particular, the very low k_{inf} in the UO₂ fuel.

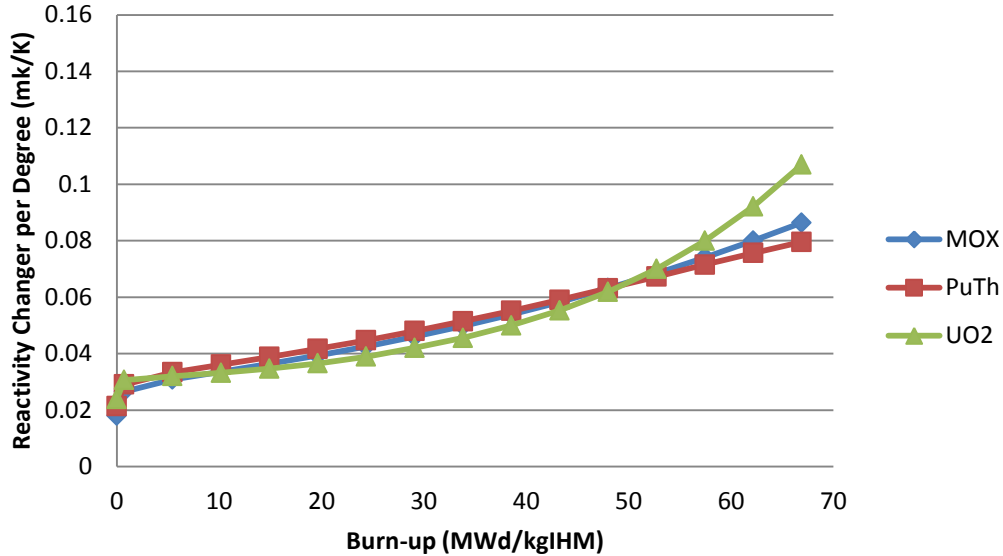


Figure 22: TCTC for the three fuel types at 2375mm

The changes in the four factors that cause the increase in the coolant temperatures are also very similar to the ICTC and OCTC cases. Shown in Figure 23, the magnitude of the TCTC is determined by the thermal utilization factor and the trend over burnup is determined by the reproduction factor, for the

same reasons as the ICTC and OCTC. The magnitude of the changes in the four factors is roughly, but not exactly, the same as the sum of their changes in the inner and outer cases. In effect, the changes are somewhat larger in the TCTC case than the ICTC case.

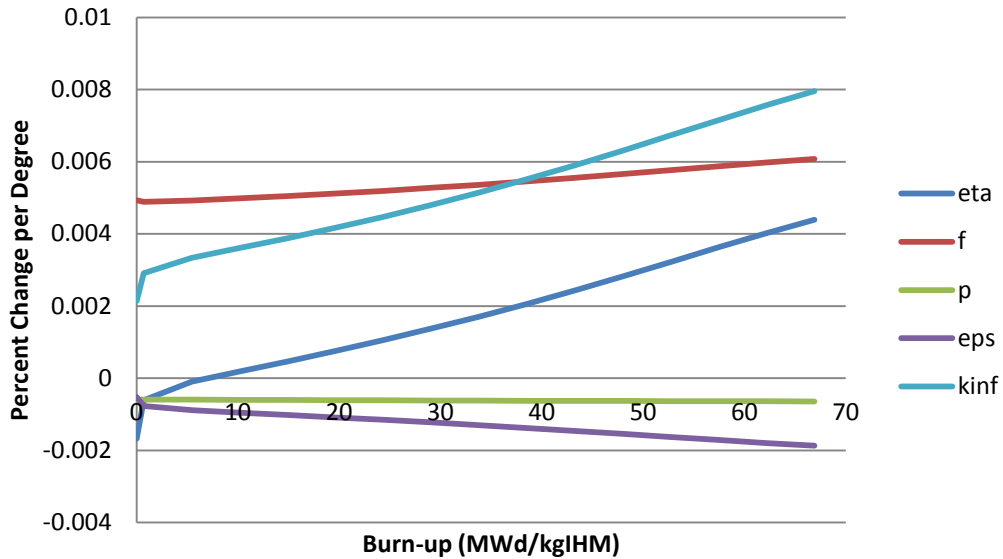


Figure 23: Change in four factors for TCTC in PuTh fuel at 2375mm

The effect of elevation in the CTC is consistent with expectations, given that the CTC is evaluated using the local density. The more dense the region of coolant is, the stronger the effect of raising its temperature. For the inner coolant, the densest portion is near the top of the core, so this area has a higher ICTC than the lower regions of the core. For the outer coolant, the top of the core is essentially voided, so the OCTC is very close to zero. The total coolant is somewhat more complex, but in general the TCTC is quite similar to the ICTC, due to the outer coolant being practically voided for much of the core. Due to the outer coolant being most dense at the bottom of the core, and the inner coolant being least dense at the bottom of the core, the TCTC does not change monotonically with height. The TCTCs for the PuTh fuel case for the 125, 2375, and 4875mm heights are shown in Figure 24, and the plots of the CTCs for the other fuel types can be found in Additional Plots.

The effect of increasing the coolant temperature is fairly similar to the effect of voiding the coolant. Both generally lead to a decrease in epithermal neutrons

and an increase in thermal and fast neutrons due to the decrease in moderation. However, the voiding should lead to a decrease in upscattering while increasing the coolant temperature should lead to an increase in upscattering. The change in upscattering should result in a large difference between the UO_2 and plutonium driven fuels for both coefficients, but this is only the case for the void coefficients.

It is not quite clear why the differences between fuels vary so significantly for the CVR and CTCs. For the CTCs, the UO_2 fuel is quite similar to the PuTh and MOX fuels, while for the CVRs the UO_2 fuel is very different. Further analysis of this difference is warranted, but would likely require manipulation of individual nuclide concentrations or cross sections, making it very resource intensive.

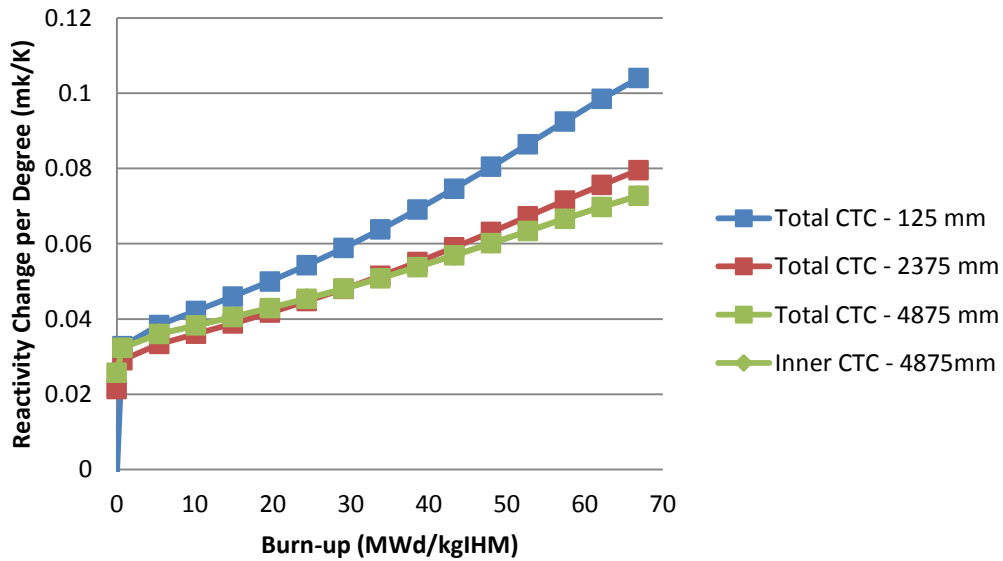


Figure 24: TCTC for the PuTh fuel at various heights

5.4 Moderator Temperature Coefficient of Reactivity

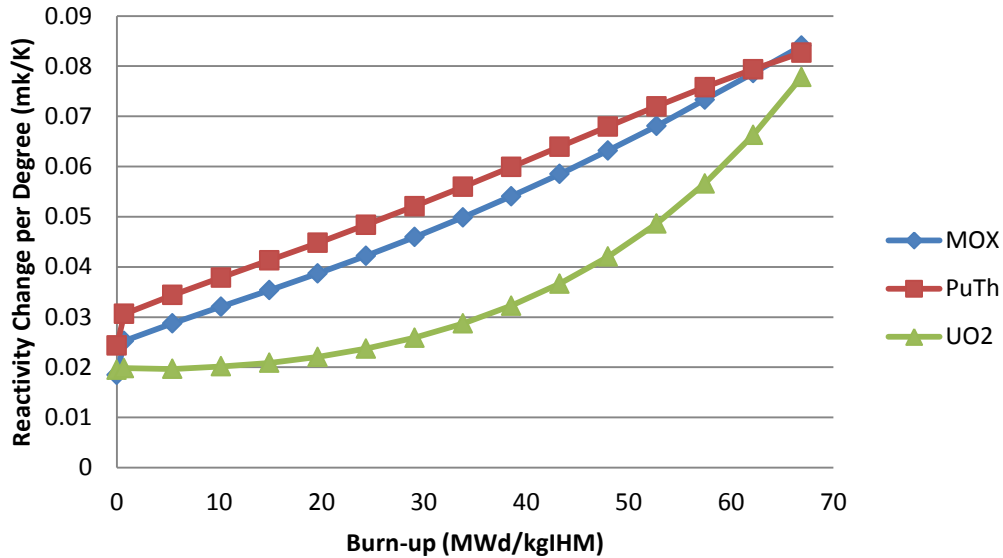


Figure 25: MTC for the three fuel types at 2375mm

Much like the CTCs, the MTCs for all three fuel types are positive and increase with burn-up for all three fuels, as seen in Figure 25. Additionally, the changes in the four factors as a result of increasing the moderator temperature are very similar. The change in the thermal utilization factor is responsible for the initial magnitude of the effect at zero irradiation, and the trend over burn-up is a result of the change in the reproduction factor. Once again, the change in the thermal utilization factor is a result of the harder neutron spectrum changing the ratio of the fission-to-absorption cross sections, and the change in the reproduction factor is a result of the changing fuel composition and decreased fissile content. These effects can be seen for the PuTh fuel at 2375mm in Figure 26, and for the

MOX and UO₂ fuel types in Additional Plots.

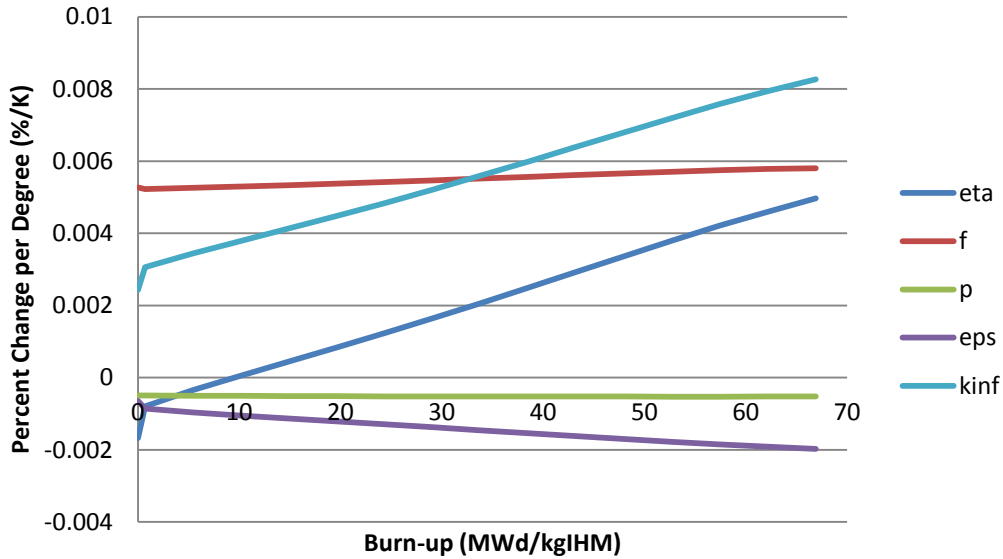


Figure 26: Change in four factors for PuTh fuel at 2375mm

Although the trends for a single height in the reactor are similar to the CTC, the MTC varies with height in a different manner. For the CTC, the density of the coolant at various heights in the reactor had a large influence on the response to an increase in temperature. Because the moderator has the same density and initial temperature throughout all locations in the core, we might not expect much variance with regards to location. However, even though the moderator’s physical properties are unchanging, the proportion of moderation it is responsible for changes.

As seen in the discussion of the TCTC, the outer coolant’s effect on reactivity is nearly negligible. Therefore, most of the moderation comes primarily from the inner coolant and the moderator. As the lower regions of the core are where the inner coolant is at its least dense, the moderator is responsible for a higher portion of the slowing of neutrons than at the top of the core. Therefore the MTC is larger in the lower portions of the core, as seen for the PuTh fuel in Figure 27.

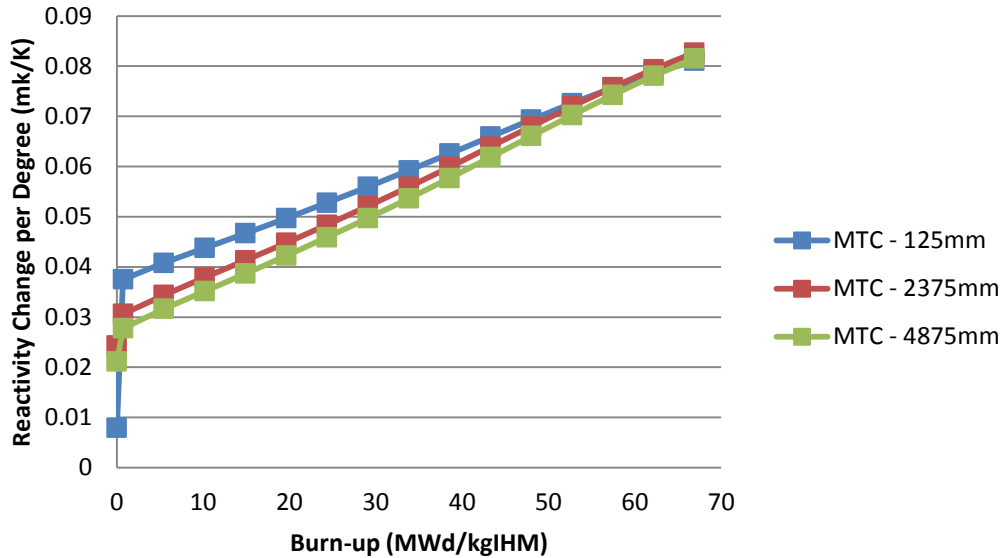


Figure 27: MTC at various heights for PuTh fuel

The UO_2 fuel has a noticeably lower MTC due to the absence of the plutonium fission peaks that are present in the other two fuel types at low irradiations. When the moderator temperature is increased, the neutron spectrum hardens and more neutrons are absorbed in the plutonium 0.3 eV fission peaks. An effect of this can also be seen in the PuTh fuel at late burn-ups. As more uranium is bred and plutonium is burnt up, the MTC decreases due to the decreasing significance of the 0.3eV peak.

5.5 Fuel Temperature Coefficient of Reactivity

The fuel temperature coefficient is the least related of the reactivity coefficients. Most of the other coefficients are driven by the efficiency of the moderation of a liquid in the core, while the FTC is driven primarily by the properties of the fuel itself. As seen in Figure 28, the FTC for the three fuel types differs more significantly than for the other reactivity coefficients, due to the primary influence of fuel composition rather than the coolant or moderator.

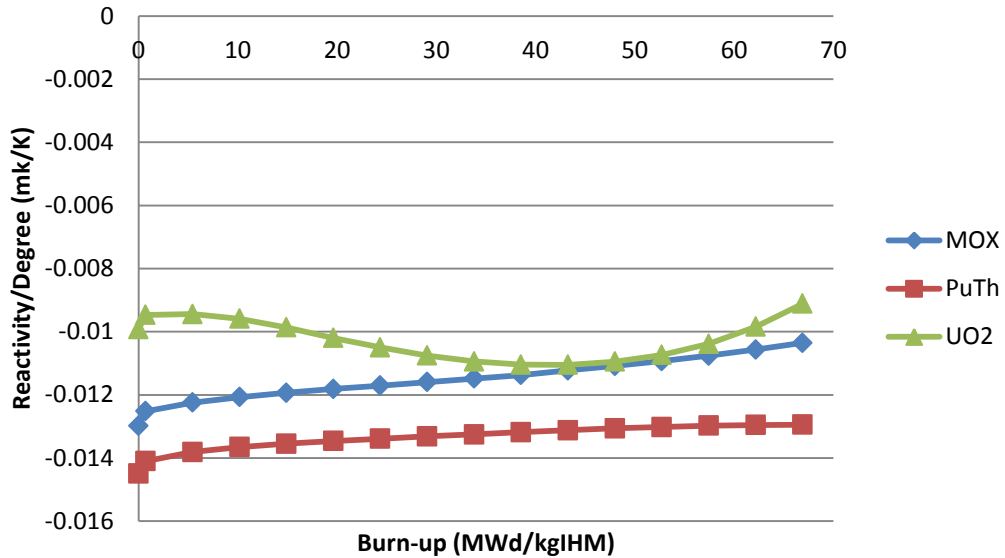


Figure 28: FTC for three fuel types at 2375mm

For the FTC, both the magnitude and the trend over burn-up are driven by the change in resonance escape probability. As the fuel temperature increases, the proportion of neutrons that successfully slow to thermal energies decreases. This is due to Doppler broadening in resonance peaks, particularly the 1eV absorption peaks found in ²⁴⁰Pu and ²⁴²Pu.

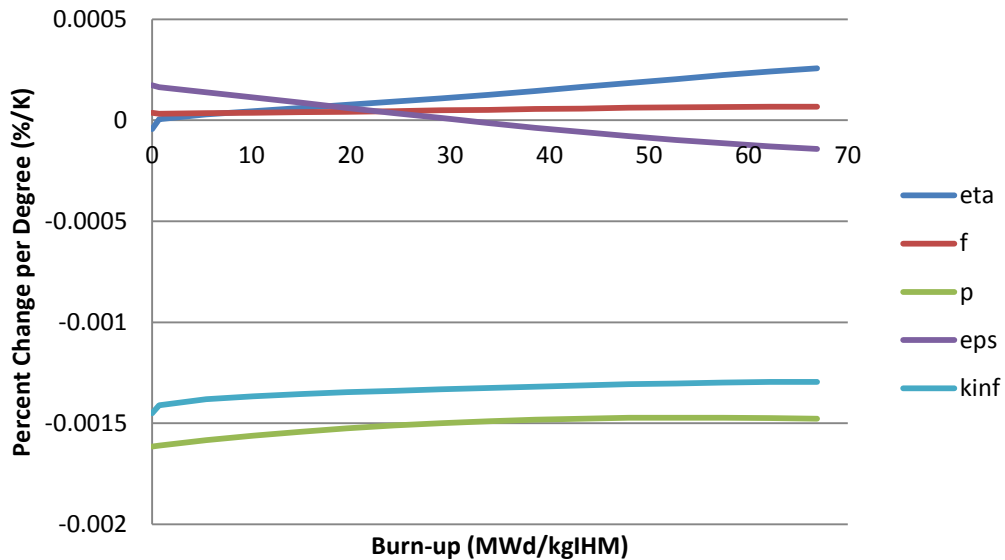


Figure 29: Change in four factors for PuTh fuel at 2375mm

The relatively high abundance of ^{240}Pu and ^{242}Pu in both the PuTh and MOX fuels (4.0% for PuTh and 3.3% for MOX) cause their FTCs to be lower at the beginning of cycle than their UO_2 counterpart. As the UO_2 fuel breeds plutonium, the even-numbered plutonium nuclides become increasingly common and contribute to the initial decrease in FTC. The strong 1eV absorption peaks, especially when Doppler-broadened, cause the resonance escape probability to drop as the nuclides’ concentration increase over burn-up. This decrease continues over burn-up as can be seen in Figure 30, but due to the rapidly increasing change in reproduction factor, it is not apparent in the FTC after 30 MWd/kgIHM. As was the case in the other reactivity coefficients, the exponentially increasing reproduction factor is a result of the changing fuel composition and low fissile content. The reproduction factor, as in the OCVR case, gives the FTC its sinusoidal shape.

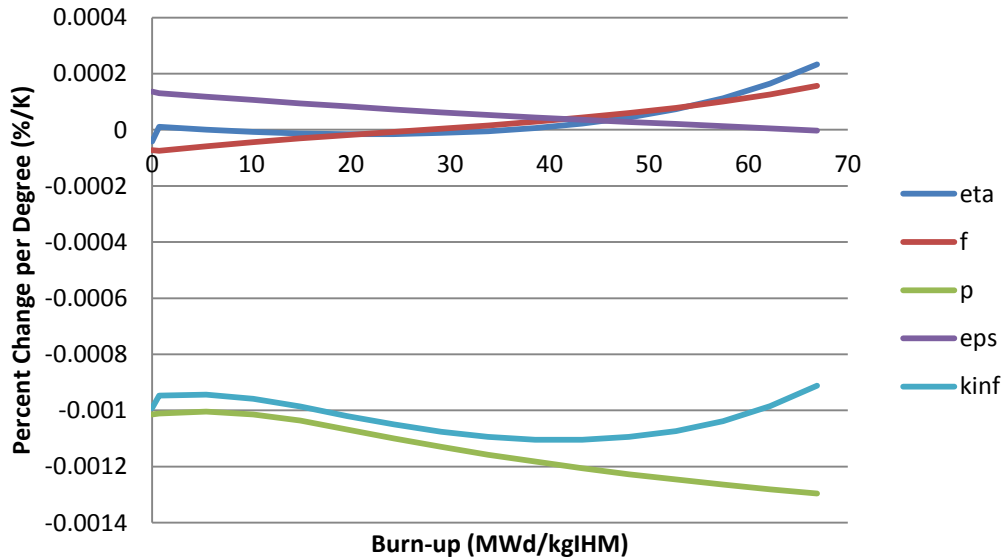


Figure 30: Change in four factors for UO2 fuel at 2375mm

A smaller but noticeable difference in the FTCs is the slight departure of the PuTh fuel's FTC relative to the MOX curve. This difference is due to the change in the fast fission factor that remains positive for the UO₂ and MOX fuels but becomes negative at high burn-ups in the PuTh fuels, as shown in Figure 29. This effect, despite all three fuels' changes in fast fission factor starting at essentially identical values, means the decline is unique to the PuTh fuel type.

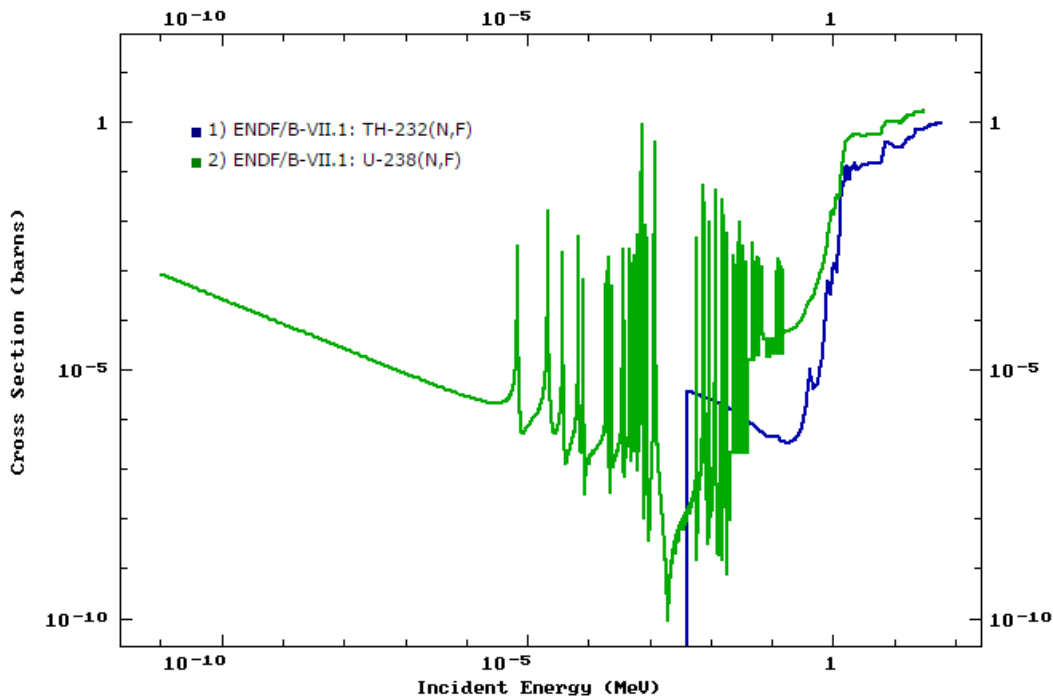


Figure 31: IAEA ENDF (n,f) cross section data for Th232 and U238 nuclides

The largest difference between PuTh and the other two fuel types is the presence of Thorium. ²³²Th does not fission below around 400eV, but ²³⁸U does, leaving a large portion of fast neutrons under-utilized by the PuTh fuel. As the fuels are burnt, the number of fast fissions occurring in the initial fissile nuclides decreases and the relative importance of fast fissions in the fertile nuclides increases. This leads to a decrease in the fast fission factor, caused by the fuel temperature increasing and Doppler broadening the resonances and absorption peaks. The result is that the change in fast fission factor decreases more rapidly for PuTh than for the other two fuel types.

5.6 Validity

Two papers have been particularly helpful in verifying the accuracy of the data. The first is a benchmark of various computer codes' evaluations of the SCWR fuel lattice by Sharpe et al. (22). The second is a journal paper by Moghrabi and Novog (23) that discussed the coefficients of reactivity at zero burn-up using NEWT.

The Sharpe et al. benchmarks cover 10 reactor heights (increments of 500mm starting at 250mm) over three burn-ups (0, 25, and 50 MWd/kgIHM) for 5 lattice codes, and in particular TRITON-NEWT. The most useful point of comparison is the multiplication factor. Although the heights used in this work and the heights in the Sharpe et al. benchmark do not align perfectly, they are quite close. In particular, the 125, 2375, and 4875mm results in this work will be compared to their closest neighbours from the benchmark, the 250, 2250, and 4750mm results.

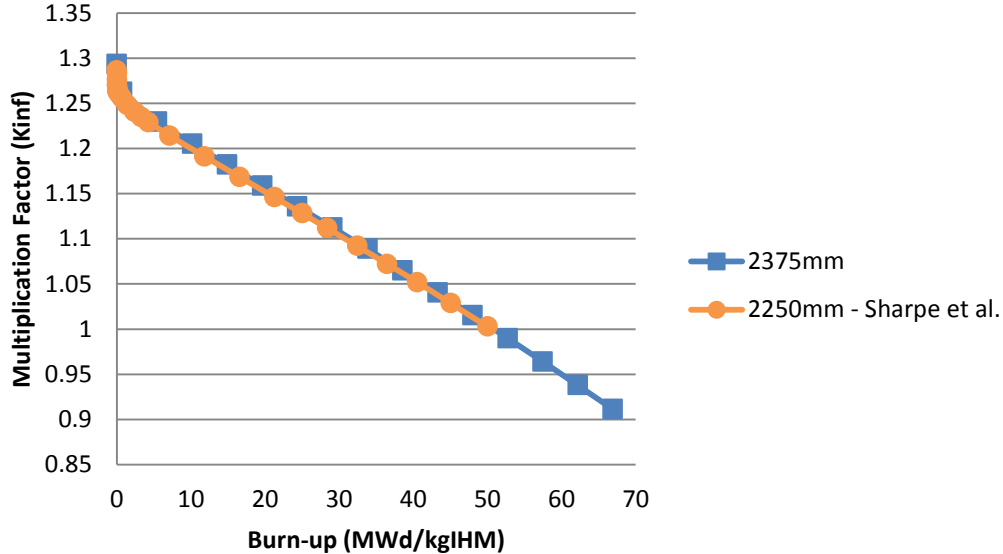


Figure 32: Comparison of Multiplication Factors to Sharpe et al. Benchmark

For the multiplication factor, the results are extremely similar for all three heights, although the lower and upper data points were excluded from Figure 32: Comparison of Multiplication Factors to Sharpe et al. Benchmark to improve clarity. The largest difference between the two data sets is the fission product

shoulder at $<1\text{MWd/kgIHM}$. The k_{inf} of Sharpe et al. decreases slightly more than the data in this work, but they realign around 10MWd/kgIHM . This difference is due to the much smaller amount of time steps in this region for this work. As fission products build up, the accuracy of their concentration and effects can be influenced by the discreteness of the time-steps used. Sharpe et al. used a smaller time-step, so it is possible that the present work is less accurate in the tracking of fission products early in the fuel's life.

However, this error is quite small, and is recovered from quite quickly, so it is unlikely that any significant influence has resulted. Additionally, the multiplication factors agree well for all other areas of burn-up, indicating that the results are similar, except for this very small region. Additionally, because the MOX and UO_2 fuels' input files are essentially identical to the PuTh fuel's input file, their results can be trusted, as well. The sole difference between the three fuel types is the one-to-one substitution of the fuel composition.

Sharpe and colleagues also analyzed the Coefficient of Void Reactivity. Once again, the heights were compared as closely as possible; however, the benchmark only gives results for 0, 25, and 50 MWd/kgIHM . In Figure 33, it is clear that the three CVRs follow the same general trends, even though the benchmark data is relatively granular. However, the magnitudes of the data differ fairly significantly.

The cause of this difference is likely the difference in Dancoff Factor handling between the two models. In the Sharpe et al. paper, all Dancoff Factors were handled by SCALE's internal model. In this work, the Dancoff Factors were interpreted using a more complicated but potentially more accurate custom solution as discussed in the Methodology: Dancoff Factors section. This might have led to significant differences in results, especially at low coolant densities, which is the case with CVR data.

As a result, because the data is similar in trend and the magnitudes are not entirely different, we can infer that the CVR data is likely to be accurate, as well. This also extends to the MOX and UO_2 fuels. As was the case for the multiplication factors, the only difference between the calculation of the PuTh CVRs and the MOX and UO_2 CVRs is the one-to-one replacement of the fuel composition.

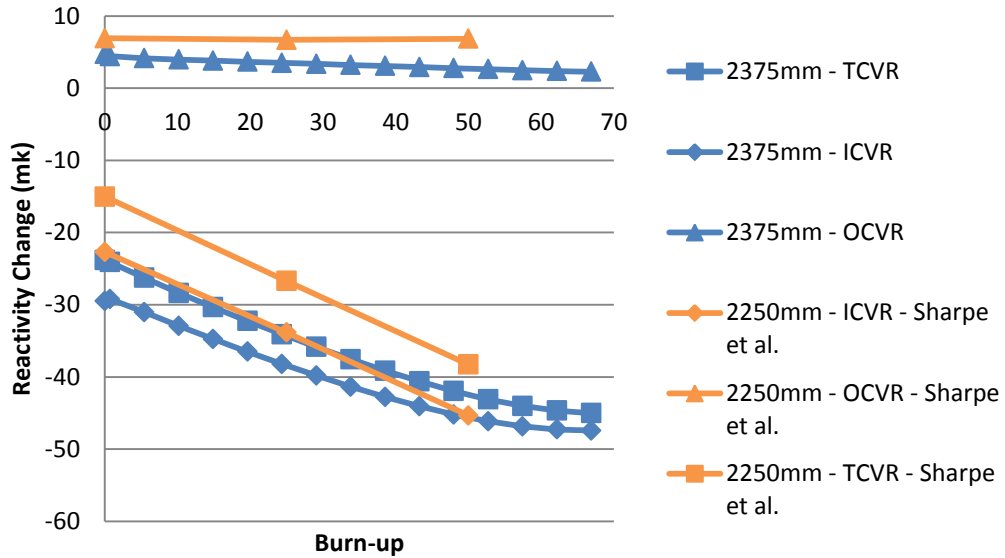


Figure 33: Comparison of CVRs to Sharpe et al. Benchmark

The Moghrabi paper has most of the reactivity coefficients that are analyzed in this work, with the exception of the inner and outer CTCs. Unlike the Sharpe et al. benchmark, the coefficients were only reported for the zero burn-up case. Although the data do not allow comparison over burn-up, they can verify the initial values of each reactivity coefficient. The Moghrabi data are presented in Table 3 alongside the data from this work, and the percent difference between the two.

Table 3: Comparison of four factors and multiplication factor to Moghrabi paper

		Reference	ICVR	OCVR	TCVR	FTC	TCTC	MTC
250mm Moghrabi	η	1.73674	1.74063	1.733649	1.733527	1.736792	1.739519	1.73707
	f	0.861505	0.845584	0.852373	0.837073	0.861488	0.857869	0.860695
	ρ	0.675033	0.748288	0.691065	0.77672	0.675911	0.675418	0.675067
	ϵ	1.276447	1.184185	1.249054	1.137148	1.27623	1.276894	1.276626
	k_{inf}	1.289201	1.314985	1.27618	1.303782	1.290671	1.287022	1.288479
4750mm Moghrabi	η	1.739422	1.740848	1.738344	1.738848	1.739474	1.741301	1.739909
	f	0.867537	0.848512	0.866366	0.847159	0.867511	0.864258	0.866808
	ρ	0.655916	0.743632	0.655693	0.74472	0.656631	0.656146	0.655968
	ϵ	1.302981	1.184775	1.300597	1.18127	1.302851	1.303619	1.303111
	k_{inf}	1.289671	1.317915	1.284332	1.313079	1.290948	1.287272	1.289181
125mm	η	1.736565	1.731548	1.740518	1.740327	1.736497	1.733001	1.734549
	f	0.860693	0.882152	0.872264	0.893299	0.860716	0.865497	0.865503
	ρ	0.682028	0.593997	0.659225	0.561292	0.680788	0.679362	0.679637
	ϵ	1.272881	1.393966	1.31039	1.466273	1.273249	1.273202	1.27275
	k_{inf}	1.297565	1.264779	1.311477	1.279475	1.295564	1.297366	1.2986
4875mm	η	1.73921	1.737288	1.74039	1.739378	1.739133	1.736775	1.736132
	f	0.866498	0.892716	0.867624	0.89415	0.86653	0.870935	0.870817
	ρ	0.658082	0.553151	0.656719	0.551564	0.657206	0.657781	0.657724
	ϵ	1.302297	1.461655	1.305514	1.466415	1.302495	1.301413	1.301586
	k_{inf}	1.291545	1.253931	1.294611	1.257933	1.290013	1.294869	1.294274
Percent difference of 250mm and 125mm	η	0.010077	0.523147	0.395456	0.391494	0.016993	0.375392	0.145234
	f	0.094298	4.233008	2.306683	6.498752	0.089626	0.885192	0.557041
	ρ	1.030904	22.98925	4.716029	32.2012	0.719019	0.582269	0.674723
	ϵ	0.27976	16.27372	4.79288	25.28401	0.233852	0.289539	0.304051
	k_{inf}	0.646676	3.892296	2.7281	1.881877	0.378412	0.80048	0.782423
Percent difference of 4750mm and 4875mm	η	0.012189	0.204726	0.117654	0.030476	0.019616	0.260234	0.217318
	f	0.119836	5.077346	0.145119	5.397256	0.113143	0.769631	0.461403
	ρ	0.329681	29.37742	0.156355	29.80156	0.087538	0.248938	0.267266
	ϵ	0.052509	20.92483	0.377379	21.53923	0.027306	0.1694	0.117119
	k_{inf}	0.145203	4.97571	0.797167	4.289792	0.072436	0.58841	0.394284

For the most part, the data match quite closely to that of the Moghrabi paper. The reference cases and the temperature coefficients of reactivity are all within less than one percent error of each other. The only cases that exceed one percent error are the CVRs. The work by Moghrabi also utilized SCALE's internal handling of Dancoff Factors, so there is expected to be some error when working at low densities. Therefore the difference between the two data sets for the CVRs is not problematic.

Chapter 6: Conclusions

Development of the Canadian SCWR design has largely relied upon the assumption of using a PuTh fuel type. Although this method was questioned in the early stages of design, the PuTh fuel type was quickly accepted as the fuel of choice. Over time, the geometry of the reactor has changed significantly, but no further analyses for the choice of fuel have taken place.

The present work re-evaluates whether the well-adopted PuTh mixture continues to be the best choice of fuel for the Canadian SCWR. To do this, UO_2 , MOX, and PuTh fuels' coefficients of reactivity and multiplication factors were considered for the normal operating conditions over the height of the core from zero burn-up to 67 MWd/kgIHM.

In evaluating the UO_2 fuel, the main drawback was its multiplication factor. UO_2 decreases in reactivity much more quickly than the PuTh or MOX fuels, resulting in the need for a higher initial reactivity. This leads to an increased cost for continued operation when compared to the lower enrichments typically used in modern-day power reactors.

Due to the rapid decrease in the multiplication factor, the UO_2 fuel's reactivity coefficients become non-linear near the end of cycle. This behaviour is undesirable, as a linear trend is more predictable and makes normal reactor operation easier to plan.

The non-linear behaviour of the UO_2 fuel also makes it more difficult to balance operation when refueling is considered. With three batches of fuel at different stages in their lifetimes, having consistent fuel performance for all three batches makes refueling a less difficult task.

The main advantage of the UO_2 fuel is that it has a smaller magnitude for all the reactivity coefficients evaluated. This makes the reactor less responsive to small perturbations in temperatures or densities and therefore easier to operate in normal conditions. However, this is also a disadvantage for the negative reactivity coefficients when transients are considered. When large changes occur in the reactor, it is desirable for the reactor to return to safe power levels as

quickly as possible and negative reactivity coefficients with a larger magnitude are more helpful in this regard.

While the UO_2 fuel is quite distinct from the MOX and PuTh fuels, the plutonium-based fuels are actually very similar. There are not many distinguishing features between these two fuel types in terms of the reactivity coefficients and multiplication factor, so much of their value is relative to the performance of the UO_2 fuel.

The PuTh and MOX fuels have more constant multiplication factors over burn-up than the UO_2 fuel. As discussed for the UO_2 fuel, this would lead to easier operation and refuelling planning, as well as being more economically favourable. These fuels also have more negative FTC and CVRs than the UO_2 that would improve their response to transients.

Because the coefficients of reactivity are so similar, the distinction between the two fuels is largely in composition. MOX fuels have more operational experience than PuTh fuels, which would likely lead to lower costs of adoption. Thorium is also chemically harder to process than uranium, making the PuTh fuel likely to be more expensive than the MOX fuel. However, the abundance of thorium in comparison to uranium might tend to reduce the lifetime cost of a PuTh reactor, if the construction of the plant were timed appropriately with a decrease in the supply of uranium.

Overall, these considerations support the continuing use of PuTh in the Canadian SCWR. However, due to the similarities in the MOX and PuTh fuel's behaviours, it seems that more research into the performance of MOX fuels in the SCWR might be warranted. Additionally, it is clear that the UO_2 fuel would not be a good choice of fuel for this reactor type. Although the UO_2 does have some advantages, the increased enrichment compared to present-day power-reactor fuels and the increased cost associated make it a less desirable fuel.

Chapter 7: Future Work

There are quite a few areas in which this work could be expanded, especially if a definitive decision on fuel composition is needed. The first major avenue would be an analysis of key reactor transients. In reactor design there is a lot of emphasis on how safely various accident scenarios are handled, and this should take into account the composition of the fuel.

It would also be valuable to consider fuel compositions other than the three analyzed in this work. It would be interesting to see similar analyses for a U-Th fuel and Accident Tolerant Fuels such as Uranium Nitrides or Silicides, as well as exploring various cladding options.

Much of the analyses of the reactivity coefficients relied on inferences based on changes of the four factors, so it would be valuable to perform a more extensive sensitivity study. There may be unexpected, underlying effects that are not immediately noticeable, but would be revealed by perturbing various cross-sections. For example, the unique decline in fast fission factor for the PuTh fuel caused by an increase fuel temperature factor would be a prime candidate for a sensitivity study.

While increasing the resolution of the time steps, meshing, and elevation heights will greatly increase the computational time and are unlikely to significantly alter the results of this work, this would increase its accuracy and make it a more useful reference for future works.

References

1. *The Evolution of CANDU Fuel Cycles and their Potential Contribution to World Peace*. **Whitlock, Jeremy J.** Bratislava, Slovakia : International Youth Nuclear Congress, 2000.
2. *Evolution of the Canadian SCWR Fuel-Assembly Concept and Assessment of the 64 Element Assembly for Thermalhydraulic Performance*. **Armando Nava Domínguez, Nihan Onder, Yanfei Rao, and Laurence Leung.** 2016, CNL Nuclear Review, p. 18.
3. *Power Flattening and Reactivity Suppression Strategies for the Canadian Supercritical Water Reactor Concept*. **MacDonald, M., Colton, A. and Pencer, J.** Saint John, NB, Canada : 35th Annual Conference of the Canadian Nuclear Society, 2015.
4. *Pre Conceptual Fuel Design Concepts for the Canadian Super Critical Water Reactor*. **McDonald, M.H., et al., et al.** Vancouver, BC, Canada : Proceedings of the 5th International Symposium on SCWR, 2011.
5. *Assessment of Candidate Fuel Cladding Alloys for the Canadian Supercritical Water-cooled Reactor Concept*. **Guzonas, D., Edwards, M. and Zheng, W.** Helsinki, Finland : The 7th International Symposium on Supercritical Water-cooled Reactors, 2015. ISSCWR7-90.
6. *Subchannel Analysis of CANDU-SCWR Fuel*. **Li, Changying, Shan, Jianqiang and Leung, Laurence K.H.** s.l. : Elsevier, 2009, Vol. Progress in Nuclear Energy.
7. *Spatial and Bulk Reactivity Systems Design and Optimization for the Canadian SuperCritical Water Reactor*. **Salaun, Frederic and Novog, David Raymond.** Hamilton, ON : CNL Nuclear Review, 2016. CNR.2016.00037.
8. **Atomic Energy of Canada Limited.** *Parameters for Transient Response Modeling for the Canadian SCWR*. Chalk River, ON, Canada : AECL, 2013. 217-123700-REPT-011.
9. *Conceptual Plant Layout of the Canadian Generation IV SuperCritical Water-cooled Reactor*. **Gaudet, M., Yetisir, M. and Sartipi, A.** Chalk River : Canadian Nuclear Laboratories, 2016.

10. **Hummel, David W.** Coupled Neutronic-Thermalhydraulic Transient Behaviour of a Pressure Tube Type Supercritical Water-cooled Reactor. Hamilton, ON, Canada : McMaster University, 2015.
11. **Grande, Lisa Christine.** Thermal Aspects of Using Alternative Nuclear Fuels in Supercritical Water-cooled Reactors. s.l. : University of Ontario Institute of Technology, 2010.
12. **Peiman, Wargha, Piro, Igor and Gabriel, Kamiel.** Thermal Aspects of Conventional and Alternative Fuels in SuperCritical Water-Cooled Reactor (SCWR) Applications. [book auth.] Prof. Amir Mesquita. *Nuclear Reactors*. s.l. : InTech, 2012.
13. *Neutronics Assessment of Thorium-based Fuel Assembly in SCWR.* **Liu, Shichang and Cai, Jiejun.** s.l. : Elsevier, 2013, Vol. Nuclear Engineering and Design.
14. *Neutronic and Thermohydraulic Characteristics of a New Breeding Thorium-Uranium Mixed SCWR Fuel Assembly.* **Liu, Shichang and Cai, Jiejun.** s.l. : Elsevier, 2013, Vol. Annals of Nuclear Energy.
15. **International Atomic Energy Agency.** *IAEA-TECDOC-1405 Thorium Fuel Cycle-Potential Benefits and Challenges.* 2005.
16. *Reactor Physics Studies for a Pressure Tube Supercritical Water Reactor (PT-SCWR).* **Boczar, P. G., et al., et al.** Toronto : 2nd Canada-China Joint Workshop on Supercritical Water-Cooled Reactors (CCSC-2010), 2010.
17. *Progression of the Lattice Physics Concept for the Canadian Supercritical Water Reactor.* **Pencer, J. and Colton, A.** Toronto, ON, Canada : Proceedings of the 34th Annual Conference of the Canadian Nuclear Society, June 9-12, 2013.
18. *Thorium Fuel Cycles in the CANDU Supercritical Water Reactor.* **Magill, Martin, et al., et al.** Vancouver, Canada : The 5th International Symposium on Supercritical Water-cooled Reactors, March 13-16, 2011.
19. **McDonald, Michael.** *Fuel and Core Physics Considerations for a Pressure Tube Supercritical Water Cooled Reactor.* Hamilton, ON, Canada : McMaster University, 2011.

20. **Harrison, Genevieve and Marleau, Guy.** *Simulation Strategy for the Evaluation of Neutronic Properties of a Canadian SCWR Fuel Channel.* s.l. : Science and Technology of Nuclear Installations, 2013.
21. *Core Neutronics for the Canadian SCWR Conceptual Design.* **Pencer, J., et al., et al.** Shenzhen, Guangdong, China : the 6th International Symposium on Supercritical Water-cooled Reactors (ISSCWR-6), 2013.
22. *A Benchmark Comparison of the Canadian Supercritical Water-cooled Reactor (SCWR) 64-element Fuel Lattice Cell Parameters using Various Computer Codes.* **Sharpe, J., et al., et al.** 2015, 35th Annual Conference of the Canadian Nuclear Society.
23. *Investigation of Reactivity Physics Phenomena in the Canadian Pressure Tube Supercritical-Water Reactor.* **Moghrabi, Ahmad and Novog, David.** 2016, CNL.
24. *Investigation of Fuel Burnup Impacts on Nuclear Reactor Safety Parameters in the Canadian Pressure Tube Supercritical Water-cooled Reactor.* **Moghrabi, Ahmad and Novog, David.** s.l. : Journal of Nuclear Engineering and Radiation Science, 2017.
25. *Coupled 3D Neutron Kinetics and Thermalhydraulic Characteristics of the Canadian Supercritical Water Reactor.* **Hummel, David and Novog, David.** s.l. : Nuclear Engineering and Design, 2015, Vol. 298.
26. *A Solid Moderator Physics Assessment for the Canadian SCWR.* **Colton, Ashlea and Pencer, Jeremy.** Chalk River, ON, Canada : Canadian Nuclear Laboratories, 2016.
27. **Jessee, M. A. and DeHart, M. D.** NEWT: A New Transport Algorithm for Two-Dimensional Discrete-Ordinates Analysis in Non-Orthogonal Geometries. s.l. : Oak Ridge National Laboratory, June 2011. Tech. Rep. ORNL/TM-2005/39 Version 6.1 Set. F21.
28. —. Triton: A Multipurpose Transport, Depletion, and Sensitivity and Uncertainty Analysis Module. s.l. : Oak Ridge National Laboratory, June 2011.
29. **Oak Ridge National Laboratory.** Scale: A Comprehensive Modeling and Simulation Suite for Nuclear Safety Analysis and Design. s.l. : Available from

Radiation Safety Information Computational Center at Oak Ridge National Laboratory as CCC-785, June 2011. ORNL/TM-2005/39.

30. **Feher, S. and Valko, J.** DANCOFF-MC: A program to calculate Dancoff factors in CANDU type fuel bundles. Netherlands : s.n., 1992. IRI-131--92-011.

31. *The Effect of Dancoff Equivalent Pitch on Voided CANDU and SCWR Lattice Cells.* **Glanfield, E. M. and Novog, D. R.** Toronto, Ontario : 36th Annual Conference of the Canadian Nuclear Society/40th Annual CNS/CNA Student Conference, 2016.

Appendix A: Raw Data

A.1 PuTh

A.1.1 125mm

	Reference Case				
	eta	f	p	eps	k _{inf}
0 days	1.736565	0.860693	0.682028	1.272881	1.297565
15 days	1.6871	0.861351	0.678893	1.280153	1.262945
115 days	1.653816	0.860054	0.677614	1.276587	1.230398
215 days	1.632299	0.858387	0.676596	1.272315	1.206165
315 days	1.611275	0.856526	0.675843	1.267983	1.182686
415 days	1.589965	0.854465	0.675352	1.263609	1.159377
515 days	1.568058	0.852181	0.67509	1.259257	1.135978
615 days	1.545343	0.849648	0.675024	1.25498	1.112296
715 days	1.52167	0.84684	0.675139	1.250823	1.088205
815 days	1.496939	0.843728	0.675433	1.246811	1.063628
915 days	1.471105	0.840274	0.675852	1.243025	1.038476
1015 days	1.444153	0.836449	0.676419	1.239468	1.012754
1115 days	1.416133	0.83222	0.677135	1.236168	0.986495
1215 days	1.387158	0.827552	0.677944	1.233205	0.959733
1315 days	1.356864	0.822457	0.678873	1.230659	0.932344
1415 days	1.32672	0.816853	0.67993	1.228359	0.905133

Total Coolant Void

	eta	f	p	eps	kinf
0 days	1.740327	0.893299	0.561292	1.466273	1.279475
15 days	1.684073	0.893955	0.556551	1.47815	1.238511
115 days	1.647253	0.892842	0.555622	1.472392	1.203201
215 days	1.622752	0.891402	0.555024	1.46524	1.176375
315 days	1.598828	0.889791	0.55471	1.457983	1.150556
415 days	1.574692	0.888002	0.55468	1.450646	1.125158
515 days	1.550009	0.88602	0.554879	1.44335	1.099885
615 days	1.52456	0.883829	0.555262	1.436177	1.074529
715 days	1.498221	0.881408	0.555809	1.429187	1.048981
815 days	1.470931	0.878738	0.556526	1.422404	1.023199
915 days	1.442692	0.875797	0.557325	1.415946	0.997086
1015 days	1.413562	0.872563	0.55825	1.409784	0.970718
1115 days	1.383671	0.869016	0.559305	1.403931	0.944181
1215 days	1.3532	0.865137	0.560394	1.398503	0.917495
1315 days	1.321743	0.860947	0.561567	1.393635	0.890582
1415days	1.291113	0.856368	0.562831	1.388924	0.864333

Inner Coolant Void

	eta	f	p	eps	kinf
0 days	1.731548	0.882152	0.593997	1.393966	1.264779
15 days	1.680404	0.882762	0.592464	1.403415	1.233405
115 days	1.646169	0.881405	0.591035	1.398721	1.199483
215 days	1.623321	0.879704	0.58992	1.392996	1.173501
315 days	1.60095	0.877823	0.589088	1.387161	1.148396
415 days	1.57833	0.87575	0.588564	1.381192	1.123636
515 days	1.555141	0.873466	0.588298	1.375207	1.098959
615 days	1.53117	0.870952	0.588247	1.369291	1.074171
715 days	1.50629	0.868183	0.588395	1.363503	1.049167
815 days	1.480432	0.865133	0.588756	1.357853	1.023904
915 days	1.453579	0.861778	0.58922	1.352512	0.998282
1015 days	1.425771	0.858091	0.589854	1.347421	0.972369
1115 days	1.39711	0.854045	0.590673	1.342585	0.946238
1215 days	1.36775	0.849622	0.591557	1.33818	0.919906
1315 days	1.337239	0.844845	0.592578	1.334283	0.893264
1415 days	1.30739	0.839626	0.593755	1.330546	0.867219

Outer Coolant Void

	eta	f	p	eps	kinf
0 days	1.740518	0.872264	0.659225	1.31039	1.311477
15 days	1.688631	0.872982	0.654966	1.319227	1.273734
115 days	1.654004	0.871833	0.65379	1.315248	1.239984
215 days	1.63162	0.87032	0.65291	1.310391	1.214932
315 days	1.609786	0.868618	0.652317	1.30546	1.190748
415 days	1.587688	0.866725	0.651997	1.300488	1.166805
515 days	1.565006	0.86462	0.651909	1.295543	1.142826
615 days	1.541524	0.862281	0.652016	1.290681	1.118606
715 days	1.517096	0.859685	0.652301	1.285948	1.094016
815 days	1.491625	0.856807	0.652757	1.281372	1.068979
915 days	1.465075	0.85361	0.653333	1.277028	1.04341
1015 days	1.437442	0.850072	0.654045	1.272926	1.017319
1115 days	1.408788	0.846164	0.65489	1.269093	0.990744
1215 days	1.379244	0.841849	0.655814	1.265603	0.963726
1315 days	1.348476	0.837141	0.656838	1.262553	0.936158
1415 days	1.31793	0.831964	0.657961	1.259753	0.908831

Total Coolant Temperature

	eta	f	p	eps	kinf
0 days	1.733001	0.865497	0.679362	1.273202	1.297366
15 Days	1.685864	0.866109	0.67839	1.279177	1.267082
115 days	1.653698	0.864851	0.677108	1.275427	1.235125
215 days	1.632815	0.863242	0.676086	1.271049	1.21125
315 days	1.612402	0.861446	0.675329	1.266616	1.188123
415 days	1.59171	0.859453	0.674835	1.262137	1.165173
515 days	1.570437	0.857243	0.674571	1.257678	1.142145
615 days	1.548375	0.854789	0.674501	1.253291	1.118844
715 days	1.525378	0.852065	0.674612	1.249017	1.095147
815 days	1.501342	0.849039	0.674903	1.244883	1.070972
915 days	1.476218	0.845676	0.675319	1.240971	1.046224
1015 days	1.449978	0.841941	0.675882	1.237285	1.020901
1115 days	1.42266	0.837799	0.676595	1.233853	0.995023
1215 days	1.394357	0.833213	0.6774	1.230761	0.96861
1315 days	1.364701	0.828188	0.678326	1.228085	0.941527
1415 days	1.335091	0.822639	0.679379	1.225672	0.914548

Inner Coolant Temperature

	eta	f	p	eps	kinf
0 days	1.735012	0.864433	0.679139	1.273322	1.296973
15 days	1.686557	0.865068	0.678697	1.279185	1.266662
115 days	1.653783	0.863787	0.677417	1.275542	1.234344
215 days	1.632519	0.862145	0.676398	1.271234	1.210226
315 days	1.611732	0.860312	0.675643	1.26687	1.186858
415 days	1.59066	0.85828	0.675152	1.262462	1.163661
515 days	1.568994	0.856028	0.67489	1.258076	1.140377
615 days	1.546523	0.853529	0.674823	1.253764	1.116812
715 days	1.5231	0.850757	0.674936	1.249568	1.092841
815 days	1.498623	0.847683	0.67523	1.245516	1.068384
915 days	1.473045	0.84427	0.675648	1.241688	1.043351
1015 days	1.446346	0.840486	0.676215	1.238087	1.017745
1115 days	1.418573	0.836299	0.676931	1.234741	0.991593
1215 days	1.389831	0.831673	0.677739	1.231732	0.964924
1315 days	1.359751	0.826617	0.678668	1.229138	0.937609
1415 days	1.329781	0.821047	0.679725	1.226796	0.910444

Outer Coolant Temperature

	eta	f	p	eps	kinf
0 days	1.734589	0.861772	0.679563	1.273983	1.294142
15 days	1.686398	0.862406	0.678591	1.280135	1.263384
115 days	1.653736	0.861131	0.67731	1.27646	1.231204
215 days	1.632611	0.859498	0.676289	1.272116	1.20722
315 days	1.61197	0.857674	0.675534	1.267713	1.183988
415 days	1.591051	0.855653	0.675041	1.263266	1.160931
515 days	1.569549	0.853411	0.674777	1.258838	1.137793
615 days	1.547253	0.850924	0.674708	1.254485	1.11438
715 days	1.524018	0.848163	0.67482	1.250246	1.090568
815 days	1.499741	0.8451	0.675112	1.24615	1.066279
915 days	1.474372	0.841696	0.675528	1.242277	1.041416
1015 days	1.447891	0.837919	0.676092	1.238633	1.015982
1115 days	1.420338	0.833735	0.676805	1.235244	0.990003
1215 days	1.391814	0.829106	0.677611	1.232195	0.963499
1315 days	1.361954	0.824041	0.678537	1.229564	0.936345
1415 days	1.332178	0.818456	0.67959	1.22719	0.909319

Moderator Temperature

	eta	f	p	eps	kinf
0 days	1.734549	0.865503	0.679637	1.27275	1.2986
15 days	1.686287	0.866149	0.678665	1.278883	1.267681
115 days	1.653639	0.864873	0.677384	1.275221	1.235417
215 days	1.632646	0.863233	0.676364	1.270874	1.211442
315 days	1.612118	0.8614	0.675609	1.266472	1.188209
415 days	1.591291	0.859368	0.675117	1.262029	1.165138
515 days	1.569861	0.857113	0.674855	1.257611	1.141973
615 days	1.547618	0.854612	0.674787	1.253268	1.118519
715 days	1.524411	0.851834	0.674901	1.249045	1.09465
815 days	1.500136	0.848752	0.675195	1.244967	1.070284
915 days	1.474741	0.845326	0.675613	1.241117	1.045324
1015 days	1.448201	0.841527	0.67618	1.237499	1.019774
1115 days	1.420557	0.83732	0.676896	1.23414	0.993658
1215 days	1.391909	0.832669	0.677705	1.231124	0.966998
1315 days	1.361901	0.827582	0.678634	1.228527	0.939674
1415 days	1.33195	0.821981	0.679691	1.22619	0.91247

Fuel Temperature

	eta	f	p	eps	kinf
0 days	1.736497	0.860716	0.680788	1.273249	1.295564
15 days	1.687115	0.861372	0.677686	1.280466	1.261049
115 days	1.653871	0.860075	0.676431	1.276863	1.228587
215 days	1.632379	0.858411	0.675433	1.272551	1.204409
315 days	1.611378	0.856553	0.674697	1.26818	1.180977
415 days	1.590091	0.854494	0.674221	1.263767	1.157712
515 days	1.568209	0.852212	0.673972	1.259377	1.134356
615 days	1.545517	0.849683	0.673917	1.255064	1.110715
715 days	1.521869	0.846877	0.67404	1.250871	1.086666
815 days	1.497163	0.843768	0.674341	1.246826	1.062129
915 days	1.471354	0.840316	0.674764	1.243009	1.037018
1015 days	1.444425	0.836493	0.675334	1.239424	1.011338
1115 days	1.416428	0.832266	0.676052	1.236098	0.985121
1215 days	1.387473	0.827599	0.67686	1.233112	0.958398
1315 days	1.357199	0.822504	0.677787	1.230546	0.931049
1415 days	1.327068	0.8169	0.67884	1.228229	0.903875

A.1.2 2375mm

	Reference Case				
	eta	f	p	eps	kinf
0 days	1.738591	0.868226	0.657898	1.302299	1.293301
15 days	1.688011	0.868877	0.657469	1.309087	1.262342
115 days	1.654122	0.867708	0.656217	1.305362	1.229476
215 days	1.632459	0.866183	0.655231	1.300889	1.205276
315 days	1.611373	0.864482	0.654547	1.296312	1.181959
415 days	1.590071	0.862594	0.654111	1.2917	1.158873
515 days	1.56824	0.860503	0.653905	1.287103	1.135778
615 days	1.545674	0.858189	0.653893	1.282579	1.11248
715 days	1.522225	0.855628	0.654049	1.278188	1.088852
815 days	1.497802	0.852795	0.654366	1.273961	1.064819
915 days	1.472351	0.849665	0.654832	1.269935	1.040327
1015 days	1.445883	0.8462	0.655395	1.266185	1.015328
1115 days	1.418436	0.842381	0.656093	1.262704	0.989886
1215 days	1.390124	0.838177	0.656887	1.259551	0.964041
1315 days	1.361132	0.833567	0.657782	1.256741	0.937926
1415 days	1.331202	0.828567	0.658772	1.254384	0.911459

	Total Coolant Void				
	eta	f	p	eps	kinf
0 days	1.740133	0.893449	0.553823	1.466248	1.262498
15 days	1.684606	0.894107	0.553361	1.478039	1.231921
115 days	1.648205	0.893034	0.55237	1.472489	1.197185
215 days	1.624364	0.891642	0.551679	1.465649	1.171091
315 days	1.601166	0.89009	0.551324	1.458622	1.146093
415 days	1.577814	0.88837	0.551215	1.451537	1.121499
515 days	1.55397	0.886471	0.551339	1.444472	1.097071
615 days	1.529428	0.884376	0.551649	1.437513	1.072607
715 days	1.50405	0.882068	0.55211	1.43075	1.047982
815 days	1.477778	0.879529	0.552721	1.424214	1.023152
915 days	1.450594	0.876739	0.553472	1.41794	0.99809
1015 days	1.422551	0.873676	0.554274	1.412051	0.972732
1115 days	1.393751	0.870322	0.555206	1.406481	0.947225
1215 days	1.364356	0.866659	0.556203	1.401316	0.921606
1315 days	1.334611	0.862673	0.557281	1.396548	0.896046
1415 days	1.304177	0.85839	0.558426	1.392367	0.870445

Inner Coolant Void

	eta	f	p	eps	kinf
0 days	1.736367	0.889674	0.559318	1.452673	1.255161
15 days	1.68273	0.890316	0.55881	1.463795	1.225471
115 days	1.647272	0.889165	0.557674	1.458509	1.191343
215 days	1.624042	0.887694	0.556824	1.452011	1.165597
315 days	1.601425	0.886063	0.55631	1.445292	1.140891
415 days	1.578646	0.884265	0.556045	1.438491	1.116566
515 days	1.555377	0.882285	0.556021	1.431676	1.092398
615 days	1.531414	0.880107	0.556194	1.424938	1.068194
715 days	1.506622	0.877713	0.556525	1.418373	1.043834
815 days	1.480939	0.875082	0.557018	1.412009	1.019277
915 days	1.454347	0.872193	0.557666	1.405881	0.994496
1015 days	1.426889	0.869025	0.558367	1.40014	0.969423
1115 days	1.39866	0.865555	0.559216	1.394695	0.944204
1215 days	1.369808	0.861766	0.560143	1.389652	0.918869
1315 days	1.340564	0.857641	0.561167	1.385	0.893584
1415 days	1.310562	0.853209	0.562277	1.380934	0.868233

Outer Coolant Void

	eta	f	p	eps	kinf
0 days	1.740432	0.871474	0.653428	1.311129	1.299435
15 days	1.688864	0.87214	0.653001	1.318258	1.26793
115 days	1.654451	0.871012	0.651766	1.31446	1.234575
215 days	1.632444	0.869524	0.650813	1.30987	1.210053
315 days	1.611031	0.867861	0.65017	1.305176	1.186452
415 days	1.589405	0.866011	0.649782	1.300448	1.163103
515 days	1.56725	0.86396	0.649626	1.295739	1.139758
615 days	1.544356	0.861687	0.649664	1.291108	1.116217
715 days	1.520576	0.859171	0.64987	1.286613	1.092351
815 days	1.495822	0.856387	0.650235	1.282286	1.068084
915 days	1.470039	0.853311	0.650746	1.278164	1.043361
1015 days	1.443243	0.849907	0.651355	1.274319	1.018139
1115 days	1.415481	0.846158	0.652092	1.270746	0.992483
1215 days	1.386872	0.842032	0.652922	1.267501	0.966439
1315 days	1.35761	0.837512	0.653847	1.264599	0.940145
1415 days	1.327455	0.832613	0.654858	1.262151	0.913527

Total Coolant Temperature

	eta	f	p	eps	kinf
0 days	1.735678	0.872509	0.65751	1.301622	1.296063
15 days	1.686977	0.873123	0.65708	1.308082	1.266012
115 days	1.653963	0.871983	0.655826	1.304201	1.233579
215 days	1.632765	0.8705	0.654837	1.299646	1.209624
315 days	1.612124	0.868845	0.654151	1.294989	1.186546
415 days	1.591269	0.867007	0.653713	1.290296	1.163704
515 days	1.569894	0.864971	0.653505	1.285616	1.140858
615 days	1.547794	0.862715	0.65349	1.281007	1.117818
715 days	1.524823	0.860216	0.653643	1.276526	1.094454
815 days	1.500891	0.857448	0.653957	1.272205	1.07069
915 days	1.475937	0.854385	0.65442	1.268082	1.046467
1015 days	1.449967	0.85099	0.654981	1.264231	1.021735
1115 days	1.42301	0.84724	0.655676	1.260647	0.996546
1215 days	1.395165	0.843102	0.656467	1.257393	0.970934
1315 days	1.366601	0.838552	0.65736	1.254484	0.945019
1415 days	1.337053	0.833601	0.658347	1.252035	0.91871

Inner Coolant Temperature

	eta	f	p	eps	kinf
0 days	1.736396	0.872166	0.657622	1.301532	1.296222
15 days	1.687257	0.872791	0.657193	1.308062	1.265939
115 days	1.654037	0.871643	0.655939	1.304221	1.233385
215 days	1.632707	0.870149	0.654951	1.299692	1.209348
315 days	1.611937	0.868482	0.654266	1.295061	1.186188
415 days	1.590951	0.866631	0.653829	1.290395	1.163262
515 days	1.569439	0.86458	0.653622	1.285743	1.14033
615 days	1.547197	0.862309	0.653608	1.281163	1.117199
715 days	1.524078	0.859794	0.653763	1.276711	1.093741
815 days	1.499992	0.857009	0.654078	1.272422	1.069881
915 days	1.474879	0.853929	0.654543	1.268331	1.045559
1015 days	1.448747	0.850516	0.655105	1.264514	1.020727
1115 days	1.421627	0.846749	0.655802	1.260965	0.995441
1215 days	1.393622	0.842595	0.656595	1.257744	0.969735
1315 days	1.364908	0.838031	0.657489	1.254868	0.943735
1415 days	1.335218	0.83307	0.658478	1.252449	0.917351

Outer Coolant Temperature

	eta	f	p	eps	kinf
0 days	1.737857	0.868576	0.657788	1.302386	1.293147
15 days	1.687726	0.869215	0.657359	1.309102	1.262425
115 days	1.654049	0.868055	0.656107	1.305337	1.229681
215 days	1.632523	0.866541	0.65512	1.300836	1.205567
315 days	1.611571	0.864852	0.654434	1.296232	1.182335
415 days	1.590406	0.862977	0.653998	1.291591	1.159335
515 days	1.568717	0.860902	0.653791	1.286966	1.136329
615 days	1.546298	0.858603	0.653778	1.282412	1.113124
715 days	1.523002	0.856058	0.653932	1.277989	1.089592
815 days	1.49874	0.853243	0.654248	1.273729	1.065659
915 days	1.473454	0.85013	0.654712	1.269669	1.041269
1015 days	1.447154	0.846683	0.655275	1.265884	1.016372
1115 days	1.419877	0.842881	0.65597	1.262367	0.991031
1215 days	1.39173	0.838693	0.656763	1.259179	0.965281
1315 days	1.362894	0.834096	0.657657	1.256335	0.939253
1415 days	1.33311	0.829105	0.658645	1.253945	0.912863

Moderator Temperature

	eta	f	p	eps	kinf
0 days	1.735686	0.872798	0.65757	1.301452	1.296447
15 days	1.686667	0.873417	0.657141	1.307963	1.266208
115 days	1.653559	0.872269	0.655886	1.304105	1.233705
215 days	1.632555	0.870768	0.654898	1.299523	1.209838
315 days	1.612096	0.869093	0.654211	1.294842	1.18684
415 days	1.591405	0.867231	0.653774	1.29013	1.164063
515 days	1.570179	0.865168	0.653566	1.285435	1.141272
615 days	1.548214	0.862882	0.653553	1.280813	1.118275
715 days	1.525363	0.860348	0.653707	1.276323	1.094943
815 days	1.501532	0.857541	0.654023	1.271998	1.071197
915 days	1.476659	0.854436	0.654488	1.267875	1.046978
1015 days	1.450745	0.850991	0.655051	1.26403	1.022229
1115 days	1.423818	0.847189	0.655747	1.260457	0.99701
1215 days	1.395976	0.842994	0.656541	1.257219	0.971349
1315 days	1.367391	0.838385	0.657437	1.254332	0.945371
1415 days	1.337809	0.833374	0.658426	1.251905	0.918994

	Fuel Temperature				
	eta	f	p	eps	kinf
0 days	1.738514	0.868258	0.656836	1.302524	1.291426
15 days	1.688019	0.868905	0.65641	1.309301	1.260562
115 days	1.654171	0.867738	0.655178	1.305543	1.227778
215 days	1.632533	0.866215	0.654208	1.301036	1.20363
315 days	1.61147	0.864516	0.653538	1.296425	1.180358
415 days	1.590192	0.86263	0.653114	1.291778	1.157313
515 days	1.568385	0.860542	0.652917	1.287148	1.134257
615 days	1.545842	0.858231	0.652913	1.282593	1.110999
715 days	1.522417	0.855672	0.653075	1.27817	1.087409
815 days	1.498019	0.852842	0.653396	1.273914	1.063415
915 days	1.472593	0.849714	0.653865	1.269861	1.038962
1015 days	1.446149	0.846252	0.65443	1.266085	1.014002
1115 days	1.418725	0.842435	0.655127	1.262581	0.988597
1215 days	1.390434	0.838232	0.65592	1.259407	0.96279
1315 days	1.36146	0.833623	0.656813	1.256579	0.936711
1415 days	1.331545	0.828623	0.657799	1.254206	0.910279

A.1.3 4875mm

	Reference Case				
	eta	f	p	eps	kinf
0 days	1.73921	0.866498	0.658082	1.302297	1.291545
15 days	1.688646	0.867136	0.657679	1.309034	1.26064
115 days	1.654707	0.865995	0.656497	1.305186	1.227841
215 days	1.633013	0.864501	0.655579	1.300606	1.203721
315 days	1.611876	0.862833	0.654955	1.295938	1.180468
415 days	1.590517	0.86098	0.654574	1.291245	1.15744
515 days	1.568623	0.858927	0.654414	1.286579	1.134394
615 days	1.545986	0.856653	0.654441	1.281999	1.111139
715 days	1.522455	0.854133	0.654629	1.277561	1.087544
815 days	1.497935	0.851345	0.654969	1.273302	1.063532
915 days	1.472367	0.848263	0.655448	1.26926	1.039048
1015 days	1.445759	0.844846	0.656023	1.265505	1.014042
1115 days	1.418148	0.841079	0.656718	1.262038	0.988577
1215 days	1.389653	0.836929	0.657503	1.258915	0.962696
1315 days	1.360459	0.832376	0.658387	1.25615	0.936544
1415 days	1.330318	0.827432	0.659338	1.253868	0.910014

	Total Coolant Void				
	eta	f	p	eps	kinf
0 days	1.739378	0.89415	0.551564	1.466415	1.257933
15 days	1.684621	0.894794	0.551111	1.477987	1.227819
115 days	1.648521	0.893741	0.550148	1.472246	1.193345
215 days	1.624938	0.892372	0.549479	1.465244	1.167465
315 days	1.601981	0.890846	0.549137	1.458064	1.14266
415 days	1.578861	0.889156	0.549035	1.450834	1.118252
515 days	1.555244	0.887289	0.549161	1.443629	1.094004
615 days	1.530923	0.885228	0.549469	1.436542	1.069718
715 days	1.505752	0.882956	0.549922	1.429661	1.045266
815 days	1.479666	0.880455	0.550521	1.423023	1.020603
915 days	1.452638	0.877703	0.551256	1.416669	0.995697
1015 days	1.424713	0.874679	0.552038	1.410724	0.970481
1115 days	1.395984	0.871363	0.552945	1.405128	0.945098
1215 days	1.366611	0.867736	0.553912	1.399969	0.919585
1315 days	1.336833	0.863782	0.554973	1.39523	0.894127
1415 days	1.306298	0.859529	0.556064	1.391151	0.868564

	Inner Coolant Void				
	eta	f	p	eps	kinf
0 days	1.737288	0.892716	0.553151	1.461655	1.253931
15 days	1.683595	0.893346	0.55268	1.472903	1.224349
115 days	1.648023	0.892264	0.551664	1.467235	1.190231
215 days	1.624788	0.890869	0.550934	1.46034	1.164567
315 days	1.602167	0.889318	0.55053	1.45325	1.139951
415 days	1.579383	0.887604	0.550365	1.446095	1.115719
515 days	1.556105	0.885713	0.550431	1.43895	1.091644
615 days	1.53213	0.883628	0.550682	1.431908	1.067532
715 days	1.507312	0.881332	0.551082	1.42506	1.043259
815 days	1.481587	0.878805	0.551631	1.418443	1.01878
915 days	1.454925	0.876026	0.552323	1.412096	0.994065
1015 days	1.427365	0.872973	0.55306	1.406159	0.969042
1115 days	1.398996	0.869623	0.553931	1.400559	0.943854
1215 days	1.36997	0.865958	0.554867	1.395398	0.918533
1315 days	1.340514	0.86196	0.555905	1.390654	0.89326
1415 days	1.310261	0.857657	0.556977	1.386577	0.867865

Outer Coolant Void					
	eta	f	p	eps	kinf
0 days	1.74039	0.867624	0.656719	1.305514	1.294611
15 days	1.689179	0.868275	0.656316	1.312419	1.263335
115 days	1.65491	0.867146	0.655138	1.308565	1.230253
215 days	1.633	0.865661	0.65423	1.303956	1.205945
315 days	1.611653	0.864002	0.653622	1.299261	1.182522
415 days	1.590085	0.862156	0.653259	1.294542	1.159331
515 days	1.567978	0.860111	0.653119	1.289852	1.136126
615 days	1.545125	0.857844	0.653166	1.285251	1.112714
715 days	1.521371	0.855333	0.653375	1.280794	1.08896
815 days	1.496624	0.852554	0.653735	1.276519	1.06479
915 days	1.470826	0.849484	0.654234	1.272463	1.040146
1015 days	1.443989	0.846081	0.654827	1.268694	1.014984
1115 days	1.416153	0.842332	0.65554	1.265215	0.989366
1215 days	1.387443	0.838203	0.656341	1.262079	0.963342
1315 days	1.358052	0.833679	0.657238	1.2593	0.937058
1415 days	1.327739	0.82877	0.658199	1.257002	0.910416

Total Coolant Temperature					
	eta	f	p	eps	kinf
0 days	1.736775	0.870935	0.657781	1.301413	1.294869
15 days	1.687823	0.871545	0.657377	1.307861	1.264716
115 days	1.654628	0.870427	0.656193	1.303885	1.232264
215 days	1.633311	0.868967	0.655273	1.299242	1.208328
315 days	1.612533	0.867337	0.654648	1.294515	1.185253
415 days	1.591533	0.865525	0.654264	1.289762	1.162406
515 days	1.57	0.863516	0.654103	1.285035	1.139544
615 days	1.547732	0.861289	0.654128	1.280392	1.116478
715 days	1.524574	0.85882	0.654314	1.275888	1.093073
815 days	1.500434	0.856084	0.654652	1.27156	1.069254
915 days	1.475246	0.853056	0.65513	1.267447	1.044959
1015 days	1.449015	0.849696	0.655702	1.263617	1.020138
1115 days	1.421769	0.845985	0.656396	1.260076	0.994843
1215 days	1.393615	0.841888	0.657179	1.256879	0.969113
1315 days	1.364725	0.837385	0.658061	1.254043	0.943081
1415 days	1.334845	0.832482	0.659011	1.251695	0.916635

Inner Coolant Temperature

	eta	f	p	eps	kinf
0 days	1.73678	0.870933	0.657783	1.301416	1.294876
15 days	1.687825	0.871543	0.657379	1.307865	1.264722
115 days	1.654628	0.870425	0.656196	1.303888	1.232269
215 days	1.633311	0.868965	0.655276	1.299245	1.208332
315 days	1.612532	0.867335	0.65465	1.294518	1.185257
415 days	1.59153	0.865523	0.654267	1.289765	1.162408
515 days	1.569997	0.863514	0.654106	1.285038	1.139546
615 days	1.547727	0.861286	0.654131	1.280395	1.116479
715 days	1.524569	0.858817	0.654317	1.275891	1.093074
815 days	1.500428	0.856082	0.654655	1.271564	1.069254
915 days	1.475239	0.853054	0.655133	1.26745	1.044958
1015 days	1.449007	0.849693	0.655705	1.263621	1.020136
1115 days	1.421759	0.845982	0.656399	1.26008	0.99484
1215 days	1.393604	0.841885	0.657182	1.256883	0.96911
1315 days	1.364713	0.837381	0.658064	1.254047	0.943076
1415 days	1.334832	0.832478	0.659014	1.251699	0.91663

Outer Coolant Temperature

	eta	f	p	eps	kinf
0 days	1.739205	0.8665	0.65808	1.302294	1.291538
15 days	1.688645	0.867138	0.657677	1.309031	1.260634
115 days	1.654707	0.865997	0.656495	1.305183	1.227836
215 days	1.633014	0.864503	0.655577	1.300602	1.203717
315 days	1.611878	0.862836	0.654953	1.295935	1.180465
415 days	1.59052	0.860982	0.654571	1.291241	1.157438
515 days	1.568626	0.858929	0.654412	1.286575	1.134393
615 days	1.545991	0.856655	0.654439	1.281995	1.111139
715 days	1.52246	0.854136	0.654626	1.277557	1.087544
815 days	1.497942	0.851348	0.654966	1.273298	1.063533
915 days	1.472375	0.848266	0.655446	1.269256	1.03905
1015 days	1.445768	0.844849	0.65602	1.265501	1.014045
1115 days	1.418159	0.841083	0.656716	1.262034	0.98858
1215 days	1.389665	0.836932	0.657501	1.258911	0.962701
1315 days	1.360471	0.83238	0.658384	1.256146	0.936549
1415 days	1.330331	0.827436	0.659335	1.253864	0.91002

	Moderator Temperature				
	eta	f	p	eps	kinf
0 days	1.736132	0.870817	0.657724	1.301586	1.294274
15 days	1.687209	0.871423	0.657321	1.308036	1.264139
115 days	1.654083	0.870301	0.656136	1.304049	1.231727
215 days	1.633066	0.868829	0.655215	1.299356	1.207954
315 days	1.612573	0.867187	0.654589	1.294581	1.185032
415 days	1.591844	0.86536	0.654206	1.289784	1.162327
515 days	1.570573	0.863334	0.654044	1.285016	1.1396
615 days	1.548559	0.861087	0.654069	1.280334	1.116661
715 days	1.525648	0.858594	0.654255	1.275793	1.093377
815 days	1.501745	0.855832	0.654594	1.271432	1.069669
915 days	1.476782	0.852774	0.655072	1.267287	1.045477
1015 days	1.450757	0.849377	0.655645	1.263431	1.020742
1115 days	1.423699	0.845626	0.65634	1.259867	0.99552
1215 days	1.395708	0.841484	0.657124	1.256652	0.969846
1315 days	1.366956	0.836932	0.658007	1.253803	0.943854
1415 days	1.337198	0.831976	0.658958	1.251444	0.917435

	Fuel Temperature				
	eta	f	p	eps	kinf
0 days	1.739133	0.86653	0.657206	1.302495	1.290013
15 days	1.688654	0.867165	0.656807	1.309221	1.259195
115 days	1.654755	0.866025	0.655641	1.305344	1.226467
215 days	1.633085	0.864533	0.654736	1.300735	1.202391
315 days	1.611971	0.862868	0.654124	1.296037	1.179177
415 days	1.590635	0.861016	0.653752	1.291315	1.156184
515 days	1.568763	0.858966	0.6536	1.286621	1.133173
615 days	1.546151	0.856694	0.653633	1.282013	1.109952
715 days	1.522643	0.854177	0.653826	1.277548	1.08639
815 days	1.498148	0.851392	0.65417	1.273263	1.062411
915 days	1.472604	0.848312	0.654652	1.269197	1.037961
1015 days	1.446019	0.844898	0.655227	1.265419	1.012989
1115 days	1.418432	0.841133	0.655923	1.261931	0.987556
1215 days	1.389958	0.836984	0.656706	1.25879	0.961708
1315 days	1.360781	0.832433	0.657588	1.256009	0.935586
1415 days	1.330655	0.827488	0.658536	1.253713	0.909086

A.2 MOX

A.1.4 125mm

	Reference Case				
	eta	f	p	eps	kinf
0 days	1.782501	0.855474	0.675211	1.264134	1.301575
15 Days	1.726508	0.856416	0.675059	1.270733	1.268381
115 days	1.693602	0.85496	0.675016	1.26489	1.2363
215 days	1.672476	0.85304	0.675158	1.257292	1.211075
315 days	1.651889	0.850902	0.675469	1.249646	1.18646
415 days	1.631143	0.848543	0.67596	1.242024	1.162029
515 days	1.609896	0.845942	0.676593	1.234495	1.13751
615 days	1.587926	0.843082	0.677384	1.227077	1.112773
715 days	1.565101	0.83993	0.678237	1.219851	1.087612
815 days	1.541315	0.836469	0.679236	1.212763	1.062032
915 days	1.516493	0.83266	0.6803	1.205909	1.035913
1015 days	1.490646	0.828478	0.681433	1.199303	1.009271
1115 days	1.463801	0.823899	0.682665	1.192918	0.982142
1215 days	1.435449	0.818934	0.683947	1.186882	0.95426
1315 days	1.407	0.813484	0.685297	1.181041	0.926375
1415 days	1.377921	0.807568	0.686713	1.175494	0.898254

	Total Coolant Void				
	eta	f	p	eps	kinf
0 days	1.793201	0.888842	0.557493	1.441831	1.28117
15 Days	1.729611	0.889793	0.557458	1.454643	1.247976
115 days	1.69325	0.888523	0.557935	1.445215	1.213126
215 days	1.669239	0.886836	0.558641	1.432706	1.184819
315 days	1.645901	0.884953	0.559508	1.420113	1.157319
415 days	1.622478	0.882871	0.560548	1.407554	1.130198
515 days	1.598575	0.880576	0.561707	1.395148	1.103139
615 days	1.573957	0.878053	0.563028	1.382906	1.07606
715 days	1.54849	0.875282	0.564345	1.370968	1.048646
815 days	1.522094	0.872241	0.565806	1.359213	1.021017
915 days	1.494708	0.868908	0.567294	1.347798	0.993032
1015 days	1.466381	0.865263	0.568819	1.336729	0.964745
1115 days	1.43718	0.861283	0.570423	1.325942	0.936221
1215 days	1.406497	0.856989	0.57203	1.315679	0.907159
1315 days	1.376079	0.85228	0.573671	1.3056	0.878413
1415 days	1.345256	0.847181	0.575339	1.295905	0.849724

Inner Coolant Void

	eta	f	p	eps	kinf
0 days	1.780752	0.877227	0.589393	1.375651	1.266569
15 Days	1.723036	0.878159	0.589133	1.385595	1.235142
115 days	1.689313	0.876683	0.58911	1.377354	1.201696
215 days	1.666992	0.874775	0.589312	1.366622	1.17442
315 days	1.645246	0.872665	0.589679	1.355802	1.147864
415 days	1.623389	0.870345	0.590258	1.344946	1.12166
515 days	1.601054	0.8678	0.590991	1.334183	1.095524
615 days	1.578025	0.865012	0.591924	1.323502	1.069366
715 days	1.554179	0.861962	0.592882	1.313098	1.042928
815 days	1.529441	0.858622	0.59405	1.302782	1.016318
915 days	1.503753	0.854975	0.595253	1.292788	0.98937
1015 days	1.477159	0.850998	0.596503	1.283117	0.962132
1115 days	1.449719	0.846664	0.597891	1.273664	0.934698
1215 days	1.420809	0.842003	0.599319	1.264676	0.906748
1315 days	1.392174	0.836904	0.600826	1.255859	0.879142
1415 days	1.363123	0.8314	0.602409	1.247383	0.851603

Outer Coolant Void

	eta	f	p	eps	kinf
0 days	1.78825	0.867225	0.653313	1.299311	1.316419
15 Days	1.729413	0.868198	0.65323	1.307195	1.282107
115 days	1.695125	0.866866	0.653412	1.300724	1.248895
215 days	1.673107	0.865076	0.653796	1.2922	1.222785
315 days	1.651682	0.863071	0.654359	1.283623	1.197364
415 days	1.630112	0.860852	0.655095	1.275086	1.172168
515 days	1.608041	0.858401	0.655965	1.266661	1.146907
615 days	1.585238	0.855701	0.656984	1.25837	1.121449
715 days	1.561561	0.852721	0.658055	1.250285	1.095562
815 days	1.536902	0.849448	0.65925	1.242364	1.069256
915 days	1.511184	0.84584	0.660507	1.234692	1.042417
1015 days	1.484421	0.841874	0.661827	1.227285	1.015065
1115 days	1.456641	0.837531	0.663222	1.220123	0.987225
1215 days	1.427354	0.832815	0.664652	1.21334	0.958643
1315 days	1.397951	0.827635	0.666129	1.206765	0.930061
1415 days	1.367922	0.822006	0.667649	1.200509	0.90126

Total Coolant Temperature

	eta	f	p	eps	kinf
0 days	1.777018	0.860521	0.674735	1.26373	1.30389
15 Days	1.723823	0.861389	0.674583	1.269933	1.272061
115 days	1.692042	0.859981	0.674535	1.263921	1.24058
215 days	1.671537	0.858134	0.674673	1.256233	1.215723
315 days	1.651549	0.856077	0.674981	1.248501	1.191475
415 days	1.631409	0.853806	0.675468	1.240796	1.167421
515 days	1.610787	0.851302	0.676098	1.233182	1.143296
615 days	1.589473	0.848545	0.676885	1.225678	1.118973
715 days	1.567337	0.845507	0.677735	1.218362	1.094248
815 days	1.54428	0.842165	0.67873	1.211181	1.069127
915 days	1.520227	0.838485	0.679791	1.204229	1.04349
1015 days	1.495189	0.83444	0.68092	1.197522	1.017352
1115 days	1.469189	0.830005	0.682149	1.191032	0.990742
1215 days	1.441735	0.825186	0.683428	1.184884	0.963399
1315 days	1.414182	0.819889	0.684775	1.178933	0.936047
1415 days	1.386016	0.814129	0.686188	1.173274	0.908456

Inner Coolant Temperature

	eta	f	p	eps	kinf
0 days	1.780176	0.859315	0.67503	1.26343	1.304636
15 Days	1.72542	0.86023	0.674877	1.26984	1.271989
115 days	1.693024	0.858793	0.674832	1.263933	1.240142
215 days	1.672146	0.856903	0.674973	1.256313	1.21504
315 days	1.651795	0.854799	0.675283	1.248649	1.190546
415 days	1.631285	0.852476	0.675773	1.241009	1.166239
515 days	1.610277	0.849915	0.676405	1.233463	1.141849
615 days	1.588554	0.847096	0.677195	1.226027	1.117245
715 days	1.565984	0.843991	0.678047	1.218781	1.092222
815 days	1.542463	0.840578	0.679045	1.211672	1.066784
915 days	1.517916	0.836822	0.680109	1.204796	1.040812
1015 days	1.492354	0.832697	0.681241	1.198166	1.014324
1115 days	1.4658	0.828177	0.682472	1.191756	0.987348
1215 days	1.43775	0.823273	0.683754	1.185691	0.959619
1315 days	1.409599	0.817885	0.685104	1.179823	0.931883
1415 days	1.380815	0.812033	0.68652	1.174248	0.903904

Outer Coolant Temperature

	eta	f	p	eps	kinf
0 days	1.77928	0.856697	0.674922	1.264432	1.30083
15 Days	1.72488	0.857591	0.67477	1.27082	1.268465
115 days	1.692604	0.856163	0.674724	1.26487	1.236756
215 days	1.671861	0.854287	0.674863	1.257201	1.211782
315 days	1.651648	0.852197	0.675172	1.249486	1.187418
415 days	1.631283	0.849891	0.675661	1.241796	1.163246
515 days	1.610432	0.847347	0.676291	1.234199	1.138998
615 days	1.588883	0.844549	0.67708	1.226711	1.114548
715 days	1.566504	0.841465	0.67793	1.219413	1.089691
815 days	1.543195	0.838076	0.678926	1.21225	1.064434
915 days	1.51888	0.834343	0.679988	1.205318	1.038655
1015 days	1.493572	0.830242	0.681119	1.198633	1.012371
1115 days	1.467295	0.825748	0.682347	1.192166	0.985614
1215 days	1.439554	0.820869	0.683627	1.186042	0.958123
1315 days	1.411719	0.815508	0.684975	1.180116	0.930627
1415 days	1.383272	0.809683	0.686388	1.174482	0.902899

Moderator Temperature

	eta	f	p	eps	kinf
0 days	1.779115	0.860382	0.674997	1.263267	1.305245
15 Days	1.724541	0.861286	0.674845	1.269652	1.272652
115 days	1.69225	0.859854	0.6748	1.263731	1.240849
215 days	1.671622	0.857966	0.67494	1.256079	1.215879
315 days	1.651503	0.855862	0.67525	1.248385	1.191507
415 days	1.631212	0.85354	0.67574	1.240721	1.167314
515 days	1.610417	0.850978	0.676372	1.23315	1.143033
615 days	1.588905	0.84816	0.677162	1.225692	1.118537
715 days	1.566542	0.845052	0.678015	1.218427	1.093615
815 days	1.543223	0.841638	0.679013	1.2113	1.068277
915 days	1.51887	0.837877	0.680077	1.204407	1.042395
1015 days	1.493491	0.833743	0.681211	1.197764	1.015985
1115 days	1.467106	0.829214	0.682442	1.191343	0.989079
1215 days	1.439223	0.824297	0.683725	1.185268	0.961413
1315 days	1.411201	0.818897	0.685076	1.179395	0.933718
1415 days	1.382526	0.813031	0.686493	1.173816	0.905767

	Fuel Temperature				
	eta	f	p	eps	kinf
0 days	1.782361	0.855507	0.674134	1.264426	1.299746
15 Days	1.726469	0.856445	0.673984	1.271017	1.266657
115 days	1.693604	0.85499	0.673955	1.265148	1.234654
215 days	1.672503	0.853074	0.674109	1.257524	1.209483
315 days	1.651939	0.850939	0.674431	1.249852	1.184918
415 days	1.631215	0.848582	0.67493	1.242205	1.160532
515 days	1.609992	0.845985	0.675569	1.234651	1.136058
615 days	1.588047	0.843128	0.676364	1.22721	1.111365
715 days	1.565247	0.839981	0.677221	1.219961	1.086247
815 days	1.541489	0.836524	0.678221	1.212851	1.060712
915 days	1.516695	0.832719	0.679286	1.205976	1.034637
1015 days	1.490879	0.828541	0.680418	1.199351	1.008042
1115 days	1.464064	0.823967	0.681647	1.192949	0.98096
1215 days	1.435745	0.819006	0.682926	1.186896	0.953127
1315 days	1.407328	0.813559	0.684272	1.181042	0.925291
1415 days	1.378282	0.807647	0.685682	1.175482	0.89722

A.1.5 2375mm

	Reference Case				
	eta	f	p	eps	kinf
0 days	1.785235	0.863184	0.655557	1.290376	1.303543
15 Days	1.728055	0.864125	0.655456	1.297788	1.270227
115 days	1.694623	0.862814	0.655547	1.291477	1.237888
215 days	1.673396	0.861056	0.655826	1.283198	1.212586
315 days	1.652797	0.859101	0.656288	1.274853	1.188005
415 days	1.632102	0.856945	0.6569	1.266564	1.163662
515 days	1.610974	0.854574	0.657645	1.258389	1.139318
615 days	1.589197	0.851972	0.65851	1.250365	1.114813
715 days	1.566632	0.849117	0.65946	1.242529	1.090007
815 days	1.543189	0.845992	0.660512	1.234872	1.06485
915 days	1.518795	0.842558	0.661602	1.227501	1.039243
1015 days	1.493475	0.838813	0.66279	1.220341	1.013258
1115 days	1.467262	0.834721	0.664012	1.213466	0.986854
1215 days	1.439603	0.830305	0.665286	1.206961	0.959802
1315 days	1.412003	0.825469	0.666589	1.200668	0.932862
1415 days	1.383898	0.820238	0.66796	1.194668	0.90582

	Total Coolant Void				
	eta	f	p	eps	kinf
0 days	1.792622	0.889036	0.554779	1.442166	1.275096
15 Days	1.729923	0.889976	0.554744	1.454782	1.242497
115 days	1.694064	0.888775	0.555187	1.445373	1.208206
215 days	1.670764	0.887168	0.555846	1.43287	1.180545
315 days	1.648197	0.885381	0.55669	1.420254	1.153769
415 days	1.625595	0.883411	0.557671	1.407713	1.127373
515 days	1.602577	0.881248	0.558772	1.395338	1.101111
615 days	1.578918	0.878877	0.559985	1.383176	1.074834
715 days	1.554478	0.876282	0.561255	1.371286	1.048376
815 days	1.529185	0.873445	0.562626	1.359625	1.021726
915 days	1.502971	0.870348	0.563982	1.348387	0.994771
1015 days	1.475898	0.866972	0.565449	1.337399	0.967645
1115 days	1.448017	0.863297	0.566912	1.326797	0.940273
1215 days	1.418644	0.859351	0.568407	1.316726	0.912428
1315 days	1.389656	0.855032	0.569899	1.306868	0.88495
1415 days	1.360319	0.850369	0.571458	1.297371	0.857623

	Inner Coolant Void				
	eta	f	p	eps	kinf
0 days	1.787548	0.885191	0.558881	1.429939	1.264537
15 Days	1.727047	0.886111	0.558761	1.441815	1.2329
115 days	1.692156	0.884855	0.559041	1.432585	1.199157
215 days	1.669482	0.883193	0.559529	1.420388	1.171837
315 days	1.647514	0.881353	0.560206	1.408049	1.145367
415 days	1.625506	0.879331	0.561033	1.39575	1.119276
515 days	1.603093	0.877116	0.561989	1.383588	1.093327
615 days	1.580055	0.874694	0.563069	1.371606	1.06738
715 days	1.556261	0.872048	0.564218	1.359874	1.041281
815 days	1.531641	0.869158	0.565492	1.348334	1.015032
915 days	1.506131	0.866009	0.566735	1.337229	0.988486
1015 days	1.479791	0.86258	0.568117	1.326336	0.961815
1115 days	1.452669	0.858852	0.569502	1.315824	0.934928
1215 days	1.424071	0.854854	0.570932	1.305826	0.907597
1315 days	1.395884	0.85048	0.57237	1.296039	0.880661
1415 days	1.367356	0.845762	0.573895	1.286599	0.853896

	Outer Coolant Void				
	eta	f	p	eps	kinf
0 days	1.787804	0.866417	0.651772	1.29853	1.310976
15 Days	1.729457	0.86738	0.651693	1.306317	1.277059
115 days	1.695487	0.866097	0.651855	1.299895	1.244285
215 days	1.673908	0.864363	0.652212	1.291427	1.218671
315 days	1.652973	0.862432	0.652753	1.2829	1.193802
415 days	1.631944	0.8603	0.653444	1.274436	1.169179
515 days	1.610476	0.857952	0.654265	1.266093	1.144555
615 days	1.58835	0.855374	0.655203	1.25791	1.119767
715 days	1.565423	0.852544	0.656222	1.249923	1.094669
815 days	1.541603	0.849446	0.657337	1.242123	1.069205
915 days	1.516815	0.846039	0.658492	1.234611	1.043287
1015 days	1.491087	0.842326	0.659736	1.227319	1.016977
1115 days	1.464451	0.838267	0.661012	1.220316	0.990237
1215 days	1.436363	0.833886	0.662332	1.213692	0.962842
1315 days	1.408321	0.829089	0.663677	1.207281	0.935552
1415 days	1.379771	0.823903	0.665082	1.201169	0.90816

	Total Coolant Temperature				
	eta	f	p	eps	kinf
0 days	1.780943	0.867649	0.655187	1.289868	1.305884
15 Days	1.725958	0.868537	0.655085	1.296933	1.273602
115 days	1.6934	0.86726	0.655174	1.290483	1.241703
215 days	1.672629	0.865555	0.65545	1.282136	1.216656
315 days	1.652467	0.863659	0.655909	1.27373	1.192328
415 days	1.632211	0.861568	0.656518	1.26538	1.168243
515 days	1.611533	0.859266	0.65726	1.257143	1.144167
615 days	1.590223	0.85674	0.658122	1.249057	1.119943
715 days	1.568148	0.853967	0.659069	1.241156	1.095433
815 days	1.545218	0.850929	0.660119	1.233433	1.070584
915 days	1.521365	0.84759	0.661206	1.22599	1.045304
1015 days	1.496609	0.843944	0.662391	1.218757	1.019657
1115 days	1.470984	0.839957	0.663611	1.211805	0.993601
1215 days	1.443947	0.835649	0.664882	1.205219	0.966909
1315 days	1.416967	0.830927	0.666182	1.198845	0.940327
1415 days	1.38949	0.825812	0.667551	1.192763	0.913641

Inner Coolant Temperature

	eta	f	p	eps	kinf
0 days	1.78208	0.867261	0.655297	1.289729	1.306213
15 Days	1.726564	0.868165	0.655195	1.296871	1.273657
115 days	1.693798	0.866878	0.655285	1.290459	1.241637
215 days	1.672899	0.865159	0.655562	1.28214	1.216507
315 days	1.652611	0.863247	0.656022	1.273759	1.192095
415 days	1.632228	0.861138	0.656632	1.265435	1.167925
515 days	1.611416	0.858817	0.657376	1.257224	1.14376
615 days	1.589965	0.85627	0.658239	1.249164	1.119441
715 days	1.56774	0.853473	0.659187	1.24129	1.094828
815 days	1.544649	0.85041	0.660238	1.233595	1.069872
915 days	1.520622	0.847044	0.661326	1.226182	1.044476
1015 days	1.495683	0.84337	0.662513	1.21898	1.018706
1115 days	1.469862	0.839353	0.663735	1.21206	0.992521
1215 days	1.442612	0.835014	0.665007	1.205506	0.965692
1315 days	1.415417	0.830258	0.666309	1.199167	0.938972
1415 days	1.387716	0.825109	0.667679	1.193119	0.912144

Outer Coolant Temperature

	eta	f	p	eps	kinf
0 days	1.784068	0.86358	0.655449	1.290513	1.303214
15 Days	1.727434	0.864505	0.655348	1.297847	1.270178
115 days	1.694216	0.863204	0.655439	1.291496	1.237963
215 days	1.673124	0.861461	0.655716	1.283189	1.212748
315 days	1.652655	0.859522	0.656177	1.274818	1.188252
415 days	1.632092	0.857385	0.656788	1.266503	1.163997
515 days	1.611102	0.855033	0.657532	1.2583	1.139745
615 days	1.589472	0.852453	0.658396	1.250249	1.115339
715 days	1.567063	0.849621	0.659345	1.242385	1.090638
815 days	1.543788	0.846522	0.660396	1.234699	1.065592
915 days	1.519573	0.843115	0.661484	1.227297	1.040104
1015 days	1.494445	0.839399	0.662671	1.220105	1.014246
1115 days	1.468435	0.835338	0.663892	1.213196	0.987974
1215 days	1.440997	0.830953	0.665164	1.206656	0.961063
1315 days	1.41362	0.826151	0.666466	1.200329	0.934265
1415 days	1.385747	0.820955	0.667835	1.194293	0.907369

	Moderator Temperature				
	eta	f	p	eps	kinf
0 days	1.780561	0.867845	0.655246	1.289798	1.305946
15 Days	1.725161	0.868744	0.655145	1.296931	1.273431
115 days	1.692481	0.867456	0.655234	1.290506	1.241447
215 days	1.671882	0.865729	0.655511	1.282139	1.216472
315 days	1.651871	0.863808	0.655971	1.273715	1.192203
415 days	1.631749	0.861689	0.656581	1.265353	1.168165
515 days	1.611194	0.859358	0.657325	1.257107	1.144126
615 days	1.589996	0.856798	0.658188	1.249013	1.119932
715 days	1.568022	0.853987	0.659137	1.241108	1.095442
815 days	1.545182	0.85091	0.660189	1.233384	1.070606
915 days	1.521399	0.847523	0.661277	1.225944	1.04532
1015 days	1.496698	0.843829	0.662465	1.218716	1.019658
1115 days	1.471106	0.839788	0.663688	1.211774	0.993571
1215 days	1.44409	0.835422	0.664961	1.205199	0.96684
1315 days	1.417091	0.830637	0.666264	1.198843	0.940195
1415 days	1.389571	0.825459	0.667636	1.192781	0.913433

	Fuel Temperature				
	eta	f	p	eps	kinf
0 days	1.785083	0.863225	0.65462	1.290594	1.301851
15 Days	1.728006	0.864162	0.654521	1.297995	1.268637
115 days	1.694616	0.862853	0.654624	1.291664	1.236372
215 days	1.673414	0.861097	0.654911	1.283365	1.211122
315 days	1.652838	0.859145	0.655379	1.275	1.186587
415 days	1.632166	0.856993	0.655996	1.266692	1.162287
515 days	1.611061	0.854625	0.656745	1.258497	1.137984
615 days	1.589309	0.852026	0.657611	1.250454	1.11352
715 days	1.566769	0.849175	0.658562	1.2426	1.088755
815 days	1.543353	0.846054	0.659614	1.234925	1.063639
915 days	1.518987	0.842624	0.660703	1.227537	1.038076
1015 days	1.493697	0.838884	0.66189	1.220361	1.012135
1115 days	1.467516	0.834796	0.663109	1.213471	0.985775
1215 days	1.43989	0.830385	0.664378	1.206953	0.958769
1315 days	1.412323	0.825553	0.665676	1.200648	0.931876
1415 days	1.384252	0.820328	0.667042	1.194637	0.904882

A.1.6 4875mm

	Reference Case				
	eta	f	p	eps	kinf
0 days	1.785603	0.861489	0.656372	1.290544	1.303039
15 Days	1.728416	0.862416	0.656303	1.297927	1.269754
115 days	1.694894	0.861128	0.656465	1.291542	1.237457
215 days	1.673579	0.859397	0.65681	1.283195	1.212195
315 days	1.652858	0.85747	0.657332	1.274794	1.187625
415 days	1.632032	0.855344	0.657996	1.266457	1.163277
515 days	1.610752	0.853016	0.65881	1.258214	1.138938
615 days	1.588819	0.850435	0.659688	1.250191	1.114373
715 days	1.56607	0.847616	0.660685	1.242323	1.08953
815 days	1.542418	0.844523	0.661739	1.234671	1.064269
915 days	1.517785	0.841121	0.66285	1.227294	1.038563
1015 days	1.4922	0.837413	0.664046	1.220145	1.012457
1115 days	1.465695	0.833357	0.665272	1.21329	0.985913
1215 days	1.438363	0.828942	0.66654	1.206733	0.959026
1315 days	1.409774	0.824182	0.667846	1.200558	0.931606
1415 days	1.381346	0.81899	0.66918	1.194623	0.904388

	Total Coolant Void				
	eta	f	p	eps	kinf
0 days	1.791301	0.889783	0.552787	1.442594	1.271026
15 Days	1.729414	0.890703	0.552758	1.455016	1.238896
115 days	1.693802	0.889525	0.55322	1.445431	1.204802
215 days	1.670691	0.887946	0.553892	1.432761	1.177285
315 days	1.648277	0.886189	0.554744	1.419985	1.150622
415 days	1.625817	0.884252	0.555728	1.407287	1.124327
515 days	1.602924	0.882124	0.556888	1.394683	1.098212
615 days	1.579386	0.87979	0.558038	1.382455	1.07197
715 days	1.555042	0.877234	0.559335	1.3704	1.045626
815 days	1.529819	0.874436	0.56066	1.358644	1.018998
915 days	1.503645	0.871378	0.562002	1.347296	0.992094
1015 days	1.476581	0.868043	0.563452	1.336214	0.96501
1115 days	1.448674	0.864409	0.564894	1.325536	0.937666
1215 days	1.420042	0.860462	0.566366	1.315244	0.910199
1315 days	1.390133	0.856222	0.56786	1.305496	0.882388
1415 days	1.360692	0.851597	0.569359	1.296008	0.855042

Inner Coolant Void					
	eta	f	p	eps	kinf
0 days	1.788408	0.888352	0.553788	1.438416	1.265551
15 Days	1.727778	0.889255	0.553723	1.450478	1.234006
115 days	1.692706	0.88806	0.554116	1.440918	1.200227
215 days	1.669951	0.886468	0.554714	1.428327	1.172908
315 days	1.647879	0.8847	0.555494	1.415615	1.146427
415 days	1.625762	0.882754	0.556411	1.402965	1.120314
515 days	1.603221	0.880619	0.557515	1.390384	1.094392
615 days	1.580049	0.878279	0.5586	1.378185	1.068344
715 days	1.556088	0.875719	0.559844	1.366133	1.042218
815 days	1.531269	0.872918	0.561124	1.35437	1.01583
915 days	1.50552	0.86986	0.562414	1.343015	0.989176
1015 days	1.478902	0.866526	0.563826	1.331908	0.962366
1115 days	1.45146	0.862894	0.565231	1.321203	0.935316
1215 days	1.423311	0.85895	0.566672	1.310878	0.908159
1315 days	1.393896	0.854716	0.568141	1.30109	0.880676
1415 days	1.364959	0.850096	0.56962	1.291563	0.853668

Outer Coolant Void					
	eta	f	p	eps	kinf
0 days	1.7873	0.862579	0.655299	1.293488	1.306767
15 Days	1.729339	0.863524	0.655239	1.301057	1.273065
115 days	1.695478	0.862242	0.65543	1.294655	1.240515
215 days	1.673944	0.860512	0.655809	1.286256	1.215074
315 days	1.653012	0.858586	0.656365	1.277806	1.190337
415 days	1.631973	0.856458	0.657062	1.269424	1.165823
515 days	1.610475	0.854127	0.657908	1.261141	1.141315
615 days	1.588316	0.851543	0.65882	1.253079	1.116576
715 days	1.565328	0.84872	0.659846	1.245177	1.091551
815 days	1.541425	0.845623	0.660928	1.237495	1.066097
915 days	1.516527	0.842216	0.662068	1.23009	1.040192
1015 days	1.490665	0.838503	0.66329	1.222917	1.013876
1115 days	1.463871	0.834442	0.664539	1.216039	0.987113
1215 days	1.436239	0.830022	0.665829	1.209462	0.960001
1315 days	1.407343	0.825259	0.667153	1.203272	0.93235
1415 days	1.378603	0.820064	0.668503	1.19732	0.904901

Total Coolant Temperature

	eta	f	p	eps	kinf
0 days	1.782089	0.866077	0.656086	1.289799	1.306078
15 Days	1.726762	0.866962	0.656017	1.29688	1.273641
115 days	1.693981	0.865702	0.656176	1.290383	1.241698
215 days	1.673037	0.864014	0.656519	1.281991	1.21663
315 days	1.65267	0.862134	0.657039	1.273549	1.192252
415 days	1.632198	0.86006	0.6577	1.265173	1.1681
515 days	1.611279	0.857785	0.658513	1.256892	1.143961
615 days	1.589717	0.855267	0.659389	1.248828	1.119607
715 days	1.567352	0.852512	0.660383	1.240919	1.094981
815 days	1.5441	0.849488	0.661435	1.233223	1.069946
915 days	1.519884	0.846162	0.662545	1.225801	1.044477
1015 days	1.494729	0.842531	0.663739	1.218604	1.018611
1115 days	1.468667	0.838557	0.664963	1.211699	0.992311
1215 days	1.441786	0.834226	0.666229	1.205091	0.965668
1315 days	1.413661	0.829552	0.667533	1.198862	0.938493
1415 days	1.385686	0.824449	0.668865	1.192874	0.91151

Inner Coolant Temperature

	eta	f	p	eps	kinf
0 days	1.782097	0.866074	0.656088	1.289801	1.306085
15 Days	1.726766	0.866959	0.656019	1.296882	1.273647
115 days	1.693983	0.865699	0.656178	1.290386	1.241702
215 days	1.673038	0.864011	0.656521	1.281993	1.216633
315 days	1.652671	0.862132	0.657041	1.273552	1.192255
415 days	1.632198	0.860057	0.657703	1.265176	1.168102
515 days	1.611277	0.857782	0.658515	1.256894	1.143963
615 days	1.589715	0.855264	0.659391	1.248831	1.119608
715 days	1.567349	0.852509	0.660386	1.240921	1.094982
815 days	1.544096	0.849485	0.661438	1.233226	1.069945
915 days	1.519878	0.846158	0.662547	1.225804	1.044475
1015 days	1.494722	0.842527	0.663741	1.218607	1.018608
1115 days	1.468659	0.838553	0.664965	1.211703	0.992307
1215 days	1.441776	0.834222	0.666232	1.205094	0.965664
1315 days	1.413651	0.829548	0.667536	1.198865	0.938487
1415 days	1.385673	0.824444	0.668868	1.192877	0.911504

Outer Coolant Temperature

	eta	f	p	eps	kinf
0 days	1.785595	0.861491	0.65637	1.290542	1.303032
15 Days	1.728413	0.862418	0.656301	1.297925	1.26975
115 days	1.694891	0.86113	0.656463	1.29154	1.237453
215 days	1.673577	0.8594	0.656808	1.283192	1.212191
315 days	1.652857	0.857473	0.65733	1.274791	1.187622
415 days	1.632032	0.855347	0.657993	1.266454	1.163275
515 days	1.610753	0.853018	0.658808	1.258211	1.138937
615 days	1.588822	0.850438	0.659686	1.250188	1.114372
715 days	1.566073	0.847619	0.660683	1.24232	1.08953
815 days	1.542422	0.844526	0.661736	1.234668	1.06427
915 days	1.517791	0.841125	0.662848	1.227291	1.038565
1015 days	1.492207	0.837417	0.664044	1.220142	1.01246
1115 days	1.465704	0.833361	0.66527	1.213286	0.985917
1215 days	1.438373	0.828946	0.666538	1.206729	0.959031
1315 days	1.409786	0.824186	0.667843	1.200554	0.931612
1415 days	1.38136	0.818994	0.669177	1.194619	0.904395

Moderator Temperature

	eta	f	p	eps	kinf
0 days	1.780678	0.8659	0.656032	1.290108	1.30498
15 Days	1.725368	0.866782	0.655963	1.2972	1.272558
115 days	1.692632	0.865517	0.656122	1.290694	1.24064
215 days	1.671965	0.863817	0.656465	1.282251	1.21572
315 days	1.651853	0.861925	0.656985	1.273765	1.191476
415 days	1.631622	0.859836	0.657646	1.265348	1.167448
515 days	1.610937	0.857548	0.658459	1.257028	1.143433
615 days	1.589608	0.855009	0.659335	1.24893	1.119193
715 days	1.567475	0.852236	0.660331	1.240986	1.094684
815 days	1.544455	0.849191	0.661383	1.233258	1.069763
915 days	1.520467	0.845837	0.662494	1.225806	1.044401
1015 days	1.495538	0.842181	0.663689	1.218581	1.018643
1115 days	1.469695	0.838177	0.664914	1.21165	0.992443
1215 days	1.443024	0.833815	0.666182	1.205018	0.965895
1315 days	1.415115	0.829107	0.667487	1.198766	0.938814
1415 days	1.387323	0.823969	0.668821	1.19276	0.911909

	Fuel Temperature				
	eta	f	p	eps	kinf
0 days	1.785453	0.86153	0.655609	1.290744	1.301679
15 Days	1.728369	0.862453	0.655541	1.298116	1.268485
115 days	1.694887	0.861166	0.655712	1.291713	1.236251
215 days	1.673596	0.859438	0.656064	1.283349	1.211033
315 days	1.652897	0.857514	0.656592	1.274931	1.186504
415 days	1.632094	0.855391	0.657259	1.266577	1.162192
515 days	1.610837	0.853066	0.658076	1.258316	1.13789
615 days	1.588929	0.850488	0.658956	1.250277	1.11336
715 days	1.566204	0.847674	0.659954	1.242392	1.088552
815 days	1.542579	0.844585	0.661007	1.234724	1.063327
915 days	1.517974	0.841187	0.662118	1.227332	1.037658
1015 days	1.492419	0.837484	0.663312	1.220169	1.01159
1115 days	1.465945	0.833432	0.664535	1.2133	0.985085
1215 days	1.438646	0.829022	0.6658	1.20673	0.958238
1315 days	1.410091	0.824266	0.667101	1.200544	0.930859
1415 days	1.381695	0.819079	0.66843	1.194598	0.903683

A.3 UO₂

A.1.7 125mm

	Reference Case				
	eta	f	p	eps	kinf
0 days	1.967679	0.783188	0.753393	1.187479	1.378694
15 Days	1.874827	0.787341	0.754877	1.194028	1.3305
115 days	1.839948	0.786205	0.754519	1.188928	1.297679
215 days	1.814384	0.783612	0.753351	1.182715	1.266799
315 days	1.789282	0.780171	0.75222	1.176382	1.235269
415 days	1.763603	0.775989	0.751401	1.170064	1.203199
515 days	1.736687	0.771091	0.750924	1.163839	1.17035
615 days	1.707127	0.765523	0.750773	1.157807	1.135975
715 days	1.676324	0.759125	0.750879	1.151858	1.100627
815 days	1.642857	0.751905	0.75119	1.146105	1.063499
915 days	1.606245	0.743798	0.751673	1.140588	1.024294
1015 days	1.566085	0.734766	0.752246	1.135375	0.982796
1115 days	1.52196	0.724753	0.752888	1.130528	0.938869
1215 days	1.473591	0.71376	0.753558	1.126141	0.892562
1315 days	1.420981	0.701875	0.75422	1.122313	0.844229
1415 days	1.364452	0.68921	0.754838	1.119151	0.794424

	Total Coolant Void				
	eta	f	p	eps	kinf
0 days	1.970058	0.833837	0.626755	1.32702	1.366266
15 Days	1.877707	0.837308	0.626927	1.33931	1.320114
115 days	1.843147	0.835934	0.626988	1.329675	1.284507
215 days	1.817623	0.833342	0.62646	1.317677	1.250344
315 days	1.792355	0.830034	0.626241	1.305507	1.2163
415 days	1.766276	0.826086	0.626502	1.293521	1.182444
515 days	1.738733	0.82151	0.62717	1.281811	1.148298
615 days	1.708397	0.81633	0.628158	1.270497	1.113005
715 days	1.67652	0.8104	0.629362	1.259366	1.076864
815 days	1.641771	0.803708	0.630718	1.248569	1.039104
915 days	1.603663	0.796182	0.632192	1.238146	0.999416
1015 days	1.561775	0.787768	0.633702	1.228189	0.957562
1115 days	1.515669	0.7784	0.635224	1.218786	0.913402
1215 days	1.465027	0.768053	0.636722	1.210083	0.866966
1315 days	1.409811	0.756784	0.638159	1.202243	0.818566
1415 days	1.350311	0.744678	0.639484	1.195452	0.768713

Inner Coolant Void					
	eta	f	p	eps	kinf
0 days	1.965876	0.812825	0.677611	1.260054	1.364342
15 Days	1.874123	0.816687	0.677665	1.269707	1.31696
115 days	1.838762	0.81556	0.677234	1.262463	1.28215
215 days	1.812707	0.81303	0.675824	1.253681	1.24869
315 days	1.787097	0.809691	0.67449	1.2447	1.214807
415 days	1.760874	0.805648	0.673559	1.235689	1.180751
515 days	1.733378	0.800929	0.673045	1.226756	1.146277
615 days	1.703384	0.795566	0.672931	1.218013	1.110738
715 days	1.671927	0.789436	0.67312	1.20935	1.074432
815 days	1.637804	0.782529	0.673548	1.200901	1.036666
915 days	1.600557	0.774786	0.674185	1.19271	0.997165
1015 days	1.559805	0.76617	0.674914	1.184874	0.955687
1115 days	1.515173	0.756633	0.675717	1.177465	0.912138
1215 days	1.466415	0.74617	0.67655	1.170604	0.866571
1315 days	1.413581	0.734867	0.677373	1.164416	0.819342
1415 days	1.357039	0.722827	0.678154	1.159033	0.770993

Outer Coolant Void					
	eta	f	p	eps	kinf
0 days	1.969745	0.800771	0.725371	1.217784	1.393314
15 Days	1.876964	0.804674	0.725529	1.225879	1.343317
115 days	1.842518	0.803441	0.725368	1.219762	1.309782
215 days	1.817234	0.800865	0.724573	1.21217	1.278251
315 days	1.792332	0.797495	0.723952	1.204471	1.246386
415 days	1.76676	0.793428	0.723725	1.196853	1.214224
515 days	1.739858	0.788676	0.723862	1.189396	1.181394
615 days	1.710157	0.783284	0.724311	1.182211	1.147032
715 days	1.679182	0.77708	0.724986	1.175142	1.111691
815 days	1.645432	0.77007	0.725832	1.168317	1.074501
915 days	1.608409	0.762181	0.726815	1.161775	1.035143
1015 days	1.567684	0.753366	0.727853	1.155587	0.99337
1115 days	1.522802	0.743559	0.728927	1.149825	0.949018
1215 days	1.473437	0.732744	0.73	1.144596	0.902109
1315 days	1.419539	0.720995	0.731032	1.14002	0.852961
1415 days	1.361381	0.708409	0.731987	1.136227	0.802107

Total Coolant Temperature

	eta	f	p	eps	kinf
0 days	1.965019	0.786075	0.753146	1.187445	1.381412
15 Days	1.874339	0.790163	0.755714	1.193435	1.335737
115 days	1.839026	0.789396	0.755336	1.188317	1.303032
215 days	1.813086	0.787109	0.754157	1.182105	1.272246
315 days	1.78777	0.78394	0.753007	1.175758	1.240827
415 days	1.762017	0.780009	0.752166	1.169426	1.208916
515 days	1.735159	0.775354	0.751676	1.163176	1.176293
615 days	1.705833	0.770026	0.751512	1.157106	1.142223
715 days	1.675344	0.763879	0.751607	1.151112	1.107229
815 days	1.642334	0.756925	0.751907	1.145302	1.07053
915 days	1.606345	0.749102	0.752375	1.139713	1.031833
1015 days	1.567001	0.740382	0.752941	1.134405	0.990955
1115 days	1.523921	0.730713	0.753576	1.129439	0.947761
1215 days	1.476866	0.7201	0.754242	1.124899	0.902315
1315 days	1.425882	0.708637	0.7549	1.120876	0.854977
1415 days	1.371323	0.696432	0.755507	1.117472	0.806294

Inner Coolant Temperature

	eta	f	p	eps	kinf
0 days	1.966705	0.78648	0.753311	1.186909	1.382989
15 Days	1.874759	0.790597	0.754796	1.193362	1.335064
115 days	1.839749	0.789587	0.754437	1.188261	1.302248
215 days	1.814063	0.787105	0.753267	1.182053	1.271367
315 days	1.788893	0.783764	0.752133	1.175722	1.23985
415 days	1.763191	0.779676	0.751311	1.169405	1.207809
515 days	1.736294	0.77487	0.750831	1.163177	1.175007
615 days	1.706817	0.769391	0.750678	1.157137	1.140703
715 days	1.676109	0.763088	0.750782	1.151179	1.105435
815 days	1.642777	0.755966	0.75109	1.145413	1.068403
915 days	1.606347	0.747963	0.751571	1.139877	1.029313
1015 days	1.566422	0.739042	0.752142	1.134638	0.987951
1115 days	1.522595	0.729151	0.752781	1.129758	0.944183
1215 days	1.474598	0.718288	0.75345	1.125327	0.89806
1315 days	1.422444	0.706545	0.75411	1.121442	0.849937
1415 days	1.366466	0.694031	0.754726	1.118208	0.800368

Outer Coolant Temperature

	eta	f	p	eps	kinf
0 days	1.965978	0.78274	0.753232	1.188021	1.377049
15 Days	1.874367	0.786891	0.754717	1.194467	1.32962
115 days	1.83918	0.785996	0.754359	1.189324	1.296948
215 days	1.813363	0.783598	0.753185	1.183073	1.266169
315 days	1.788115	0.780328	0.752047	1.176699	1.234761
415 days	1.762385	0.776302	0.751221	1.170338	1.202847
515 days	1.735509	0.771555	0.750738	1.164064	1.170196
615 days	1.7061	0.766137	0.750581	1.157975	1.136077
715 days	1.675519	0.759896	0.750681	1.151965	1.101028
815 days	1.642377	0.752843	0.750987	1.146143	1.064261
915 days	1.606211	0.744916	0.751465	1.140547	1.025491
1015 days	1.566637	0.736083	0.752034	1.135241	0.984511
1115 days	1.523267	0.726293	0.752671	1.130286	0.941198
1215 days	1.475851	0.715548	0.753337	1.125769	0.895612
1315 days	1.424424	0.703943	0.753995	1.121785	0.848115
1415 days	1.369331	0.691585	0.754608	1.118436	0.799258

Moderator Temperature

	eta	f	p	eps	kinf
0 days	1.966473	0.786689	0.753305	1.186911	1.383184
15 Days	1.873751	0.790864	0.754789	1.193432	1.334863
115 days	1.838592	0.78988	0.754431	1.188337	1.301984
215 days	1.812862	0.787417	0.753259	1.182126	1.271094
315 days	1.787676	0.784095	0.752123	1.17579	1.239585
415 days	1.761991	0.780026	0.7513	1.169465	1.207572
515 days	1.735143	0.775239	0.750819	1.163226	1.174817
615 days	1.705715	0.769783	0.750665	1.157175	1.140565
715 days	1.67512	0.763501	0.750768	1.1512	1.105381
815 days	1.64193	0.756402	0.751076	1.145416	1.068451
915 days	1.605671	0.748422	0.751557	1.139861	1.029478
1015 days	1.565944	0.739524	0.752129	1.1346	0.988243
1115 days	1.52234	0.729656	0.752768	1.129697	0.944611
1215 days	1.474587	0.718813	0.753437	1.125242	0.898626
1315 days	1.42269	0.707087	0.754098	1.121332	0.850639
1415 days	1.366971	0.694585	0.754715	1.118072	0.801194

	Fuel Temperature				
	eta	f	p	eps	kinf
0 days	1.967601	0.783127	0.752563	1.18765	1.377213
15 Days	1.874843	0.787278	0.75404	1.19421	1.329132
115 days	1.83995	0.786155	0.75369	1.189093	1.29635
215 days	1.814372	0.783571	0.752517	1.182864	1.265483
315 days	1.789262	0.780139	0.75137	1.176515	1.233951
415 days	1.763579	0.775965	0.750529	1.170184	1.201874
515 days	1.736665	0.771075	0.750028	1.163945	1.169021
615 days	1.707113	0.765514	0.749853	1.157899	1.134652
715 days	1.676321	0.759125	0.749937	1.151938	1.09932
815 days	1.642872	0.751913	0.750227	1.146174	1.06222
915 days	1.606283	0.743815	0.75069	1.140646	1.023055
1015 days	1.566155	0.734793	0.751246	1.135423	0.981612
1115 days	1.522072	0.724792	0.751871	1.130567	0.937753
1215 days	1.473756	0.713811	0.752527	1.126171	0.891529
1315 days	1.421212	0.701942	0.753175	1.122335	0.843292
1415 days	1.364764	0.689293	0.753779	1.119164	0.793596

A.1.8 2375mm

	Reference Case				
	eta	f	p	eps	kinf
0 days	1.968389	0.79452	0.730848	1.209296	1.382215
15 Days	1.874761	0.798595	0.730993	1.217139	1.332068
115 days	1.840729	0.797739	0.730638	1.211316	1.299601
215 days	1.814073	0.79558	0.729541	1.204367	1.26808
315 days	1.7893	0.792557	0.728554	1.197153	1.236874
415 days	1.764076	0.788843	0.727912	1.189994	1.205401
515 days	1.737729	0.784467	0.727627	1.182964	1.173375
615 days	1.708843	0.779483	0.727663	1.176169	1.140011
715 days	1.678899	0.773741	0.727944	1.16947	1.105877
815 days	1.646488	0.767253	0.728424	1.162985	1.070177
915 days	1.611182	0.759967	0.729044	1.156755	1.032606
1015 days	1.572622	0.751851	0.729746	1.150839	0.992983
1115 days	1.530439	0.742845	0.730501	1.145295	0.951157
1215 days	1.48442	0.732965	0.731275	1.140219	0.907213
1315 days	1.434567	0.722268	0.732009	1.135705	0.861393
1415 days	1.381161	0.710846	0.732726	1.131847	0.814234

	Total Coolant Void				
	eta	f	p	eps	kinf
0 days	1.96968	0.833729	0.624203	1.327648	1.360908
15 Days	1.876398	0.83728	0.624365	1.340127	1.31456
115 days	1.842711	0.836167	0.624285	1.330459	1.279779
215 days	1.815852	0.833932	0.623621	1.318813	1.245418
315 days	1.790896	0.830932	0.623246	1.306755	1.211963
415 days	1.7653	0.827318	0.623326	1.294883	1.17879
515 days	1.738401	0.823108	0.623812	1.283285	1.145471
615 days	1.708898	0.818339	0.624617	1.27208	1.111162
715 days	1.678051	0.812874	0.62564	1.261054	1.076184
815 days	1.644586	0.806711	0.626822	1.250349	1.039801
915 days	1.608075	0.799793	0.628112	1.240006	1.001716
1015 days	1.568156	0.792076	0.629446	1.230103	0.961736
1115 days	1.524457	0.783499	0.630796	1.220714	0.919721
1215 days	1.476751	0.77406	0.632128	1.211974	0.87575
1315 days	1.425031	0.763801	0.633382	1.204025	0.830053
1415 days	1.369573	0.752795	0.634582	1.197003	0.78315

	Inner Coolant Void				
	eta	f	p	eps	kinf
0 days	1.96757	0.827001	0.63619	1.309491	1.35558
15 Days	1.874915	0.830665	0.636295	1.321182	1.309269
115 days	1.840816	0.829727	0.635977	1.31228	1.274717
215 days	1.813633	0.827598	0.634887	1.301698	1.24044
315 days	1.788485	0.824663	0.633993	1.290666	1.20687
415 days	1.7628	0.821093	0.633542	1.279699	1.173488
515 days	1.73591	0.816915	0.633519	1.2689	1.139963
615 days	1.706568	0.812166	0.633862	1.25839	1.105549
715 days	1.67592	0.806724	0.634468	1.248003	1.070541
815 days	1.642762	0.800586	0.635277	1.237878	1.034245
915 days	1.606676	0.7937	0.636232	1.228065	0.996373
1015 days	1.567322	0.786031	0.637261	1.218644	0.956736
1115 days	1.524354	0.777523	0.638335	1.209685	0.915208
1215 days	1.477577	0.768181	0.639412	1.201322	0.871874
1315 days	1.42702	0.758056	0.640431	1.193683	0.826975
1415 days	1.372988	0.747224	0.641429	1.186891	0.781046

	Outer Coolant Void				
	eta	f	p	eps	kinf
0 days	1.969457	0.799611	0.724091	1.217452	1.388258
15 Days	1.875628	0.803607	0.724246	1.225649	1.337959
115 days	1.841809	0.802657	0.723969	1.219555	1.305257
215 days	1.815326	0.800445	0.723051	1.212213	1.273602
315 days	1.790657	0.797394	0.722293	1.204614	1.242358
415 days	1.765485	0.793666	0.721902	1.197103	1.210909
515 days	1.739141	0.789286	0.721871	1.189751	1.178921
615 days	1.710177	0.784307	0.722149	1.182667	1.145555
715 days	1.680136	0.77857	0.722655	1.175693	1.111392
815 days	1.647572	0.77209	0.723341	1.168951	1.075603
915 days	1.612048	0.764811	0.724152	1.16248	1.037881
1015 days	1.573192	0.756697	0.72503	1.156341	0.998035
1115 days	1.530621	0.747684	0.725948	1.150594	0.955902
1215 days	1.484103	0.737785	0.726872	1.145336	0.911559
1315 days	1.433618	0.72705	0.727744	1.14067	0.86524
1415 days	1.379431	0.71557	0.728584	1.136695	0.817477

	Total Coolant Temperature				
	eta	f	p	eps	kinf
0 days	1.966372	0.797628	0.730637	1.209048	1.385516
15 Days	1.874535	0.801657	0.730783	1.2167	1.336147
115 days	1.840157	0.801081	0.730428	1.210847	1.303762
215 days	1.813224	0.799157	0.729325	1.203876	1.272291
315 days	1.788288	0.796342	0.728331	1.196639	1.241163
415 days	1.763008	0.792819	0.727682	1.189451	1.209807
515 days	1.7367	0.788629	0.72739	1.182385	1.177942
615 days	1.707987	0.783828	0.72742	1.175544	1.1448
715 days	1.678263	0.778277	0.727695	1.168795	1.110917
815 days	1.646173	0.77199	0.72817	1.162251	1.075522
915 days	1.611301	0.764919	0.728784	1.15595	1.038318
1015 days	1.573305	0.757036	0.72948	1.149949	0.999129
1115 days	1.53184	0.748284	0.73023	1.144304	0.957813
1215 days	1.486717	0.738684	0.730999	1.139103	0.914464
1315 days	1.437964	0.728293	0.731727	1.134437	0.869329
1415 days	1.38588	0.717202	0.732439	1.130395	0.822942

Inner Coolant Temperature

	eta	f	p	eps	kinf
0 days	1.967003	0.79779	0.730714	1.208805	1.386109
15 Days	1.874712	0.801819	0.73086	1.216499	1.336461
115 days	1.840469	0.801153	0.730504	1.210663	1.304037
215 days	1.813631	0.799156	0.729404	1.203709	1.272536
315 days	1.788758	0.796278	0.728413	1.196488	1.241372
415 days	1.763503	0.792696	0.727766	1.189318	1.209966
515 days	1.737188	0.788449	0.727477	1.182273	1.178034
615 days	1.708426	0.783592	0.727509	1.175455	1.144803
715 days	1.678628	0.777981	0.727786	1.168732	1.110816
815 days	1.646426	0.77163	0.728263	1.162216	1.075292
915 days	1.611397	0.76449	0.72888	1.155948	1.037931
1015 days	1.573192	0.756529	0.729578	1.149985	0.998553
1115 days	1.531455	0.747691	0.73033	1.144383	0.957011
1215 days	1.485986	0.737994	0.731101	1.139234	0.913394
1315 days	1.436802	0.727494	0.731832	1.134631	0.867945
1415 days	1.384192	0.716282	0.732545	1.130663	0.821199

Outer Coolant Temperature

	eta	f	p	eps	kinf
0 days	1.967749	0.794343	0.730775	1.209539	1.381596
15 Days	1.874567	0.798419	0.73092	1.217342	1.331724
115 days	1.840397	0.797653	0.730565	1.211502	1.299296
215 days	1.813644	0.795567	0.729465	1.204536	1.267807
315 days	1.788808	0.792608	0.728476	1.197305	1.236637
415 days	1.763557	0.788952	0.727831	1.190128	1.205214
515 days	1.737216	0.784633	0.727543	1.183078	1.173255
615 days	1.708379	0.779707	0.727577	1.176259	1.13998
715 days	1.67851	0.774024	0.727855	1.169535	1.105952
815 days	1.646213	0.7676	0.728334	1.16302	1.070382
915 days	1.611067	0.760384	0.728952	1.156758	1.03297
1015 days	1.57272	0.752346	0.729651	1.150803	0.993539
1115 days	1.530814	0.743426	0.730405	1.145215	0.951943
1215 days	1.485148	0.733645	0.731177	1.140084	0.90827
1315 days	1.435737	0.723058	0.731909	1.135506	0.862769
1415 days	1.38287	0.711758	0.732624	1.131571	0.815974

Moderator Temperature					
	eta	f	p	eps	kinf
0 days	1.966601	0.797097	0.730709	1.209059	1.384904
15 Days	1.873065	0.801224	0.730855	1.216881	1.334707
115 days	1.838532	0.800583	0.730498	1.211062	1.302157
215 days	1.811625	0.798596	0.729395	1.204101	1.270637
315 days	1.786688	0.795727	0.728402	1.196872	1.239457
415 days	1.76141	0.792154	0.727753	1.18969	1.208058
515 days	1.73511	0.787914	0.727463	1.182629	1.176157
615 days	1.706365	0.783067	0.727494	1.175796	1.142962
715 days	1.676661	0.777463	0.72777	1.169051	1.109053
815 days	1.644589	0.771119	0.728247	1.162511	1.073629
915 days	1.609728	0.763987	0.728863	1.156217	1.03639
1015 days	1.571728	0.756035	0.729561	1.150224	0.997157
1115 days	1.530233	0.747206	0.730314	1.144592	0.955781
1215 days	1.485046	0.737519	0.731085	1.139411	0.912349
1315 days	1.436178	0.727029	0.731816	1.134772	0.867103
1415 days	1.383915	0.715827	0.732531	1.130767	0.820573

Fuel Temperature					
	eta	f	p	eps	kinf
0 days	1.968307	0.794462	0.730107	1.209461	1.380844
15 Days	1.87478	0.798535	0.730254	1.217297	1.330807
115 days	1.84073	0.797692	0.729904	1.211459	1.298374
215 days	1.814059	0.795545	0.728801	1.204495	1.266864
315 days	1.789277	0.792533	0.727799	1.197266	1.235654
415 days	1.764048	0.788828	0.727135	1.190093	1.204172
515 days	1.737702	0.784461	0.726827	1.18305	1.172143
615 days	1.708824	0.779486	0.726841	1.176242	1.138785
715 days	1.678891	0.773753	0.727101	1.169532	1.104667
815 days	1.646498	0.767275	0.727563	1.163036	1.068995
915 days	1.611217	0.76	0.728165	1.156796	1.031465
1015 days	1.572691	0.751896	0.72885	1.150871	0.991896
1115 days	1.530551	0.742903	0.729591	1.145319	0.950136
1215 days	1.484587	0.733039	0.730351	1.140234	0.906271
1315 days	1.434803	0.722359	0.731071	1.135711	0.860545
1415 days	1.381483	0.710957	0.731776	1.131844	0.813492

A.1.9 4875mm

	Reference Case				
	eta	f	p	eps	kinf
0 days	1.968388	0.793063	0.729487	1.211337	1.379434
15 Days	1.874794	0.797111	0.729644	1.219255	1.329468
115 days	1.840717	0.796321	0.729339	1.21334	1.297141
215 days	1.815257	0.794165	0.728322	1.206134	1.266391
315 days	1.789369	0.791269	0.727421	1.198905	1.234794
415 days	1.764215	0.787624	0.726864	1.191631	1.203553
515 days	1.737951	0.783321	0.72666	1.184502	1.171775
615 days	1.709161	0.77842	0.726769	1.17762	1.138672
715 days	1.679308	0.772763	0.727115	1.170852	1.104795
815 days	1.646997	0.766367	0.727653	1.164302	1.069349
915 days	1.611796	0.759183	0.728323	1.158013	1.032035
1015 days	1.573341	0.75117	0.729071	1.15204	0.992655
1115 days	1.531254	0.742271	0.729869	1.146447	0.951063
1215 days	1.485331	0.732506	0.730679	1.141323	0.907339
1315 days	1.435555	0.721923	0.731487	1.136758	0.861757
1415 days	1.382207	0.710601	0.73219	1.132866	0.814707

	Total Coolant Void				
	eta	f	p	eps	kinf
0 days	1.969114	0.833797	0.622456	1.328312	1.357502
15 Days	1.876002	0.837361	0.622612	1.340799	1.311374
115 days	1.842183	0.836354	0.622531	1.331074	1.276691
215 days	1.816644	0.834149	0.62182	1.319161	1.243013
315 days	1.790355	0.831297	0.621377	1.307259	1.208962
415 days	1.764833	0.827767	0.621386	1.295323	1.175849
515 days	1.738048	0.823642	0.621803	1.283661	1.142625
615 days	1.708714	0.81896	0.62255	1.272379	1.108466
715 days	1.678036	0.813589	0.623509	1.261301	1.073662
815 days	1.644773	0.807523	0.624638	1.250531	1.037489
915 days	1.608496	0.800711	0.625878	1.240122	0.999654
1015 days	1.568845	0.793104	0.627166	1.230145	0.95995
1115 days	1.525439	0.784643	0.628474	1.220683	0.918242
1215 days	1.478069	0.77533	0.629764	1.211861	0.874605
1315 days	1.426718	0.765198	0.631031	1.203805	0.829313
1415 days	1.371664	0.754319	0.632144	1.196698	0.782714

Inner Coolant Void					
	eta	f	p	eps	kinf
0 days	1.967771	0.8309	0.627051	1.321016	1.354362
15 Days	1.875237	0.834508	0.627179	1.333133	1.308434
115 days	1.841147	0.833634	0.626985	1.323729	1.273855
215 days	1.815408	0.831519	0.626066	1.312282	1.240206
315 days	1.788986	0.828739	0.625372	1.300815	1.206087
415 days	1.763407	0.825268	0.625125	1.289255	1.172878
515 days	1.736629	0.821197	0.625297	1.277914	1.139574
615 days	1.707397	0.816565	0.625826	1.266897	1.105402
715 days	1.676852	0.811249	0.626585	1.25606	1.07063
815 days	1.643795	0.805243	0.627537	1.245499	1.034564
915 days	1.607805	0.7985	0.62862	1.23527	0.996915
1015 days	1.568537	0.790974	0.629764	1.225446	0.957479
1115 days	1.525629	0.782612	0.630943	1.216109	0.916132
1215 days	1.478892	0.773418	0.632114	1.207382	0.872952
1315 days	1.428335	0.763429	0.633279	1.199379	0.828229
1415 days	1.374254	0.752722	0.634292	1.192285	0.782296

Outer Coolant Void					
	eta	f	p	eps	kinf
0 days	1.969181	0.795197	0.727013	1.214435	1.382537
15 Days	1.875259	0.799212	0.727174	1.222517	1.332345
115 days	1.841343	0.798335	0.726906	1.216502	1.299903
215 days	1.816003	0.796118	0.725976	1.209141	1.269093
315 days	1.790195	0.793175	0.725184	1.201765	1.237477
415 days	1.765076	0.789492	0.724747	1.194359	1.206235
515 days	1.738809	0.785156	0.724662	1.187113	1.174453
615 days	1.709959	0.780226	0.724884	1.18013	1.141312
715 days	1.680024	0.774539	0.725335	1.173269	1.107376
815 days	1.647588	0.768111	0.725968	1.166636	1.071829
915 days	1.61221	0.760892	0.726727	1.160273	1.03437
1015 days	1.573518	0.752837	0.727556	1.154236	0.994795
1115 days	1.531122	0.74389	0.728429	1.148589	0.95295
1215 days	1.484803	0.734064	0.729307	1.143426	0.908911
1315 days	1.434529	0.723407	0.730176	1.138839	0.862942
1415 days	1.380569	0.711996	0.730937	1.134945	0.815438

Total Coolant Temperature

	eta	f	p	eps	kinf
0 days	1.966829	0.796717	0.729329	1.210798	1.383777
15 Days	1.87475	0.800715	0.729487	1.218545	1.334383
115 days	1.840431	0.800141	0.729182	1.212614	1.302101
215 days	1.81476	0.798167	0.728161	1.205403	1.271372
315 days	1.788766	0.795431	0.727255	1.198165	1.239822
415 days	1.763579	0.791935	0.726693	1.190878	1.208656
515 days	1.737355	0.787775	0.726484	1.183732	1.176983
615 days	1.708705	0.783013	0.726589	1.176824	1.144028
715 days	1.67902	0.777502	0.72693	1.170028	1.110315
815 days	1.646948	0.771258	0.727464	1.163443	1.075068
915 days	1.612062	0.764234	0.728131	1.15711	1.037988
1015 days	1.574012	0.756393	0.728874	1.151084	0.998884
1115 days	1.532431	0.747679	0.729668	1.145425	0.95761
1215 days	1.487131	0.738115	0.730474	1.140219	0.914253
1315 days	1.438111	0.727748	0.731277	1.135553	0.869087
1415 days	1.385661	0.716659	0.731977	1.131538	0.822501

Inner Coolant Temperature

	eta	f	p	eps	kinf
0 days	1.966833	0.796718	0.729328	1.210797	1.383779
15 Days	1.87475	0.800716	0.729487	1.218544	1.334383
115 days	1.840432	0.800142	0.729181	1.212613	1.302101
215 days	1.814762	0.798168	0.72816	1.205403	1.271372
315 days	1.788769	0.795431	0.727254	1.198164	1.239821
415 days	1.763582	0.791934	0.726693	1.190878	1.208656
515 days	1.737357	0.787773	0.726484	1.183732	1.176982
615 days	1.708707	0.783012	0.72659	1.176824	1.144028
715 days	1.679022	0.7775	0.726931	1.170028	1.110314
815 days	1.646949	0.771255	0.727465	1.163443	1.075066
915 days	1.612062	0.764231	0.728131	1.157111	1.037985
1015 days	1.57401	0.756389	0.728875	1.151085	0.99888
1115 days	1.532428	0.747675	0.729669	1.145426	0.957605
1215 days	1.487125	0.73811	0.730475	1.14022	0.914246
1315 days	1.438102	0.727742	0.731279	1.135555	0.869077
1415 days	1.385649	0.716652	0.731979	1.13154	0.822489

Outer Coolant Temperature

	eta	f	p	eps	kinf
0 days	1.968384	0.793061	0.729488	1.211339	1.379432
15 Days	1.874794	0.797109	0.729645	1.219256	1.329469
115 days	1.840716	0.796321	0.72934	1.213341	1.297142
215 days	1.815255	0.794165	0.728322	1.206135	1.266391
315 days	1.789367	0.791269	0.727421	1.198906	1.234794
415 days	1.764212	0.787625	0.726864	1.191631	1.203553
515 days	1.737949	0.783322	0.72666	1.184503	1.171775
615 days	1.709159	0.778421	0.726769	1.17762	1.138673
715 days	1.679306	0.772765	0.727114	1.170852	1.104796
815 days	1.646996	0.76637	0.727652	1.164302	1.069351
915 days	1.611796	0.759186	0.728323	1.158013	1.032037
1015 days	1.573342	0.751173	0.72907	1.15204	0.992659
1115 days	1.531258	0.742275	0.729868	1.146446	0.951068
1215 days	1.485337	0.732511	0.730678	1.141321	0.907347
1315 days	1.435564	0.721928	0.731485	1.136756	0.861766
1415 days	1.38222	0.710608	0.732189	1.132864	0.814719

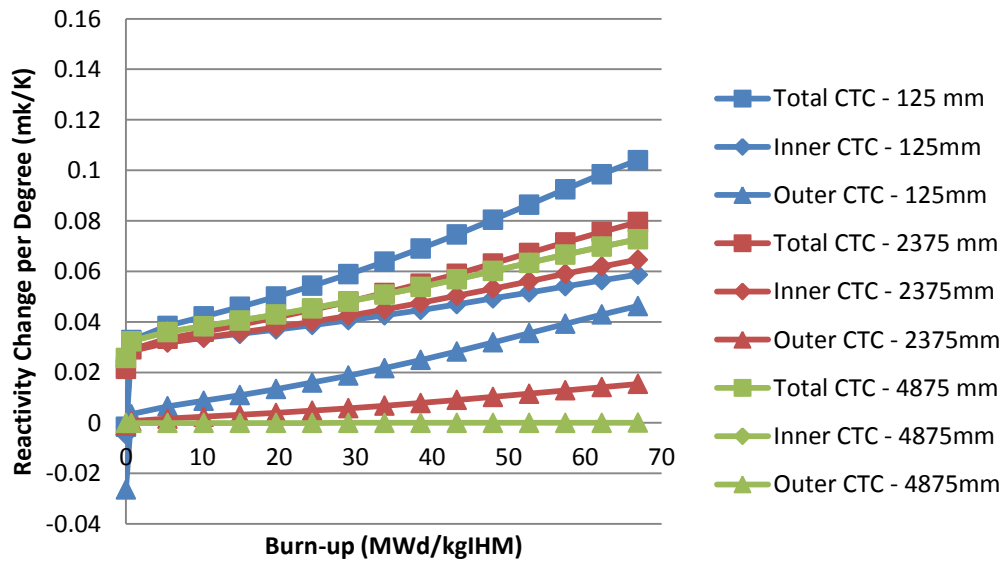
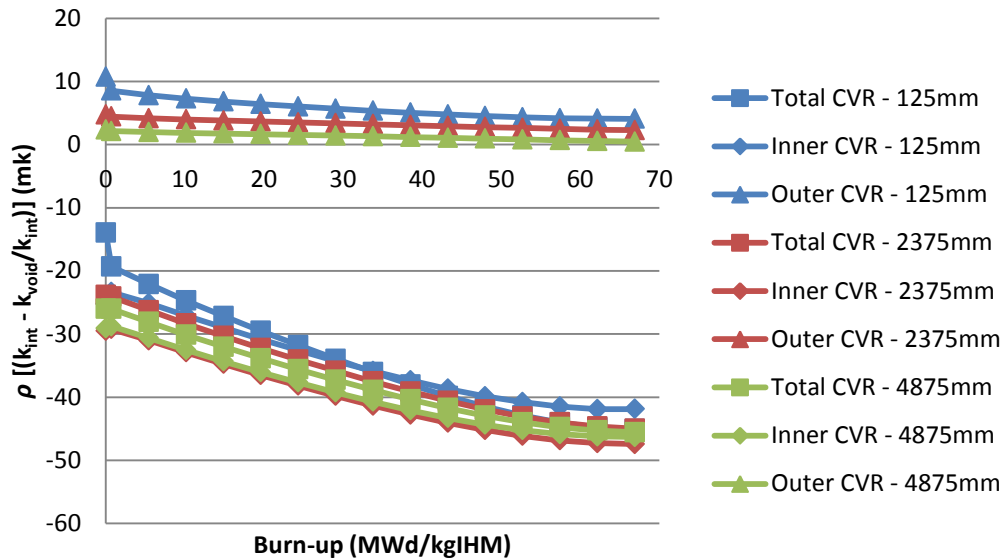
Moderator Temperature

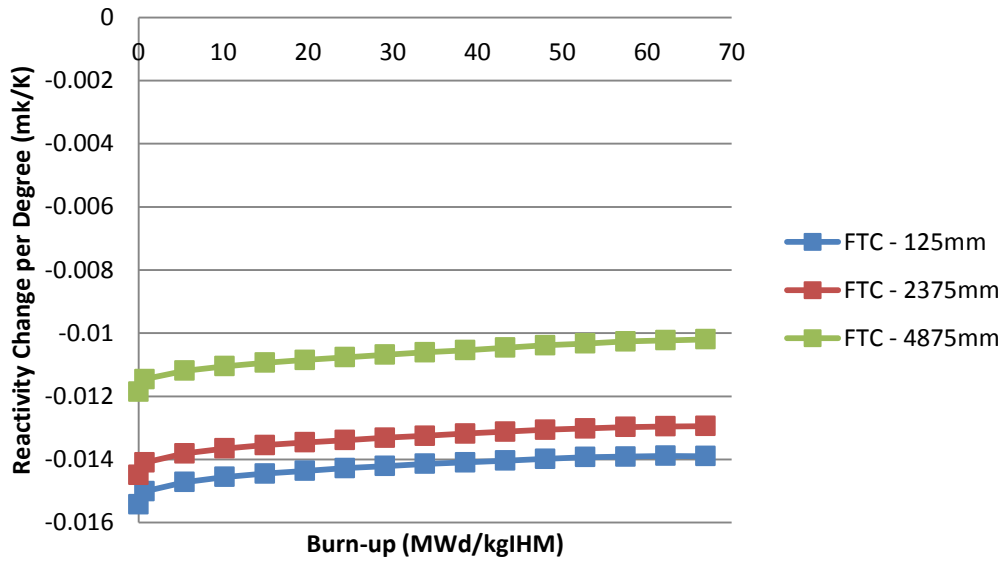
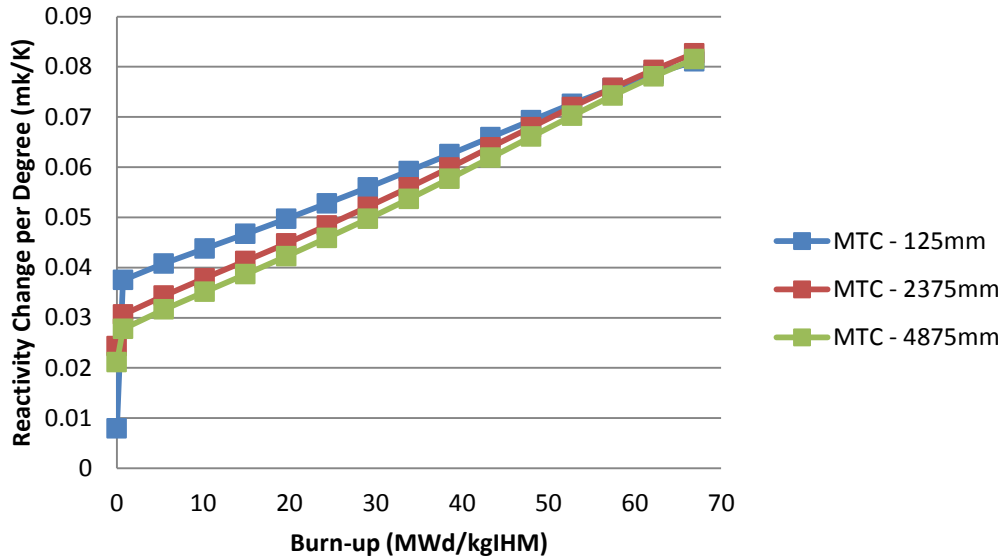
	eta	f	p	eps	kinf
0 days	1.966425	0.795253	0.729329	1.211251	1.381466
15 Days	1.87299	0.799358	0.729487	1.219144	1.331525
115 days	1.838367	0.798802	0.72918	1.213229	1.299119
215 days	1.812596	0.796831	0.728156	1.206009	1.268359
315 days	1.786551	0.794095	0.727248	1.198756	1.236805
415 days	1.761326	0.790598	0.726684	1.191454	1.205642
515 days	1.7351	0.786437	0.726473	1.18429	1.173995
615 days	1.706449	0.781677	0.726577	1.177364	1.141072
715 days	1.676838	0.776163	0.726918	1.170544	1.107432
815 days	1.644875	0.769917	0.727451	1.163932	1.072281
915 days	1.610134	0.762892	0.728117	1.157572	1.035321
1015 days	1.572267	0.755051	0.728861	1.151516	0.996362
1115 days	1.530909	0.746339	0.729655	1.145825	0.95526
1215 days	1.485874	0.736777	0.730462	1.140584	0.912101
1315 days	1.43716	0.726416	0.731266	1.135882	0.86716
1415 days	1.385056	0.715332	0.731967	1.131829	0.820819

	Fuel Temperature				
	eta	f	p	eps	kinf
0 days	1.968306	0.793005	0.728896	1.2115	1.378344
15 Days	1.874815	0.797051	0.729055	1.219411	1.328479
115 days	1.84072	0.796275	0.728754	1.213481	1.296179
215 days	1.815244	0.794131	0.727731	1.206261	1.265433
315 days	1.789348	0.791245	0.726815	1.199018	1.23383
415 days	1.764189	0.787609	0.726239	1.19173	1.202579
515 days	1.737926	0.783315	0.726015	1.184589	1.170796
615 days	1.709144	0.778423	0.726106	1.177694	1.137698
715 days	1.679302	0.772776	0.726433	1.170915	1.103834
815 days	1.647009	0.766391	0.726955	1.164354	1.068413
915 days	1.611832	0.759217	0.727612	1.158055	1.031134
1015 days	1.573411	0.751216	0.728346	1.152073	0.991802
1115 days	1.531367	0.742332	0.729132	1.146471	0.950268
1215 days	1.485499	0.732582	0.72993	1.141338	0.906617
1315 days	1.435792	0.722016	0.730726	1.136763	0.861118
1415 days	1.38253	0.710714	0.731419	1.132861	0.814164

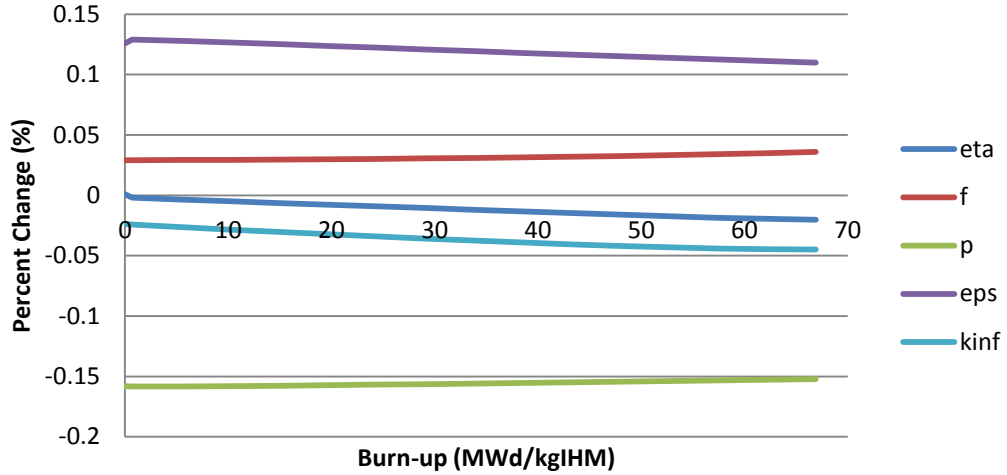
Appendix B: Additional Plots

B.1 PuTh

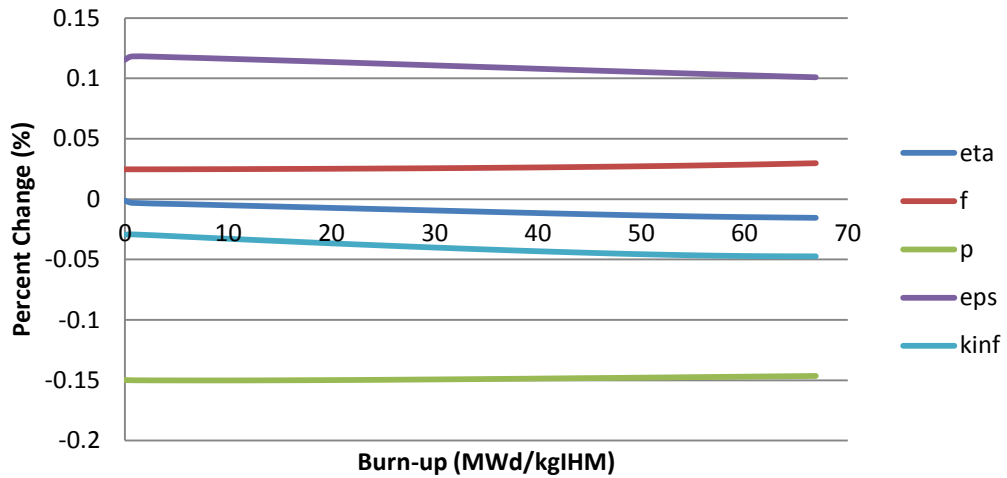




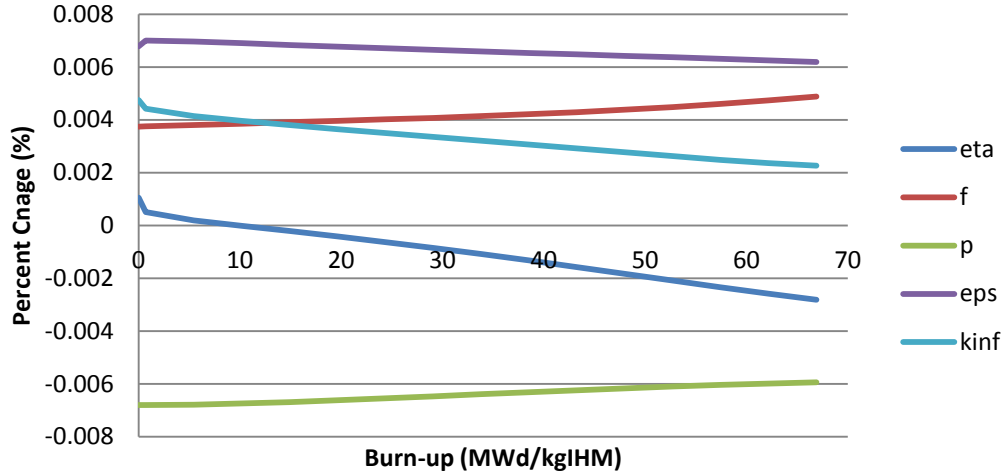
Total Coolant Void



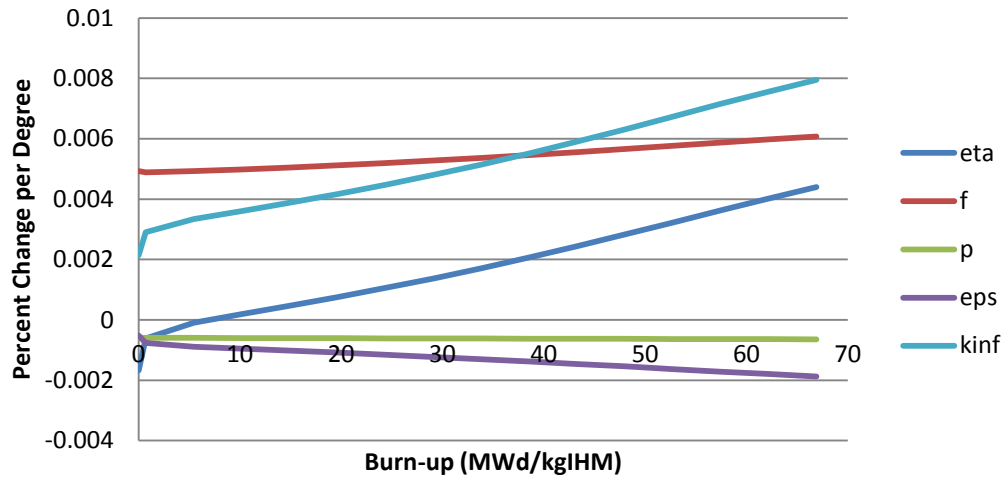
Inner Coolant Void



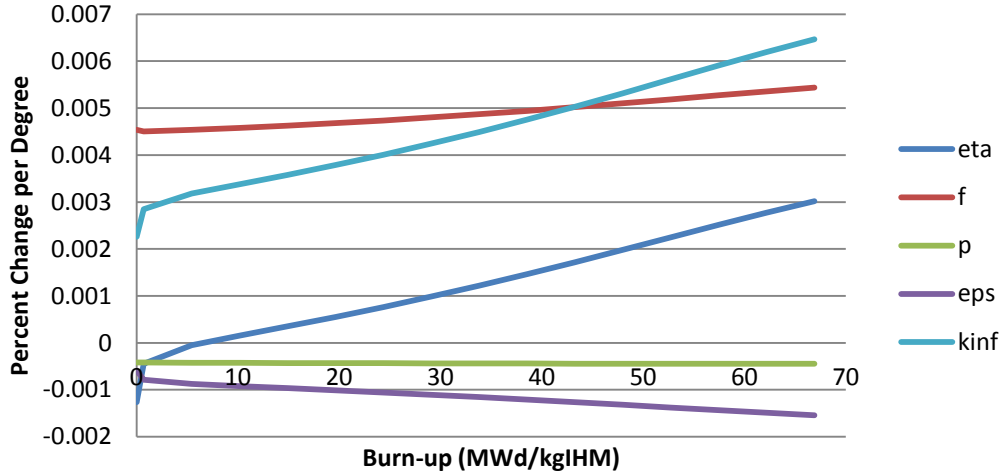
Outer Coolant Void



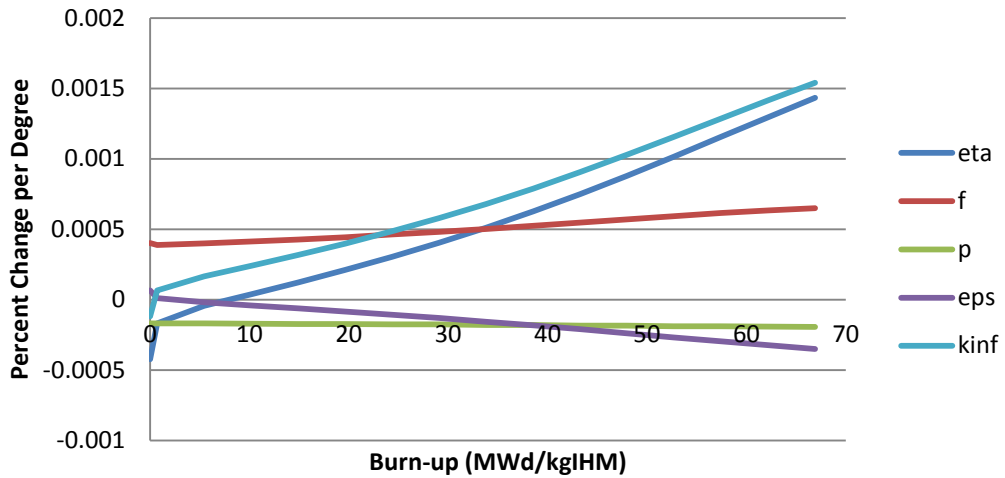
Total Coolant Temperature



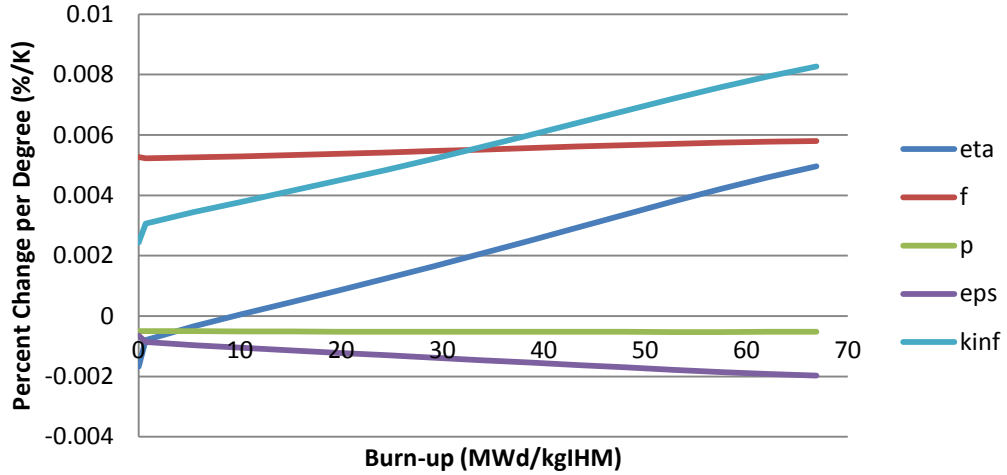
Inner Coolant Temperature



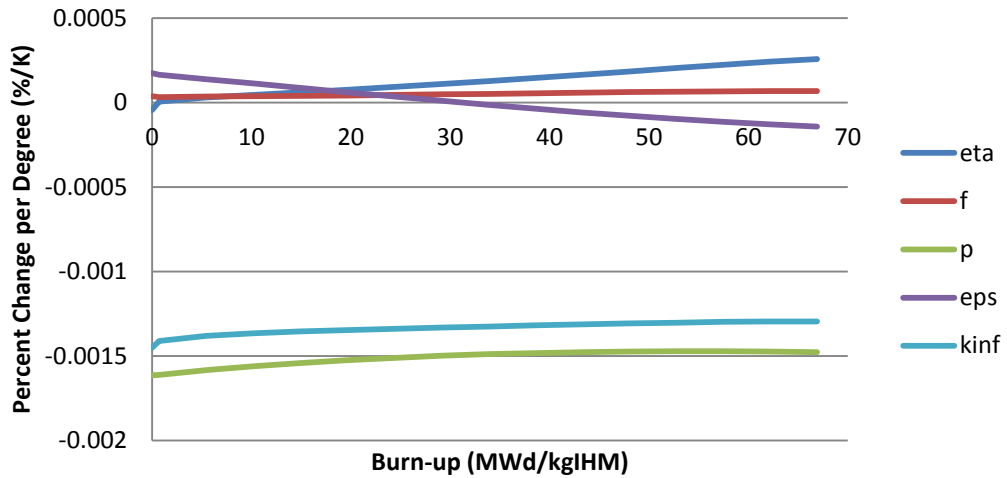
Outer Coolant Temperature



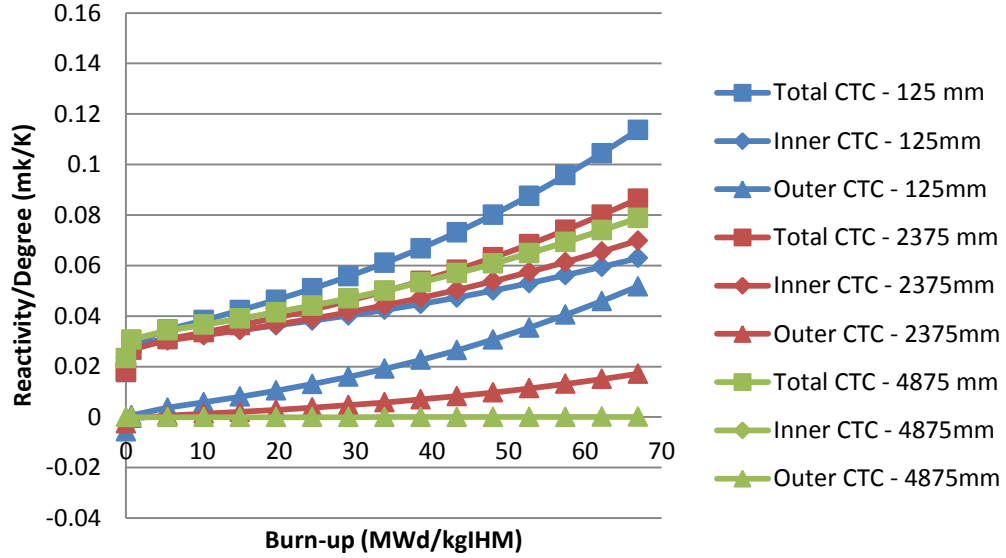
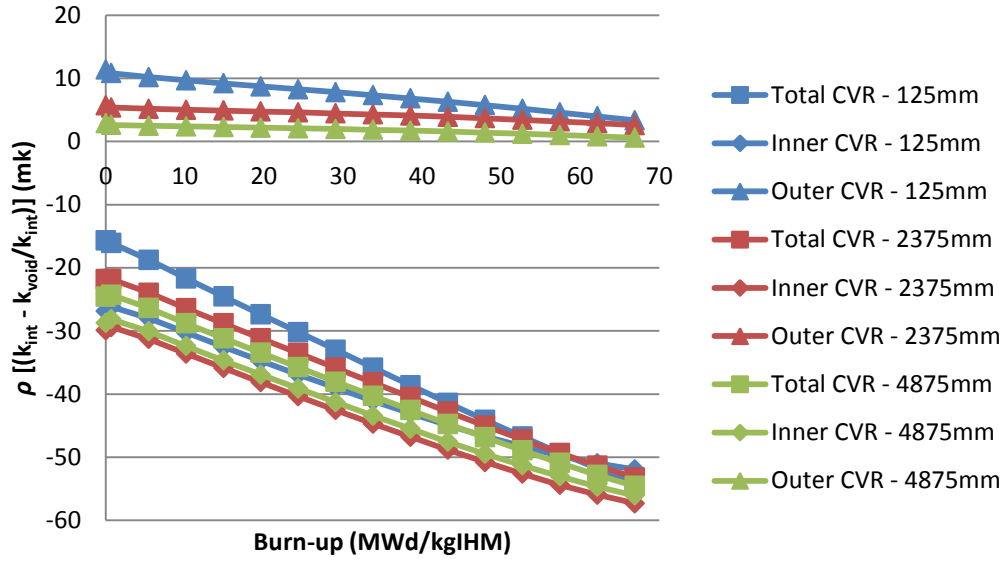
Moderator Temperature

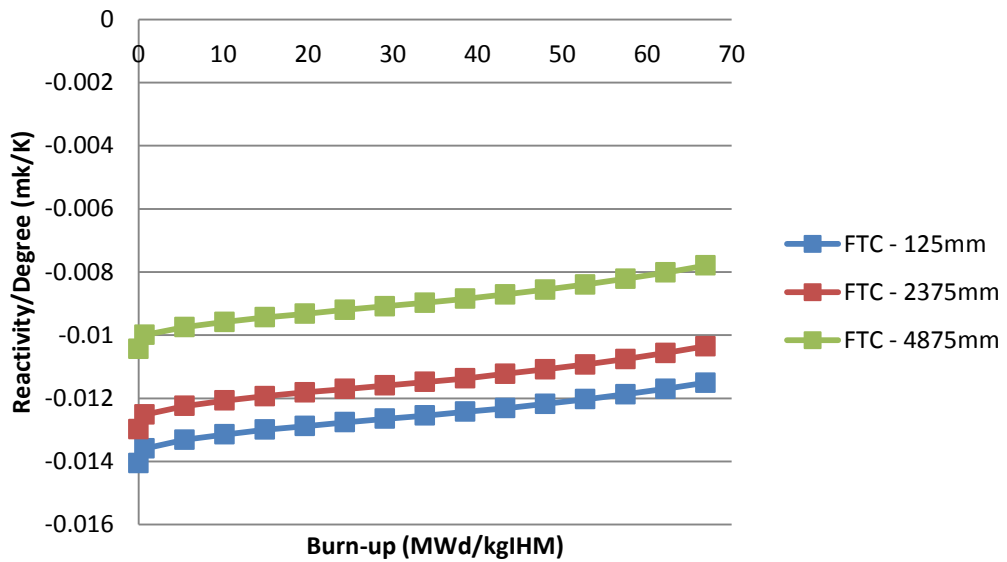
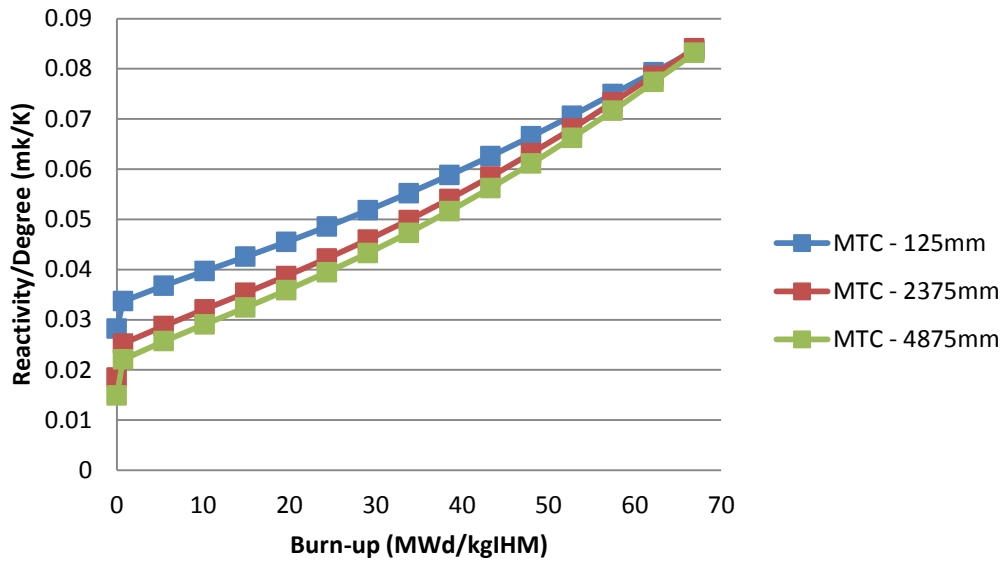


Fuel Temperature

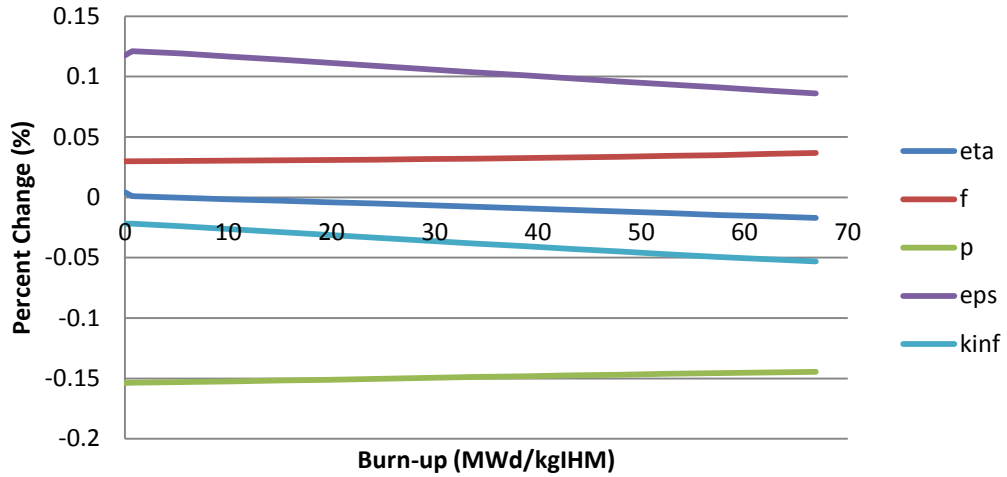


B.2 MOX

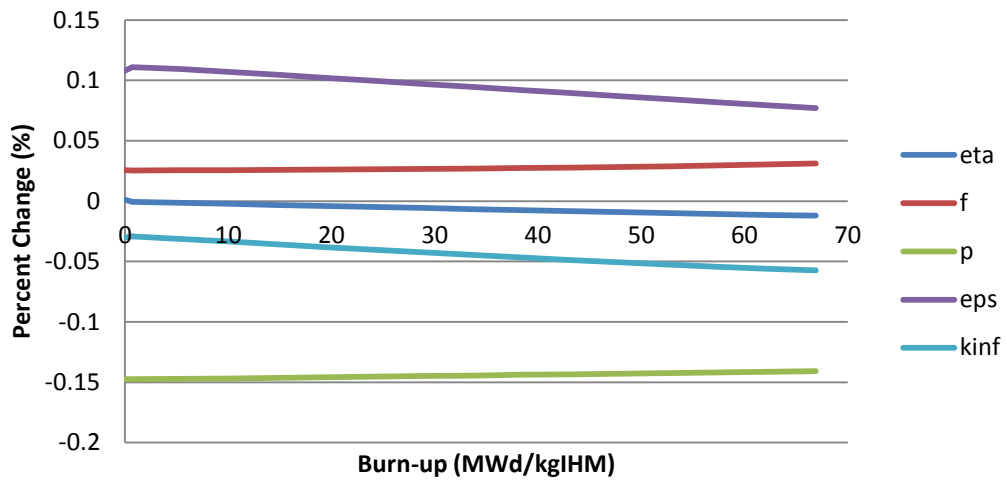




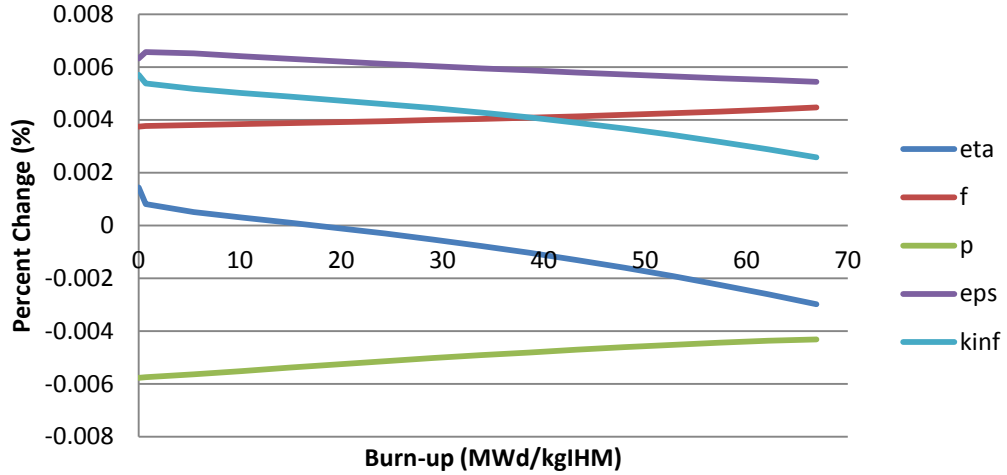
Total Coolant Void



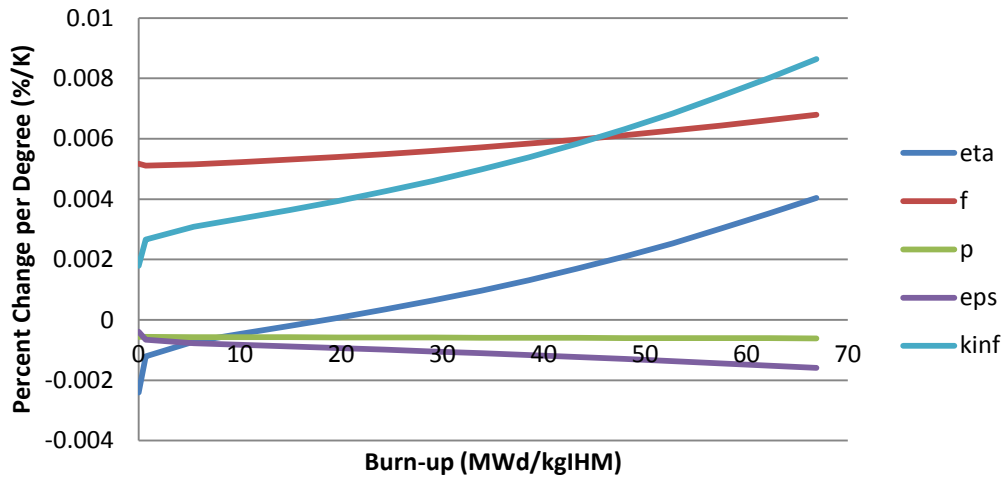
Inner Coolant Void



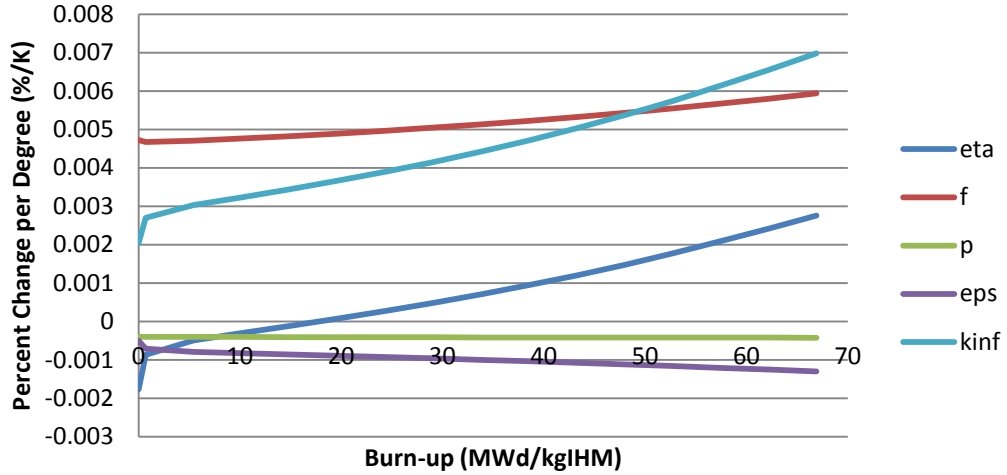
Outer Coolant Void



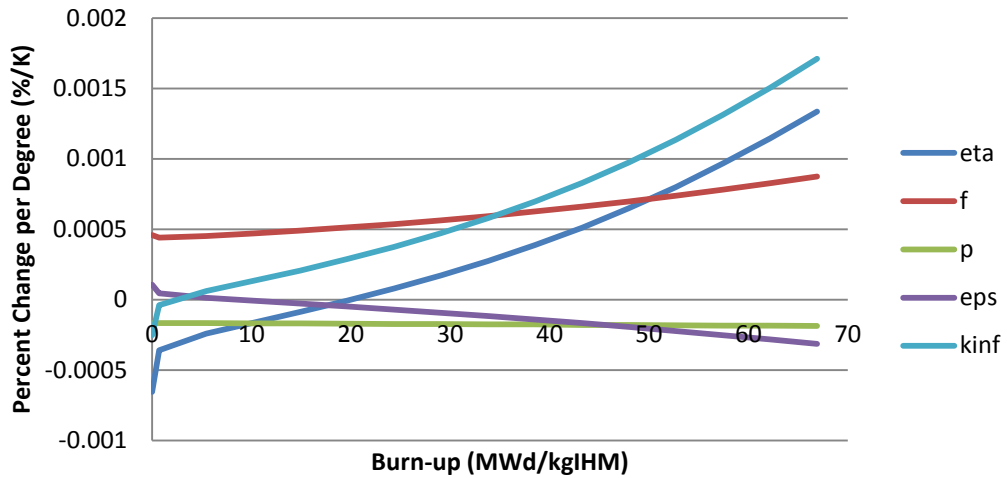
Total Coolant Temperature



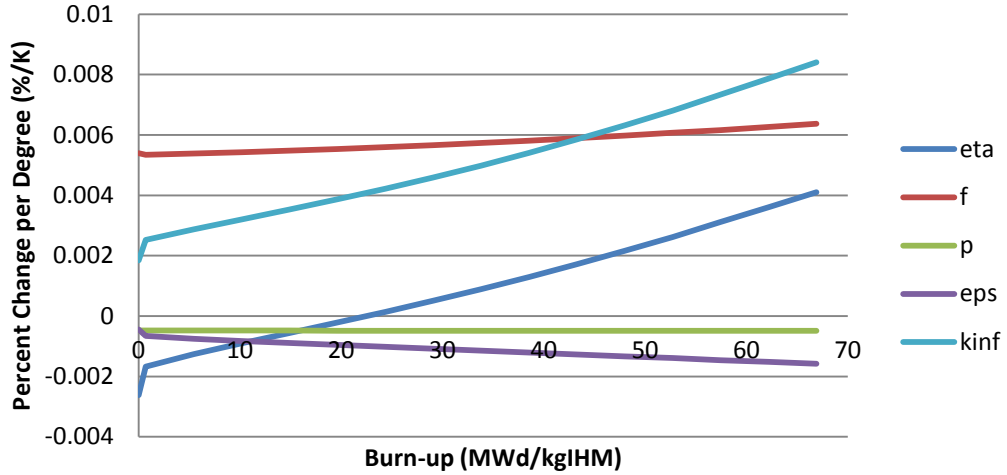
Inner Coolant Temperature



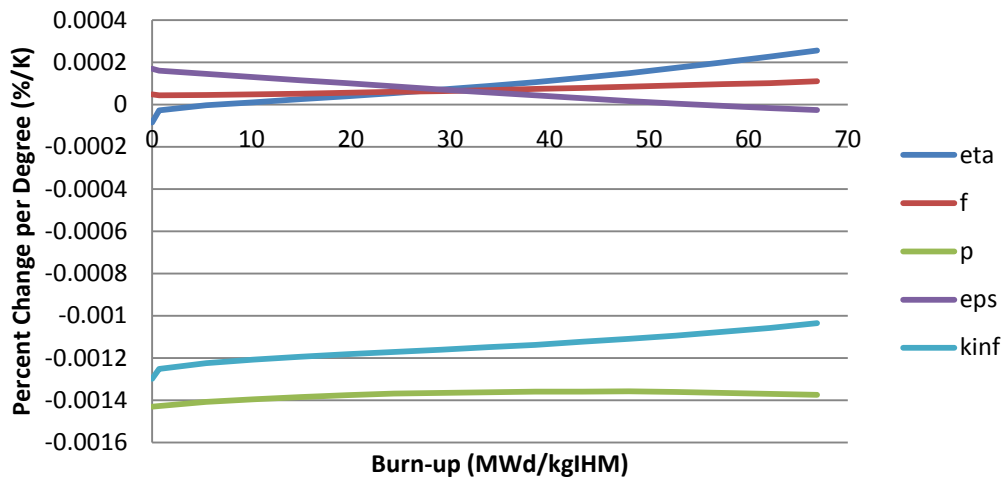
Outer Coolant Temperature



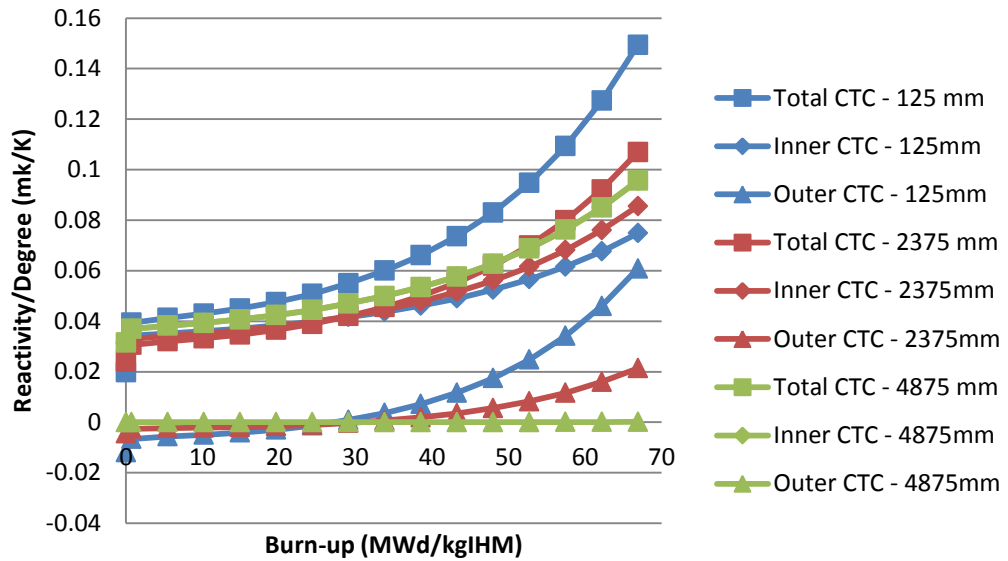
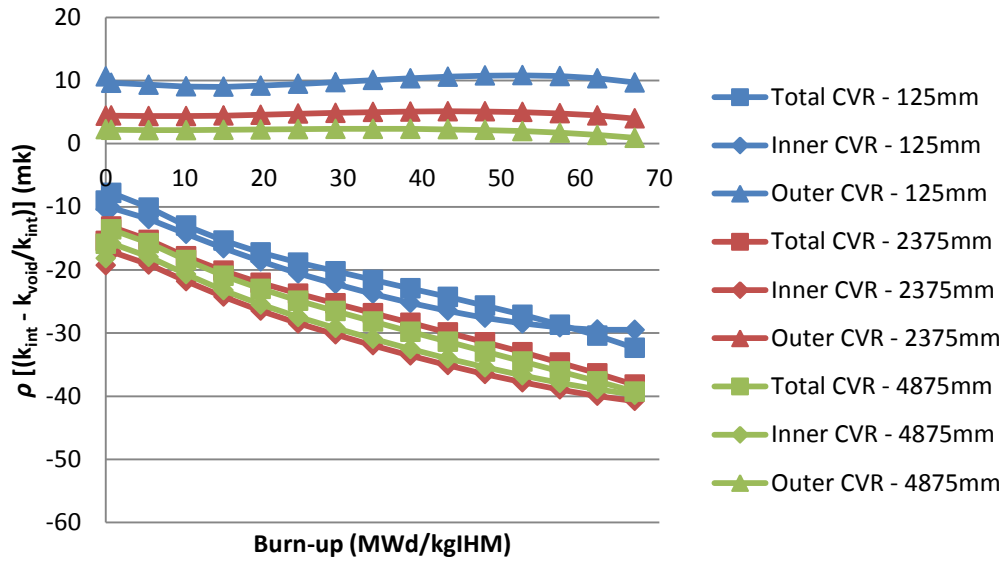
Moderator Temperature

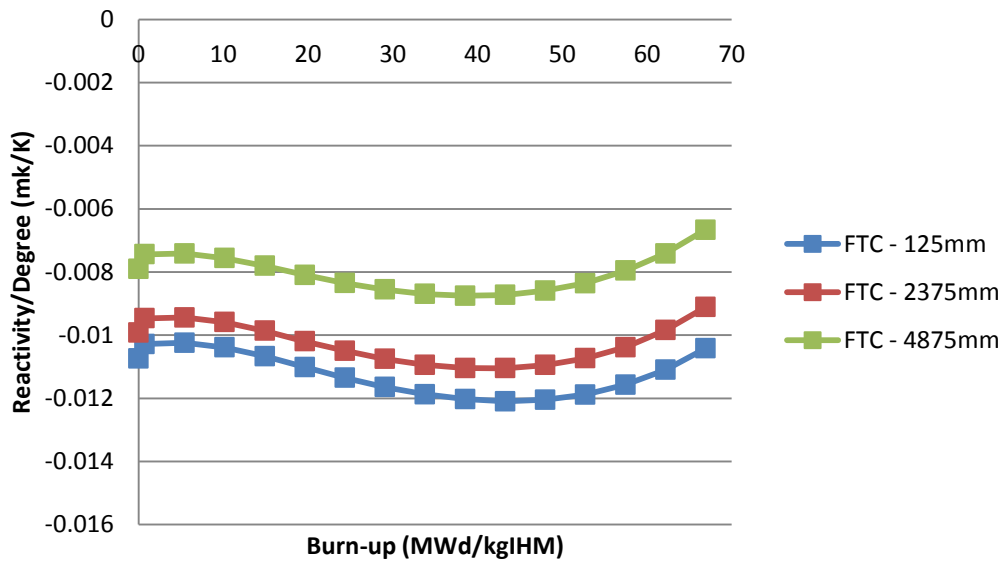
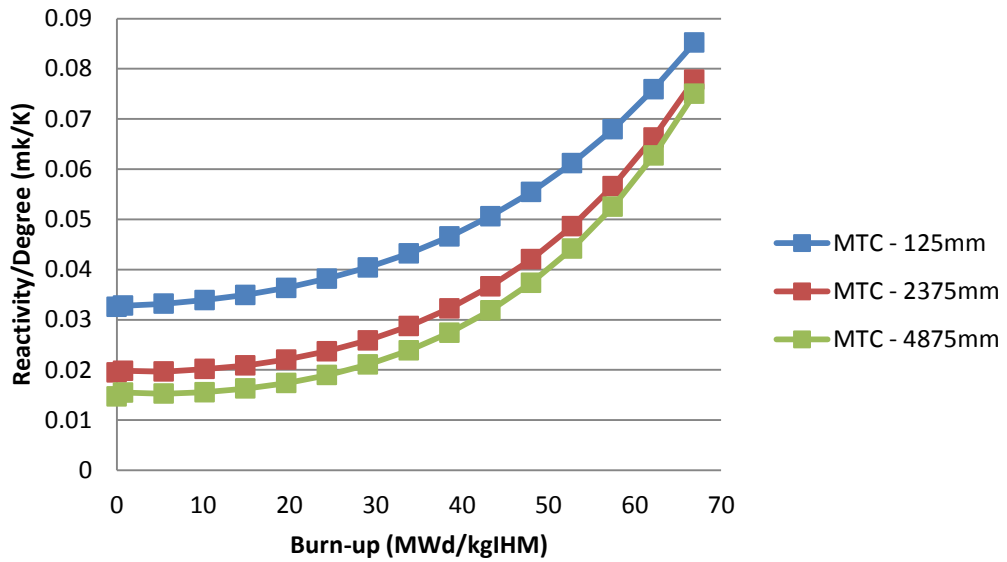


Fuel Temperature

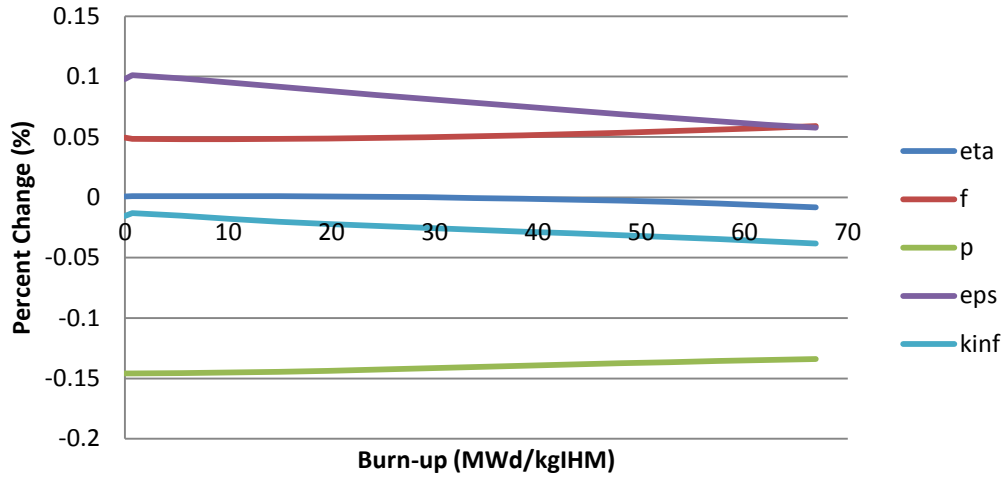


B.3 UO₂

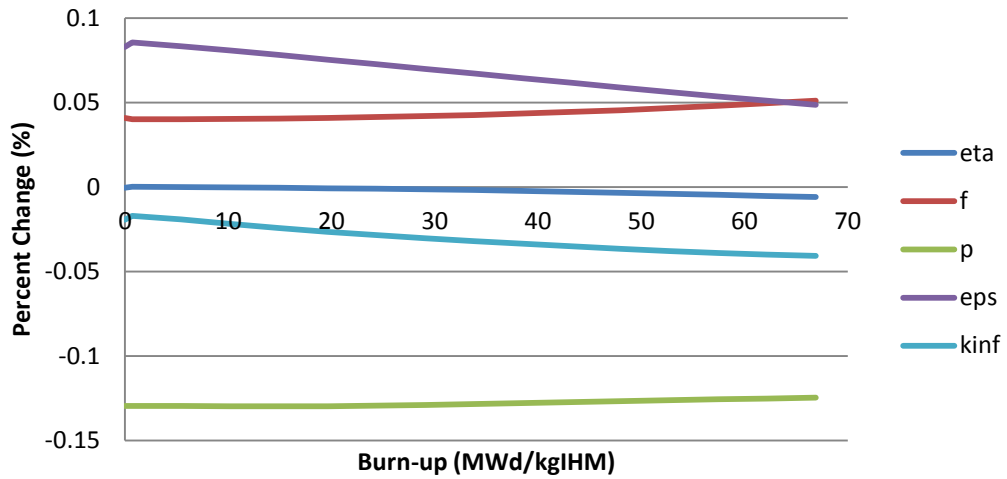




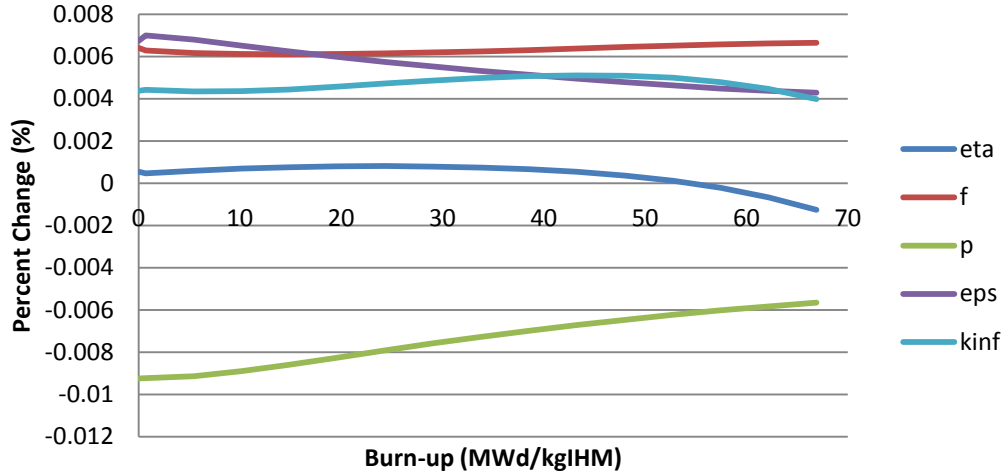
Total Coolant Void



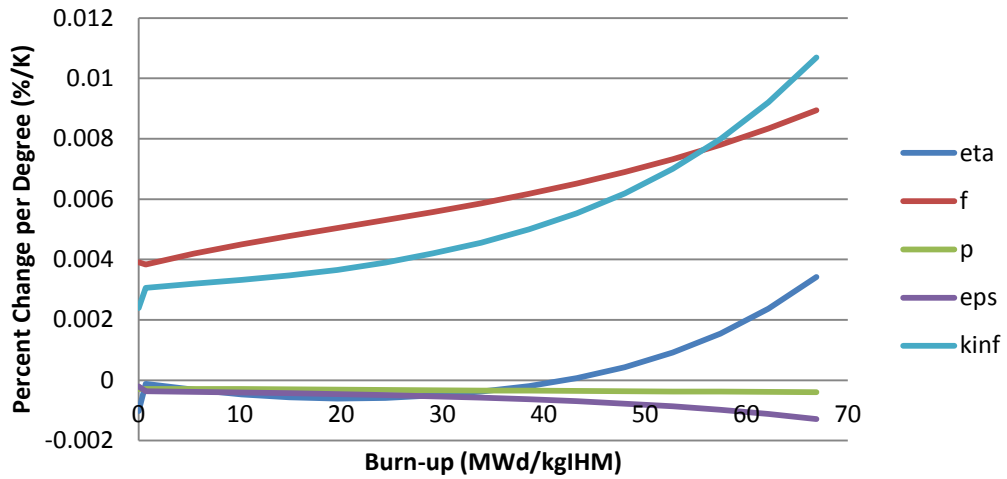
Inner Coolant Void



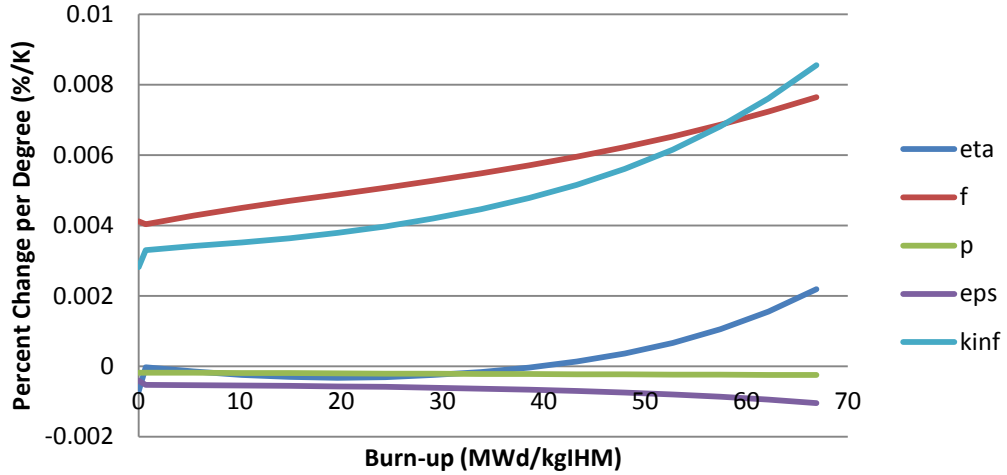
Outer Coolant Void



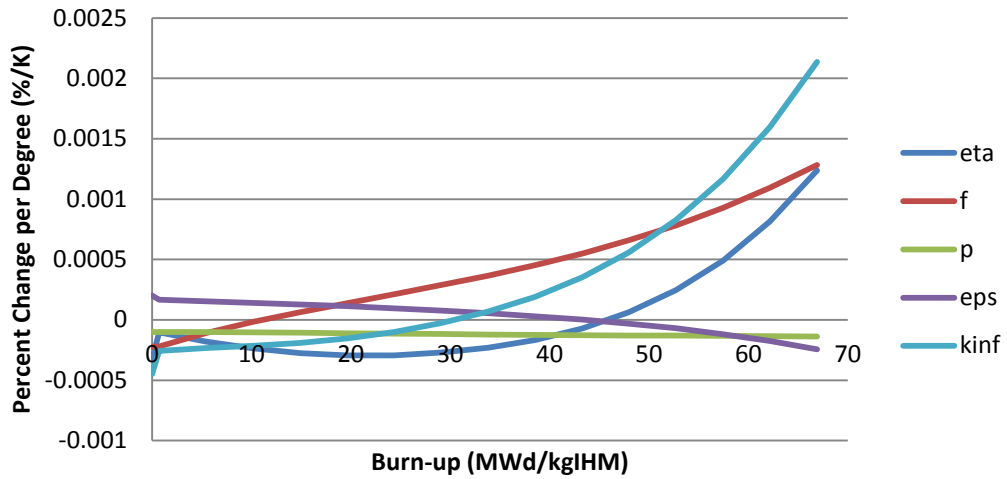
Total Coolant Temperature



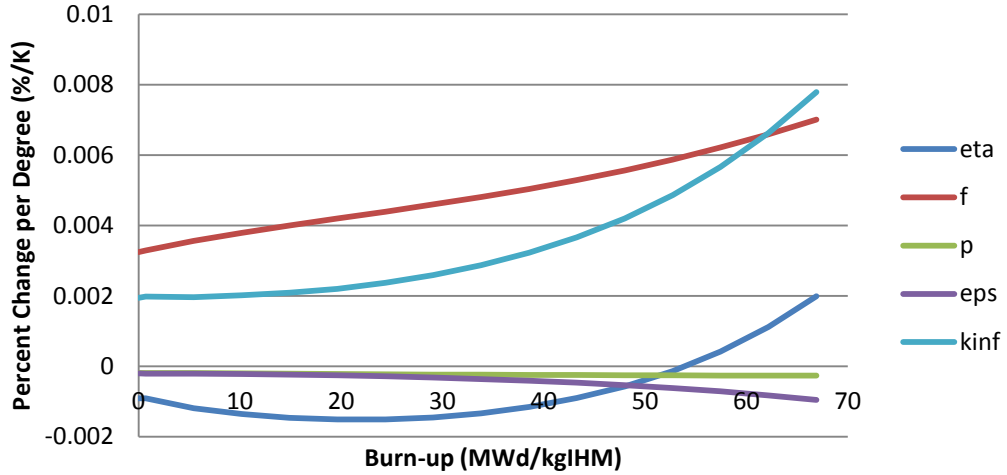
Inner Coolant Temperature



Outer Coolant Temperature



Moderator Temperature



Fuel Temperature

